

**SYNTHESIS OF POLYMER COATED IRON OXIDE FOR THE
DISINFECTION OF BACTERIA**

TAN QING ZUAN

**A project report submitted in partial fulfilment of the
requirements for the award of Bachelor of Engineering
(Honours) Chemical Engineering**

**Lee Kong Chian Faculty of Engineering and Science
Universiti Tunku Abdul Rahman**

May 2021

DECLARATION

I hereby declare that this project report is based on my original work except for citations and quotations which have been duly acknowledged. I also declare that it has not been previously and concurrently submitted for any other degree or award at UTAR or other institutions.

Signature :  _____

Name : Tan Qing Zuan

ID No. : 17UEB02896

Date : 4/5/2021

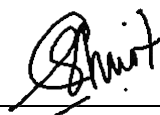
APPROVAL FOR SUBMISSION

I certify that this project report entitled **“SYNTHESIS OF POLYMER COATED IRON OXIDE FOR THE DISINFECTION OF BACTERIA”** was prepared by **TAN QING ZUAN** has met the required standard for submission in partial fulfilment of the requirements for the award of Bachelor of Engineering (Honours) Chemical Engineering at Universiti Tunku Abdul Rahman.

Approved by,

Signature

:



Supervisor

:

Ts. Dr. Shuit Siew Hoong

Date

:

7/5/2021

The copyright of this report belongs to the author under the terms of the copyright Act 1987 as qualified by Intellectual Property Policy of Universiti Tunku Abdul Rahman. Due acknowledgement shall always be made of the use of any material contained in, or derived from, this report.

© 2021, Tan Qing Zuan. All right reserved.

ACKNOWLEDGEMENTS

I would like to thank everyone who had contributed to the successful completion of this project. I would like to express my gratitude to my research supervisor, Ts. Dr. Shuit Siew Hoong for his invaluable advice, guidance and his enormous patience throughout the development of the research.

In addition, I would also like to express my gratitude to my loving parents and friends who had helped and given me encouragement throughout the period in completing the final year project.

Last but not least, I would like to offer my best regards to all who had supported me towards the completion of this project.

ABSTRACT

Water is an important element in human daily life. However, there are more than 2.2 billion people do not have access to clean and safe drinking water. The presence of pathogenic *E. coli* in water will cause bloody diarrhea, kidney failure or even death. There are a lot of water treatment techniques to purify the microorganism polluted water. However, these disinfection methods are known to have their downsides including the production of harmful by-products or high energy consumption. The use of Fenton reaction to remove *E. coli* had emerged as a promising disinfection technique in recent years. Conventional Fenton reaction which uses iron and hydrogen peroxide (H_2O_2) as reagents possess limitations such as narrow pH working range or production of iron sludge. Recent research moves towards the use of heterogenous Fenton reaction which uses iron oxide (Fe_3O_4) and H_2O_2 as reagents. In addition, the use of polymer to coat on Fe_3O_4 enhanced the colloidal stability of the core. In this paper, the synthesis and characterization method of polydimethyldiallyl ammonium chloride (PDDA) functionalized Fe_3O_4 , the effect of parameters (pH, catalysts dosage), and comparison with other disinfection techniques were reviewed. PDDA functionalized Fe_3O_4 can be easily synthesized by in-situ or post synthesis coating. The characterization of PDDA functionalized Fe_3O_4 showed that the coating of PDDA onto the Fe_3O_4 core would not perturb to original crystallinity of Fe_3O_4 nanoparticles. By comparing with other disinfection methods, Fenton reaction requires higher cost and disinfection contact time but a comparable efficiency. The most important benefit of Fenton reaction is the environmental friendly nature. Hence Fenton reaction using PDDA functionalized Fe_3O_4 can be a good alternative in wastewater treatment industry.

TABLE OF CONTENTS

DECLARATION		i
APPROVAL FOR SUBMISSION		ii
ACKNOWLEDGEMENTS		iv
ABSTRACT		v
TABLE OF CONTENTS		vi
LIST OF TABLES		ix
LIST OF FIGURES		x
LIST OF SYMBOLS / ABBREVIATIONS		xiii
CHAPTER		
1	INTRODUCTION	1
1.1	General Introduction	1
1.2	Importance of the Study	2
1.3	Problem Statement	3
1.4	Aim and Objectives	5
1.5	Scope and Limitation of the Study	5
1.6	Contribution of the Study	6
1.7	Outline of the Report	6
2	LITERATURE REVIEW	7
2.1	Water Pollution	7
2.2	<i>E. coli</i>	11
2.3	Methods of Bacteria Disinfection	14
2.3.1	Chemical Disinfection	14
2.3.2	Physical Disinfection	16
2.3.3	Advanced Oxidation Processes (AOPs)	18
2.4	Fenton Reaction	19
2.4.1	Iron Oxide (Fe ₃ O ₄)	21
2.4.2	Polydimethyldiallyl ammonium chloride (PDDA) coated Fe ₃ O ₄	22

2.5	Characterization Study	23
2.5.1	Scanning Electron Microscopy (SEM)	23
2.5.2	Transmission Electron Microscopy (TEM)	24
2.5.3	Fourier Transform Infrared Spectroscopy (FTIR)	25
2.5.4	X-ray Diffraction (XRD)	28
2.5.5	Brunauer-Emmett-Teller (BET)	30
2.5.6	Thermogravimetric Analysis (TGA)	31
2.6	Reusability Test	33
3	METHODOLOGY	34
3.1	Framework for the Methodology of Literature Review	34
	Search the literature pertinent to the review	35
3.1.1	Formulate the Problem	35
3.1.2	Search the Literature Pertinent to the Review	36
3.1.3	Screening for Inclusion	36
3.1.4	Evaluating the Quality of Primary Studies	37
3.1.5	Extracting Data	38
3.1.6	Analysing and Synthesizing Data	38
4.1	Synthesis of PDDA coated Fe ₃ O ₄	40
4.2	Characterization of PDDA coated Fe ₃ O ₄	43
4.3	Effect of Parameters in the Fenton Degradation of Microorganisms	50
4.3.1	Effect of pH	50
4.3.2	Effect of Temperature	55
4.3.3	Effect of Fenton Reagent Concentration	56
4.4	Comparison with Other Disinfection Methods	69
4.4.1	Cost	69
4.4.2	Disinfection By-Products (DBPs) Formation	71
4.4.3	Contact Time Required for Disinfection	73
4.4.4	Efficiency of Different Disinfection Processes	75

5	CONCLUSIONS AND RECOMMENDATIONS	85
5.1	Conclusions	85
5.2	Recommendations for future work	86
	REFERENCES	87

LIST OF TABLES

Table 2.1:	Absorption Bands of Common Functional Groups (Guerrero-Pérez and Patience, 2019)	26
Table 2.2:	Comparison between Volumetric Gas Adsorption Technique and DVS (Naderi, 2015)	30
Table 4.1:	Kinetic Parameters and Time Required to Achieve log-3 Activation of <i>E. coli</i> (Fernández, et al., 2020)	53
Table 4.2:	Concentrations of H ₂ O ₂ and Inactivation Rate of <i>E. coli</i>	61
Table 4.3:	Concentrations of Iron and Corresponding Inactivation Rate of <i>E. coli</i>	67
Table 4.4:	Comparison of Cost of Treatment for Four Different Methods	69
Table 4.5:	Comparison of Costs for Different Disinfection Methods	71
Table 4.6:	Disinfection Rate of Fenton Reaction, Ozonation, Chlorination and Electrochemical disinfection	74
Table 4.7:	Treatment Time and Disinfection Rate for Different Disinfection Methods	74
Table 4.8:	Disinfection Rate of Fenton Reaction, Ozonation and Chlorination	78
Table 4.9:	Comparison of CT Values for Different Disinfection Methods	79
Table 4.10:	Experimental Conditions and Efficiency of Different Disinfection Methods	82

LIST OF FIGURES

Figure 2.1:	Overall Quality Status of Rivers from Year 2008 to 2017 in Malaysia (DOE, 2017)	9
Figure 2.2:	Current Approach to Monitor and Identify Bacteria (Nurliyana, et al., 2018)	10
Figure 2.3:	<i>E. coli</i> Cell (Nurliyana, et al., 2018)	11
Figure 2.4:	(a) Multiple Tube Fermentation Method. (b) Plate Count Enumeration Method (Nurliyana, et al., 2018)	13
Figure 2.5:	Disinfection by Chlorine Gas (Saqib Ishaq, Afsheen and Khan, 2019)	15
Figure 2.6:	Ozone Contacting Method (Saqib Ishaq, Afsheen and Khan, 2019)	16
Figure 2.7:	UV Disinfection Method (Saqib Ishaq, Afsheen and Khan, 2019)	17
Figure 2.8:	Schematic Diagram of Photocatalysis using Semiconductor (Saqib Ishaq, Afsheen and Khan, 2019)	19
Figure 2.9:	Mechanism of Fenton Process (O'Dowd and Pillai, 2020)	20
Figure 2.10:	Configurations of SEM (Choudhary and Priyanka, 2017)	23
Figure 2.11:	Schematic Diagram of TEM (Tang and Yang, 2017)	25
Figure 2.12:	Different Types of FTIR (Guerrero-Pérez and Patience, 2019)	27
Figure 2.13:	Pictorial Representation of ATR-FTIR (Schuttlefield and Grassian, 2008)	27
Figure 2.14:	Schematic Diagram of XRD System (Bunaciu, Udriștioiu and Aboul-Enein, 2015)	29
Figure 2.15:	Thermobalances Design of TGA	32

Figure 3.1:	Overall Flowchart to Conduct Literature Review	35
Figure 3.2:	Citavi Program	37
Figure 4.1:	TEM Image of PDDA Coated Fe ₃ O ₄ (a)-(c) in Suspension and (d) in Powder (Li, et al., 2016)	44
Figure 4.2:	FTIR Spectrum of Pristine PDDA and PDDA Coated Fe ₃ O ₄ (Li, et al., 2016)	45
Figure 4.3:	TEM Images of (A) Fe ₃ O ₄ Nanoparticles (B) PDDA Coated Fe ₃ O ₄ (Qu, et al., 2015)	45
Figure 4.4:	XRD Patterns of Fe ₃ O ₄ Nanoparticles (Red) and PDDA Coated Fe ₃ O ₄ (Black)	46
Figure 4.5:	SEM Images of (a) Fe ₃ O ₄ and (b) PDDA Coated Fe ₃ O ₄ (Chen, Ju and Chen, 2018)	47
Figure 4.6:	TEM Images of Fe ₃ O ₄ Nanoparticles (Left) and PDDA Coated Fe ₃ O ₄ (Chen, Ju and Chen, 2018)	47
Figure 4.7:	Comparison of FTIR Spectrum of PDDA Coated Fe ₃ O ₄ , PDDA and Fe ₃ O ₄ (Chen, Ju and Chen, 2018)	48
Figure 4.8:	TGA Curves of (a) Fe ₃ O ₄ and (b) PDDA Coated Fe ₃ O ₄ (Chen, Ju and Chen, 2018)	49
Figure 4.9:	TEM Image of PDDA Coated Fe ₃ O ₄ (Jang, et al., 2014)	49
Figure 4.10:	Effect of pH on Iron Catalysts in Fenton Process (O'Dowd and Pillai, 2020)	51
Figure 4.11:	<i>E. coli</i> Degradation Rate at Different pH Values (Moradi, et al., 2017)	53
Figure 4.12:	Graph of Time Required for <i>E. coli</i> Disinfection at Different pH (Tong, et al., 2019)	54
Figure 4.13:	Inactivation Percentage of Different H ₂ O ₂ Dosage (Middle Column) (Fernández, et al., 2020)	58

Figure 4.14:	Effect of FSCNC in heterogenous Fenton-like reaction (Feng, et al., 2019)	65
Figure 4.15:	Efficiency of <i>E. coli</i> Inactivation under Different AOPs System with UV-Vis (Rincón and Pulgarin, 2006)	75
Figure 4.16:	Efficiency of <i>E. coli</i> Inactivation under Different AOPs System Without UV-Vis (Rincón and Pulgarin, 2006)	76
Figure 4.17:	Inactivation of <i>E. coli</i> Using Different Chlorine Dosages (Rodriguez-Chueca, et al., 2015)	77
Figure 4.18:	Inactivation of <i>E. coli</i> After Different Contact Time (Rodriguez-Chueca, et al., 2015)	77
Figure 4.19:	<i>E. coli</i> Inactivation in Milli-Q Water (■) UV (●) UV/ H ₂ O ₂ (▲) Fe ²⁺ / H ₂ O ₂ /UV (Rubio, et al., 2013)	80
Figure 4.20:	Disinfection Efficiency of PVA-AgNP (Alkawareek, et al., 2019)	81
Figure 4.21:	Disinfection Efficiency of PAH-AgNP (Alkawareek, et al., 2019)	81
Figure 4.22:	(a) Initial <i>E. coli</i> ; (b) <i>E. coli</i> After Chlorination Disinfection; (c) <i>E. coli</i> After Ozonation Disinfection; (d) Fenton Treatment for 10 min; (e) Electrochemical Disinfection at 16 mA/cm ² ; (f) Electrochemical Disinfection at 25 mA/cm ² (Diao, et al., 2004)	83

LIST OF SYMBOLS / ABBREVIATIONS

A	absorbance, nm
b'	effective path length, m
c	concentration, mol dm ⁻³
C	dimensionless constant
d_p	penetration depth per reflection, m
N	number of reflections
n_1	index of refraction of the internal reflection element
n_2	index of refraction of the sample medium exposed to crystal
n_{21}	ratio of n_2 to n_1
P	equilibrium partial vapor pressure of absorbate gas, Pa
P_0	saturated pressure of absorbate gas, Pa
V_a	volume of gas adsorbed, mm
V_m	volume of gas adsorbed to form monolayer, mm
$W(t)$	mass of sample at t, g
W_0	initial mass, g
W_∞	residual mass, g
d	interplanar spacing generating the diffraction
α	extent of conversion
ε	molar absorptivity, dm ³ mol ⁻¹ cm ⁻¹
θ	angle of diffraction
λ	wavelength of X-ray, nm
$[\text{H}_3\text{O}_2]^+$	oxonium ions
$\cdot\text{OH}$	hydroxyl radicals
1,1-DCP	1,1-dichloro-2-propanone
AAc	acrylic acid
AgNP	silver nanoparticles
AOPs	advanced oxidation processes
ATR	attenuated total reflection
BET	Brunauer–Emmett–Teller
BOD	biochemical oxygen demand

CFU	colony forming units
CH	chloral hydrate
Cl ₂	chlorine
CO ₂	carbon dioxide
COD	chemical oxygen demand
Cu-IDS	copper with iminodisuccinic acid
DBPs	disinfection by-products
DO	dissolved oxygen
DOE	Department of Environment
DRIFTS	diffuse reflection
DVS	gravimetric dynamic vapour sorption technique
<i>E. coli</i>	Escherichia coli
Fe(H ₂ O) ₆ ³⁺	hexaaquairon ion
Fe ₃ O ₄	iron oxide
Fe-MABs	hybrid alginate montmorillonite iron enriched beads
FSCNC	Fe ₃ O ₄ /SiO ₂ /C nanocomposites
FTIR	Fourier transform infrared spectroscopy
H ⁺	hydrogen ions
H ₂ O	water
H ₂ O ₂	hydrogen peroxide
HAAs	haloacetic acids
HANs	haloacetonitriles
HC	haemorrhagic colitis
HUS	hemolytic uremic syndrome
IONPs	iron oxide nanoparticles
IR	infrared
KBr	potassium bromide
KPS	potassium persulfate
MF	magnetic Fe ₃ O ₄ -deposited MoS ₂ flower-like spheres
MMA	methyl methacrylate
MNPs	magnetic nanoparticles
MoS ₂	Molybdenum disulfide
N ₂	nitrogen gas
NaOH	sodium hydroxide

NDMA	N-nitrosodimethylamine
NH ₃ -N	ammoniacal nitrogen
NH ₄ OH	ammonium hydroxide
NWQS	national water quality standers
O ₂ ⁻	superoxide radical
O ₃	ozone
PAH	polyallylamine hydrochloride
PDDA	polydimethyldially ammonium chloride
ppm	parts per million
PVA	polyvinyl alcohol
RAIRS	specular reflection
SEM	scanning electron microscope
TEM	transmission electron microscopy
TGA	thermogravimetric analysis
THM	trihalomethane
TiO ₂	titanium dioxide
TIR	transmission
TMAOH	tetramethylammonium hydroxide
TSS	total suspended solid
TTP	thrombocytopenic purpura
UV	ultraviolet
WQI	water quality index
XRD	X-ray diffraction
ZnO	zinc oxide

CHAPTER 1

INTRODUCTION

1.1 General Introduction

Water is an important element in human daily life. There are only 3% of water on earth is fresh water and only 1.2% is consumable drinking water (National Geographic Society, 2020). Water resources was found to be depleted due to the rapid growth of civilization and industrialization. Daily water usage will cause contamination of water by adding a lot of compounds into the waste source, producing wastewater. These natural organic, inorganic, and artificial compounds include oil, dirt, chemicals, metals, and animal wastes. Apart from that, the presence of pathogens such as bacteria, viruses, protozoans also became a major concern because they posed threats to human life. The threat is crucial for the communities in developing countries since most of them are still using open water sources such as rivers or dams (Motshekga, Sinha Ray and Maity, 2018).

The contamination by microorganisms in water supplies emerged as a major environmental issue in the world. Amongst the microorganisms, bacteria is one of the most distinct group of human pathogens present in wastewater. Bacteria is chosen to be the indicator in the tracking of the efficiency of a wastewater treatment process. *Escherichia coli* (*E. coli*) is often used to monitor the water quality because it is a representation of the fecal contamination. Some of the bacteria will be beneficial to their host while some bacteria will become the pathogens in the wastewater. These pathogenic bacteria in water will cause adverse health effect to human if they are not properly treated.

To overcome the bacterial contamination of wastewater, a lot of disinfection processes had been developed. Disinfection means to destroy or inactivate the pathogenic microorganisms which will cause health hazards (Forney, 2008). The wastewater will need to undergo additional flocculation and filtration process to ensure a more efficient disinfection process. The conventional methods of disinfection of bacteria in water were adsorption using activated carbon, air stripping, high temperature incineration,

chlorination, coagulation and biological treatment (Singh, et al., 2019). In recent years, iron-oxide (Fe_3O_4) based magnetic nanoparticles (MNPs) were widely studied for the effectiveness of bacterial removal in wastewater (Xu, et al., 2019). Moreover, advanced oxidation processes (AOPs) such as photocatalysis process had been developed to replace the conventional methods for the disinfection of bacteria. Fe_3O_4 nanoparticles coupled with non-magnetic semiconductor photocatalysts to achieve a better performance in disinfection process. Polymer coated nanocomposites were found effective in the disinfection process as well.

Fe_3O_4 is known as the most abundant metal oxides which can be synthesized industrially at ambient conditions. Fe_3O_4 can be used in a wide range of industries such as biomedical, industrial catalysis and so on. Fe_3O_4 containing absorbents can be easily functionalized with other materials such as polymers, metals and so on. Besides, it can be separated easily from another suspension by utilizing a magnetic field. In common practice, Fe_3O_4 will be functionalized with different materials to obtain the required properties in the nanocomposites. Functionalization is also to ensure a uniform size and well dispersion of the Fe_3O_4 nanoparticles. Recently, polymer coated Fe_3O_4 has been developed due to the development in the polymer properties and the unique properties of the nanomaterials inside polymer (Li, et al., 2016). Both synthetic polymer and natural polymer could be used to coat Fe_3O_4 nanoparticles.

1.2 Importance of the Study

It was reported that magnetic nanoparticles were efficient in wastewater treatment. However, limited study was reported on the effectiveness of the disinfection of bacteria in wastewater by using polymer coated Fe_3O_4 . Only few studies reported on the usage of polymer coated Fe_3O_4 in the biomedical field. Studies that investigated the effectiveness of nanocomposites in the disinfection process included magnetic barium phosphate nanoflakes with Fe_3O_4 nanoparticles, silver-loaded magnetic particles, and Fe_3O_4 nanoparticles. Motshekga, Sinha Ray and Maity (2018) employed alginate nanocomposites to study the bacteria disinfection of water. Zhang, et al. (2019) studied the removal of *E. coli* from water using magnetic

Fe₃O₄/phosphate nanocomposites. Hence, it is important to study the use of polymer coated Fe₃O₄ for the disinfection of bacteria.

1.3 Problem Statement

One of the major environmental issues currently is the insufficient access to clean drinking water and sanitation (Singh, et al., 2019). As reported by United Nations World Water Development 2019, there were more than 2 billion people encountered water shortage and 2.2 billion people did not have access to clean drinking water. Diarrhea illness is known as one of the top five major causes of death around the world. There were more than 1.3 million deaths of children caused by diarrheal illness every year globally (Liu, et al., 2013). Water is often contaminated by pollutants such as organic molecules, detergents, pesticides, herbicides, plastics, heavy metals, and pathogens. Contaminated water is the main culprit for these deaths caused by diarrheal illness because it is the main transmission pathway of pathogens. The disease-causing pathogens include viruses, bacteria and protozoans (Forney, 2008). By introducing wastewater treatment process to the wastewater, the concentration of the microbial pathogens could be reduced.

Conventional methods of bacteria disinfection possessed limitations such as high cost, time-intensive or even the formation of toxic by-products. The most commonly used chlorination process was found to produce carcinogenic and mutagenic substances due to the reaction between chlorine and organic compounds in wastewater (Motshekga, Sinha Ray and Maity, 2018). Therefore, it is vital to develop a disinfection method that is more cost-effective and without the formation of hazardous by-products. Over the last few years, much attentions had been focusing on Fe₃O₄ magnetic nanoparticles due to their special magnetic properties, non-toxicity and cost-effective to produce (Businova, et al., 2011a). The effectiveness of Fe₃O₄ as disinfectant agent had been proven in the removal of viruses (Nangmenyi, et al., 2011). Fe₃O₄ is capable to interact with many biological molecules in the different processes due to their unique superparamagnetic properties and a wide choice of surface functionalization. The surface charge of Fe₃O₄ will adsorb the impurities from water by dissociating the surface hydroxyl group. Moreover, when the Fe₃O₄ is used as a catalyst in heterogenous Fenton reaction, high

efficiency can be achieved. Hence, the problem with this issue is to replace the conventional disinfectants by using Fe_3O_4 magnetic nanoparticles as catalysts in Fenton reaction.

Conventional wastewater treatment includes physical, chemical, or biological technologies which no single technology is known to be the best method (Crini and Lichtfouse, 2019). The commonly used method in wastewater treatment is adsorption process using activated carbon, carbon nanotubes and so on (Zare, et al., 2015). In adsorption process, organic or inorganic compounds in wastewater will be adsorbed onto the surface on the adsorbent. One of the limitations of adsorption process is that additional separation process is required to remove the adsorbent from solution. To overcome this problem, Fenton reaction can be employed to degrade the bacteria in wastewater. In Fenton reaction, Fe_3O_4 will react with hydrogen peroxide (H_2O_2) to form hydroxyl radical ($\cdot\text{OH}$). The $\cdot\text{OH}$ will then oxidize the bacteria in wastewater causing degradation. Harmless products which is carbon dioxide and water will be formed. Hence, Fenton reaction is a good alternative in wastewater treatment due to its environmental friendly nature.

Apart from that, the use of naked or non-functionalized Fe_3O_4 magnetic nanoparticles in water treatment process will cause the environmental problems, release toxic compounds and safety hazards. The Fe_3O_4 nanoparticles became a pollutant in the treated water when metal ions leaked into water. Fe_3O_4 nanoparticles are used to be isolated by matrices to obtain uniform size and well dispersion of the particles (Li, et al., 2016). The surface coating of Fe_3O_4 nanoparticles will affect its properties such as colloidal stability and magnetism (Barrow, et al., 2015). To obtain better colloidal stability in hydrophilic conditions and stop the iron core from degrading, polymer is usually used to functionalized Fe_3O_4 nanoparticles. Therefore, Fe_3O_4 encapsulated in polymer matrix will make sure that the nanoparticles is contained and will not further pollute the treated water.

1.4 Aim and Objectives

The main aim of this study is to review the synthesis of polymer coated Fe_3O_4 and investigate its effectiveness to remove *E. coli* in wastewater.

The specific objectives of this study include:

- i. To review the synthesis and characterization methods of PDDA functionalized Fe_3O_4 .
- ii. To review the effect of parameters in the degradation of *E. coli* using PDDA functionalized Fe_3O_4 via Fenton reaction.
- iii. To compare the degradation of *E. coli* using PDDA functionalized Fe_3O_4 via Fenton reaction with other disinfection techniques.

1.5 Scope and Limitation of the Study

The first scope of this study is to review and compare the synthesis and characterization of polymer coated Fe_3O_4 . The synthesis method of PDDA coated Fe_3O_4 such as in situ coating and post synthesis coating will be reviewed. Next, the polymer coated Fe_3O_4 will be characterized by using scanning electron microscope (SEM), transmission electron microscopy (TEM), X-ray diffraction (XRD), Brunauer–Emmett–Teller analysis (BET), Fourier transform infrared spectroscopy (FTIR) and thermogravimetric analysis (TGA).

Next, the effect of parameters on the effectiveness of PDDA functionalized Fe_3O_4 in disinfection of bacteria such as effect of pH, concentration of PDDA functionalized Fe_3O_4 , concentration of H_2O_2 and so on will be reviewed.

Finally, the effectiveness of other disinfection method will be reviewed and compare with the effectiveness of degradation of *E. coli* using PDDA functionalized Fe_3O_4 via Fenton reaction.

In this project, not all the disinfection methods will be reviewed to compare the effectiveness of degradation of *E. coli* using PDDA functionalized Fe_3O_4 via Fenton reaction. For the effect of parameters, only important parameters such as pH and dosages of catalysts will be reviewed.

1.6 Contribution of the Study

In this paper, the synthesization and characterization methods of PDDA functionalized Fe_3O_4 are reviewed. Moreover, the effect of parameters on Fenton reaction including pH and catalysts dosage as well as comparison with other disinfection methods with Fenton reaction are reviewed. This report can provide an overview of the bacteria degradation via Fenton reaction. In addition, the findings can provide a reference for the experiments to investigate the use of PDDA coated Fe_3O_4 to disinfect bacteria via Fenton reaction.

1.7 Outline of the Report

There are five main chapters in this report. Chapter 1 is about the general introduction, problem statement, aims and scope of this study. Water pollution issues and the limitations of conventional disinfection methods are outlined in this chapter. In Chapter 2, literature reviews which include the type of disinfection methods, the *E. coli* contamination issue in Malaysia as well as introduction of PDDA coated Fe_3O_4 are included in this chapter. Next, the methodology of this study are presented in Chapter 3. The reviews based on the objectives are presented in Chapter 4 and Chapter 5 gives a brief conclusion of the whole report.

CHAPTER 2

LITERATURE REVIEW

2.1 Water Pollution

Back in the day, groundwater is known to be pollutant free where there are no microbes in the water sources underground especially in the confined aquifers. However, the presence of microbes and pathogens are detected in groundwater recently. The groundwater is usually polluted by nearby sources of contaminated surface water such as leakage from waste lagoon, septic tanks, landfill and so on (Polo-López, Nahim-Granados and Fernández-Ibáñez, 2018). Surface water will always show a higher level of contamination than ground water which contains a higher number of pathogens inside water. Nevertheless, it is very difficult to trace and check every contaminated water source since different tests are required for each type of pathogen. It is not practical due to the time and cost issue. *E. coli*, as an indicator of faecal contamination, is the most used microbial indicators of water quality.

Pollution in surface water and groundwater has emerged as an important environmental issue as it possesses health issue to the society. The rapid growth of industrialization and civilization had increased the number of pollutants such as toxic compounds, dyes, detergents, pesticides, herbicides, organic compounds, heavy metals as well as pathogens. Even in regions which were seemed to be rich in water, insufficient access to drinking water had become a major issue as well due to the increase civilization and industrialization (Singh, et al., 2019). The breeding of bacteria in water had become a serious issue due to the increasing water pollution problem (Liu, et al., 2018). The quality of drinking water had been affected due to the increasing number of bacteria inside water. Millions of people around the world are suffering from diseases caused by microbes in water (Mukherjee and De, 2015).

Water quality is a term used to define whether the water is suitable to be used to sustain daily activities for living organisms. More than 90 % of the water used comes from rivers (Lee Goi, 2020). Hence, the water quality of rivers possesses a serious impact to human life. In Malaysia, the water quality

of river is monitored by the Department of Environment (DOE) by using water quality index (WQI). The degree of pollution of the river is classified into 5 categories which is class I, II, III, IV and V. These classes are classified based on few parameters, namely ammoniacal nitrogen ($\text{NH}_3\text{-N}$), chemical oxygen demand (COD), biochemical oxygen demand (BOD), dissolved oxygen (DO), pH and total suspended solid (TSS). The details of the classification are tabulated in Table 2.1 below. The water which has WQI within the range of 81 – 100, 60 – 80 and 0 – 59 are considered clean, slightly polluted, and polluted respectively (Huang, et al., 2015). Table 2.2 below illustrates the uses of different classes of WQI. From 477 rivers monitored in 2017, 46 % were clean, 43 % were slightly polluted and 11% were polluted. The overall quality status of the monitored rivers from year 2008 to year 2017 are illustrated in Figure 2.1.

Table 2.1: Classification of River Water Quality (Lee Goi, 2020)

Parameter	Unit	Class				
		I	II	III	IV	V
NH₃-N	mg/L	<0.1	0.1-0.3	0.3-0.9	0.9-2.7	>2.7
BOD	mg/L	<1	1-3	3-6	6-12	>12
COD	mg/L	<10	10-25	25-50	50-100	>100
DO	mg/L	>7	5-7	3-5	1-3	<1
pH	-	>7	6-7	5-6	<5	-
TSS	mg/L	<25	25-50	50-150	150-300	>300
WQI		<92.7	76.5-92.7	51.9-76.5	31.0-51.9	<31.0

Table 2.2: Uses of Water Based on Different WQI (Huang, et al., 2015)

Class	Uses
I	Natural environment conservation. Water Supply I – Practically no treatment required Fishery I – Very sensitive aquatic species
IIA	Water Supply II – Conventional treatment required
IIB	Fishery II – Sensitive aquatic species Recreational use body contact
III	Water Supply III – Treatment required extensively Fishery III – Common, of economic value and tolerant species; livestock drinking
IV	Irrigation
V	None of the above

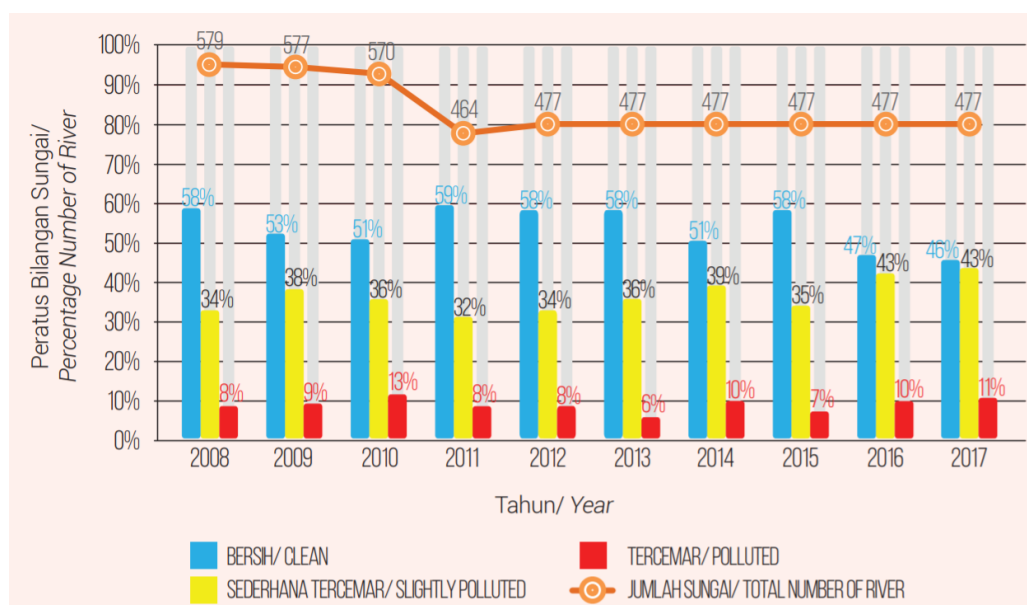


Figure 2.1: Overall Quality Status of Rivers from Year 2008 to 2017 in Malaysia (DOE, 2017)

As reported by UN-Water (2020), the water usage had increased by six times over the last ten years and still rising by about 1 % every year. Due to the climate change as well as increasing frequency of the extreme events such as storms, floods, droughts, more countries will be affected by the situation

that water supply is not sufficient. The risk of water pollution and pathogen contamination will increase due to floods or droughts.

Wastewater treatment and sewage management become an arising concern in developing countries due to the presence of bacteria and viruses carrier. Due to the water shortage problem, the community started to search for new and effective water treatment process to disinfect wastewater (La Obra Jiménez, et al., 2020). It is very crucial to employ effective disinfection method to microbes by destroying their biological structure so that they do not have to ability to grow in water anymore. Many analytical methods are developed to monitor the contaminations of microbes in water. One of the newly developed technologies in investigating molecular biology is known as quantitative polymerase chain reaction. This reaction enables the detection of antibiotic-resistance bacteria. Antibiotic-resistance bacteria is one the most concerned health issues in society. However, to study and monitor the contamination of microbes in water, culture-based methodologies are still most frequently used. Current approaches to monitor and identify bacteria in water is illustrated in Figure 2.2 below.

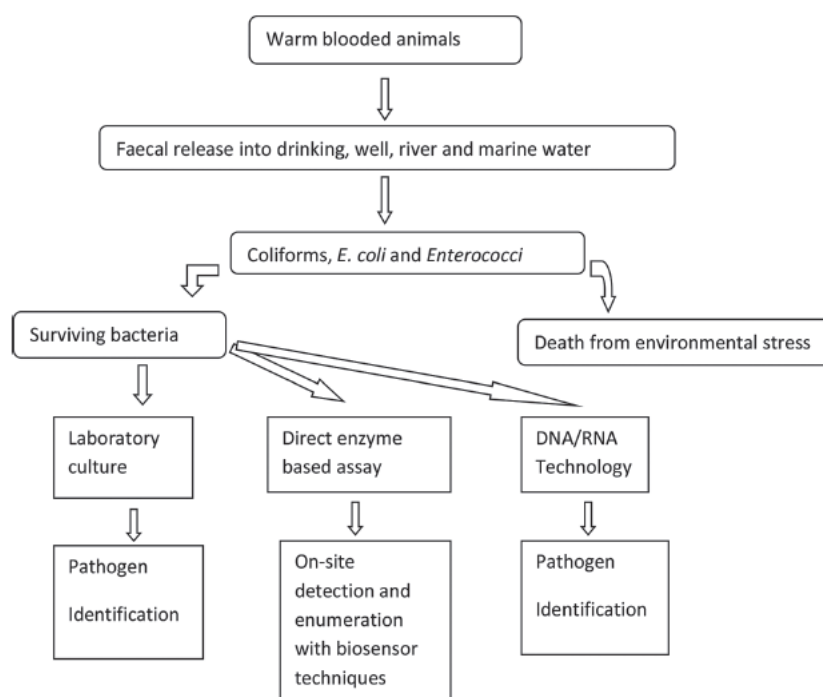


Figure 2.2: Current Approach to Monitor and Identify Bacteria (Nurliyana, et al., 2018)

2.2 *E. coli*

E. coli is classified in the gram-negative bacteria family and is grouped in Enterobacteriaceae. *E. coli* is known as the most infecting organisms within the group. *E. coli* is rod-shaped and non-spore forming with diameter and length of about 0.5 μm and between 1 to 3 μm , respectively (Nurliyana, et al., 2018). Figure 2.3 below shows an image of *E. coli* cell.

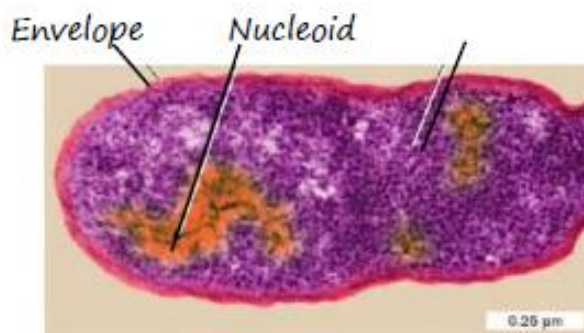


Figure 2.3: *E. coli* Cell (Nurliyana, et al., 2018)

Most of the *E. coli* strains colonize the gastrointestinal tract of humans and animals without causing any harm to them (Lim, Yoon and Hovde, 2012; Odonkor and Mahami, 2020). *E. coli* will be released into the environment through faeces. The presence of *E. coli* in food or water indicates recent faecal contamination or poor sanitation conditions in food processing facilities. There are a lot of pathotypes elements in water, and it is almost impossible to isolate them for testing. The requirement to test a large variety of pathogens will be time consuming and expensive as well (Nurliyana, et al., 2018). Hence, *E. coli* is often known as the indicator of faecal contamination in water (Price and Wildeboer, 2017; Nurliyana, et al., 2018; Odonkor and Mahami, 2020) and it can be tested to detect the water quality.

It is very important to monitor the amount of *E. coli* bacteria in water. *E. coli* will become pathogenic by obtaining virulence factors through plasmids, transposons and so on (Lim, Yoon and Hovde, 2012). *E. coli* infection becomes a vital health concern around the world. Even the total number of *E. coli* infections are lower than the enteric pathogens, the *E. coli* infection shows a much higher hospitalization and death rates (Lim, Yoon and Hovde, 2012). Even low amount of these pathogenic *E. coli* will possess a

significant risk such as gastroenteritis (Price and Wildeboer, 2017). Pathogenic *E. coli* possess risk to human as it can cause some diseases such as bloody diarrhoea, kidney failure and may cause death (Nurliyana, et al., 2018). Most of the *E. coli* infection cases start with non-bloody diarrhoea and healed without additional complication. However, some of the cases will progress to bloody diarrhoea or hemorrhagic colitis (HC). Some of these patients may even progress to life-threatening diseases such as hemolytic uremic syndrome (HUS) or thrombocytopenic purpura (TTP) (Lim, Yoon and Hovde, 2012).

To detect the presence of *E. coli* in environmental waters, laboratory-based methods usually involved. Conventionally, the number of bacteria present in water will be enumerated using microbiological tests such as multiple tube fermentation, plate count enumeration as well as membrane filtration method (Price and Wildeboer, 2017). Figure 2.4(a) and Figure 2.4(b) below illustrates the multiple tube fermentation method and plate count enumeration method. In multiple tube fermentation method, the total bacteria form will be enumerated based on the theory of dilution using most probable number. The sample will be diluted into few fermentation tubes. The presence of gas in the dilution tube indicates bacteria present in water. Plate count enumeration method is another method similar to multiple tube fermentation, but the number of *E. coli* cell can be approximated more easily. This is because a lot of tubes are required in the multiple tube fermentation method, but the *E. coli* cell are spread evenly one the plate in plate count enumeration method. In membrane filtration method, the water sample will be filtered to trap the bacteria and the bacteria will be cultured in agar. After incubation, the number of *E. coli* colonies will be calculated using plate count enumeration method (Nurliyana, et al., 2018). However, these methods become less preferable due to time consuming and the requirement of microbiological expert to perform the culture of bacteria to get an accurate result.

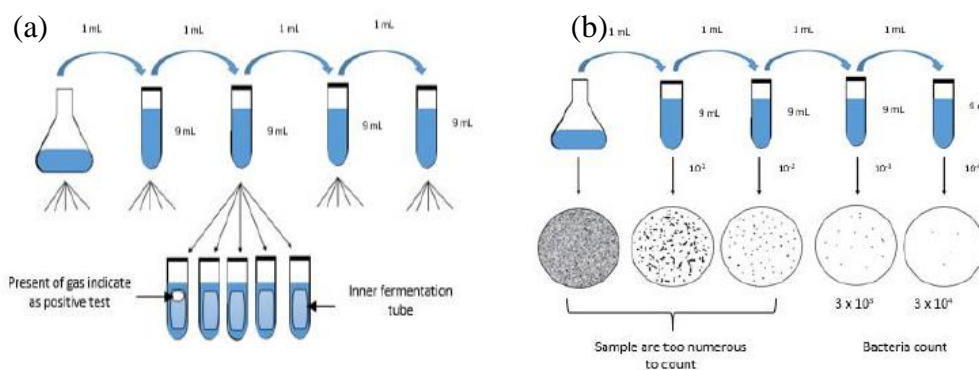


Figure 2.4: (a) Multiple Tube Fermentation Method. (b) Plate Count Enumeration Method (Nurliyana, et al., 2018)

In Malaysia, the prevalence of *E. coli* ranged from 22.6% to 88.0% (Frederick, 2011). However, most studies of prevalence of *E. coli* concentrated in beef samples. *E. coli* had been the headlines due to the outbreak of food poisoning of twenty athletes at Terengganu in year 2012 (New, et al., 2017). *E. coli* can survive in water and it will be transmitted when the contaminated water is used for cleaning and food processing. However, it is very hard to categorize the type of foodborne pathogens that cause severe risk to communities in Malaysia because few data are available.

Al-Badaii and Shuhaimi-Othman (2015) studied the *E. coli* contamination of Semenyih River at Kuala Lumpur Malaysia. Eight sampling points were chosen across the river. It was found that *E. coli* population ranged from 246 CFU/100 mL and 160500 CFU/100 mL. Sampling point 1 and 7 had the lowest and highest *E. coli* population respectively. Serious contamination occurred at the river especially from sampling point 3 onwards. Urban activities near sampling point downstream had contributed to the high *E. coli* population. At sampling point 1, the river had been classified as class I based on WQI. Sampling point 2 and 3 were classified as class II while the rest of the sampling points were class III. The prevalence of *E. coli* was studied along Kelantan River and its adjacent coastal water at 15 sampling points (Bong, et al., 2020). The *E. coli* population was found to be ranging from 31 CFU/ 100 mL to 160000 CFU/ 100 mL. The *E. coli* population had exceeded the allowable limit of 10 CFU/ 100 mL for class II river in Malaysia. Fecal contamination was found, mainly from the untreated sewage discharged from

housing areas. The use of traditional septic tank which the sewage only treated partially before discharged had contributed to this fecal contamination. *E. coli* can adapt to the stress of the environment very quickly. Hence, the prevalence of *E. coli* possessed health risks to the locals who consumed the water directly and indirectly. Various studies had shown that the rivers in Malaysia was contaminated by *E. coli* and exceeded the threshold limit for national water quality standers (NWQS) for Malaysia rivers (Al-Badaii and Shuhaimi-Othman, 2015; Othman, Sakai and Chowdhury, 2015; Bong, et al., 2020). Hence, it is very important to perform immediate action to ensure that the water is treated in an efficient way.

2.3 Methods of Bacteria Disinfection

2.3.1 Chemical Disinfection

Disinfection of bacteria by chemical means applying chemical disinfectants directly to remove the pathogens in wastewater. The typical way of chemical disinfections includes injecting ozone, chlorine, and chlorine dioxide into the wastewater stream directly. Chlorine gas or calcium hypochlorite in solid and aqueous form will be used as chemical disinfectant (Saqib Ishaq, Afsheen and Khan, 2019). Figure 2.5 below showed the set up of the disinfection using chlorine gas. Chlorine gas is known as the most effective disinfectants as it can remove nearly all pathogens in water. It is also relatively cheaper as compared to other physical disinfectant such as ultraviolet light. The chlorine that is leftover after the chlorination process can be reused. Meanwhile, the effectiveness of the leftover chlorine may be further evaluated. Even though chlorination is used widely in treating wastewater in large-scale, it has some limitations. The water treated using chlorination will have a different taste or odour. Moreover, chlorine is a volatile gas which may cause hazards if it is not handled properly. The by-products that formed during chlorination such as trihalomethanes (THMs) may be harmful to the end users since THMs is known to be mutagenic and carcinogenic (Mukherjee and De, 2015).

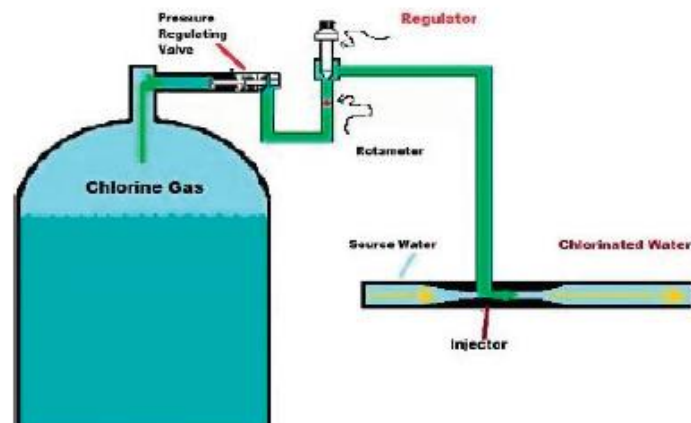


Figure 2.5: Disinfection by Chlorine Gas (Saqib Ishaq, Afsheen and Khan, 2019)

Ozone is an unstable form of oxygen where a new molecule formed from three molecules. Highly reactive radicals are formed when ozone decomposes rapidly. Ozone is used in wastewater treatment industry as an oxidant due to its higher oxidation potential than chlorine. In terms of oxidation capacity, only hydroxyl radical and fluoride is stronger than ozone. Ozone will oxidize and lyse the cell wall of the microorganisms. It works in a different way from chlorination, which diffuse through the cell wall and destroy the microorganisms. Figure 2.6 below demonstrated the configuration of the disinfection using ozone. In disinfection using ozone, no chemicals required and only a short reaction time required to kill the microbes in water. Ozone not only can remove all organic matters in wastewater, it can remove algae as well. Basically, ozone can be produced from dry and clean ambient air or pure oxygen. Ozone is generated when the stream of gas passed through an electric field. During the disinfection process, ozone will be dissolved in water to kill the microbes. Since ozone is unstable in atmospheric pressure, onsite generation is essential. Ozone is also known as one of the greenhouse gases and it is toxic in high concentration.

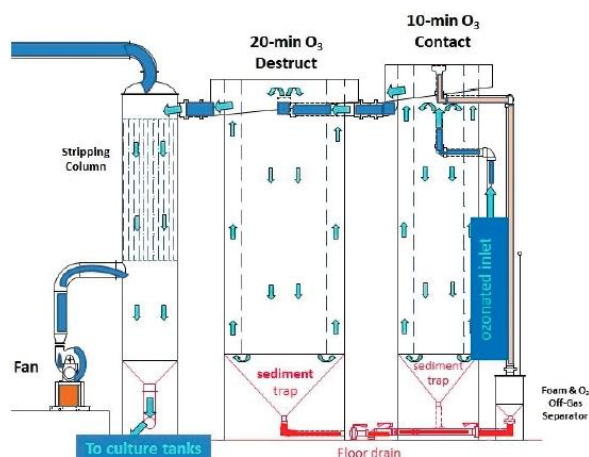


Figure 2.6: Ozone Contacting Method (Saqib Ishaq, Afsheen and Khan, 2019)

2.3.2 Physical Disinfection

Disinfection of bacteria using physical method simply means no chemical will be involved during the disinfection process. The bacteria will be destroyed by causing damage to their structure using physical method to inhibit their microbial function. Since chemical is not added during disinfection process, the physical agents will generate reactive chemical species to disinfect the pathogens in water (Linden and Murphy, 2017). One way of doing this is to degrade the physical properties of microorganisms while the other way is to change the water chemistry that leads to degradation. At large scale disinfection, physical method will be more cost and time effective.

Heat is known as one of the most traditional way of disinfection. Heat can be supplied by using open flame from fuels, solar and microwave heating. Heat disinfection is known to be more effective to in deactivating bacteria as compared to viruses. The enzymes and proteins within the cell of microbes will be denatured by heat sterilization and hence lead to cell death. In addition, dry heat can cause dehydration and cell lysis of microbes. The working principal of heat disinfection is to heat the water up to the minimum deactivation temperature then held the matrix at that temperature for constant time. Normally high temperature will require shorter disinfection time as compared to low temperature. The main advantage of disinfection using heat is complete disinfection can be achieved, easy to conduct as no tools are required and will not change the water chemistry. However, disinfection using heat will

require high energy and inefficient in large scale processes (Linden and Murphy, 2017).

As an alternative technology to chemical disinfection, ultraviolet (UV) radiation treatment is known as one of the effective method in deactivating bacteria and viruses in water (Matsumoto, Tatsuno and Hasegawa, 2019). UV irradiation disinfects microbes by destroying their nucleic acids and intercellular proteins in the form of photons. The replication of nucleic acid is hindered leading to deactivation of bacteria. The most effective wavelength of UV irradiation reported to be in the range of 200 to 280 nm with peak absorbance at 260 nm. As shown in Figure 2.7, UV disinfection requires only simple set up to achieve high efficiency of disinfection rate.

UV light disinfection is applicable to all type of waterborne pathogens. It is cost effective, does not change water quality and requires short disinfection time only. UV disinfection will not affect by parameters such as temperature, pH or organic matters present in water. Last but not least, there are not any harmful by products to the environment and human due to the small footprint of UV disinfection (Saqib Ishaq, Afsheen and Khan, 2019). However, there are some disadvantages of UV disinfection such as there will not be any disinfectant left, high energy requirement to generate the ultraviolet light and interference caused by excessive particles.

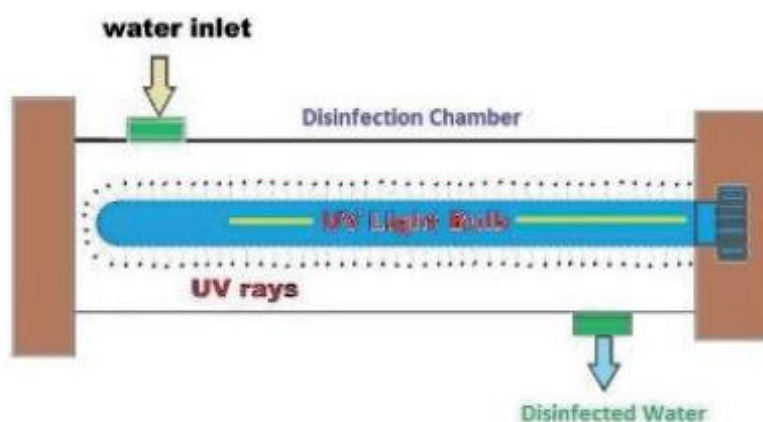


Figure 2.7: UV Disinfection Method (Saqib Ishaq, Afsheen and Khan, 2019)

2.3.3 Advanced Oxidation Processes (AOPs)

Recently, AOPs has emerged as a promising wastewater purification method due to its efficiency in oxidation and strong practicality (Liu, et al., 2018). AOPs is employed to replace the conventional method of bacterial disinfection to completely remove high levels of pollutants. Reactive oxygen species will be generated in AOPs to disinfect bacteria or virus. The main oxidizing agents used in AOPs is $\cdot\text{OH}$ and sulfate radicals. The radicals will be able to inactivate pollutants in wastewater then transform to lower or non-toxic products (Deng and Zhao, 2015).

The main type of AOPs reaction is $\cdot\text{OH}$ based AOPs which can be further classified to ozone-based AOPs, UV-based AOPs and Fenton-related AOPs. $\cdot\text{OH}$ are required to pair with other oxidizing agents such as H_2O_2 and O_3 , irradiation such as UV and catalysts such as Fe^{2+} due to its short lifetime. In ozone-bases AOPs, $\cdot\text{OH}$ can be produced mainly from three ways, which is ozonation, peroxone ($\text{O}_3/\text{H}_2\text{O}_2$) system and photolysis of H_2O_2 . In UV-based AOPs, photons produced from catalysts or oxidants will generate $\cdot\text{OH}$. Semiconductors such as TiO_2 or ZnO or Fenton catalysts can be used to drive the AOPs (Fernández, et al., 2020). Similar to ozone based AOPs, $\cdot\text{OH}$ can be produced under UV irradiation in the presence of O_3 and H_2O_2 but in a higher amount. For example, two $\cdot\text{OH}$ can be produced in the presence of UV irradiation from H_2O_2 whereas only one $\cdot\text{OH}$ will be formed without UV irradiation (Deng and Zhao, 2015). In Fenton process, $\cdot\text{OH}$ will be produced in the presence of H_2O_2 and iron.

Photocatalysis is one of the AOPs process which satisfy the principle of green chemistry. Photocatalysis is the acceleration of photoreaction in existence of catalysts. Many researches are done to design environmental friendly and efficient photocatalysts. There are two types of catalysts used in photocatalysis which is heterogenous and homogenous. In photocatalysis process, organic pollutants are degraded by UV visible light or solar energy into inorganic ions, carbon dioxide and water (Singh, et al., 2019). No harmful by product will be formed from this oxidation or reduction process of organic pollutants. A wide range of photocatalytic materials can be used such as metallic semiconductor, metal sulfide and noble metals. The electronic structure of the semiconductors is responsible for the photocatalysis process.

The heterogenous photocatalysis is advantageous over homogenous due to its stability, lower cost, and non-selective catalytic activity. It can be applied in ambient temperature and pressure as well. The major disadvantage of photocatalysis is the poor absorption of visible light and easily combine with electron-hole pair. Figure 2.8 below show the mechanism of the photocatalysis using semiconductor as catalysts in disinfection process.

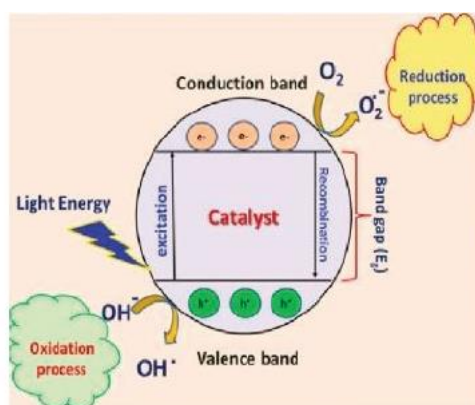


Figure 2.8: Schematic Diagram of Photocatalysis using Semiconductor (Saqib Ishaq, Afsheen and Khan, 2019)

2.4 Fenton Reaction

Fenton process was discovered in 1894 when tartaric acid is oxidized to dihydroxy maleic acid by using oxidizing agents and iron (O'Dowd and Pillai, 2020). In the nineties, this process is frequently used to oxidize the organic compounds in water. When the H_2O_2 is decomposed by the catalyst, which is iron, $\cdot\text{OH}$ will be produced. This $\cdot\text{OH}$ will act as the oxidizing agent in Fenton reaction. The mechanism of Fenton process is illustrated in Figure 2.9. $\cdot\text{OH}$ is a very strong oxidizing agent that it will break down organic compounds and kill microorganisms in water. $\cdot\text{OH}$ is the second strongest oxidizing agent after fluoride, which drive the oxidative capacity of Fenton reaction (Polo-López, Nahim-Granados and Fernández-Ibáñez, 2018). Hence Fenton process is known to be an effective process to disinfect bacterial through the reaction of Fe^{2+} and H_2O_2 (Tong, et al., 2019). Harmless substances such as H_2O and CO_2 will be formed when the organic compounds are broken down and microorganisms are killed. Fe^{3+} from the Fenton process can be recycled to from $\cdot\text{OH}$. Fe^{3+} can react with H_2O_2 to form $\cdot\text{OH}$. However, it has a very low

efficiency due to its low kinetics. Fenton process which is applied using light or UV is known as photo-Fenton process.

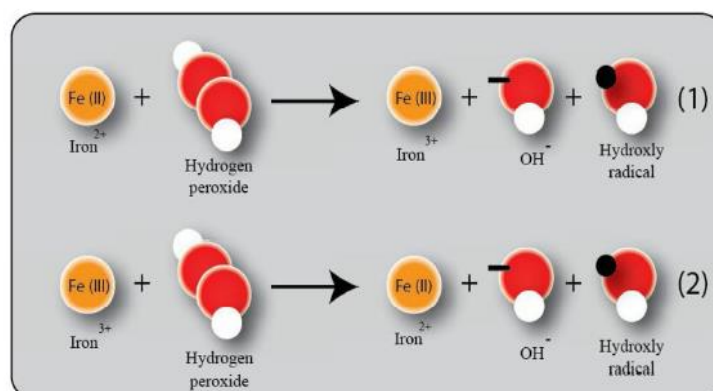


Figure 2.9: Mechanism of Fenton Process (O'Dowd and Pillai, 2020)

There are two types of Fenton process, which includes homogenous and heterogenous Fenton reaction. Homogenous Fenton process involves catalysts and substrate in the same phase. It has a higher kinetics than the heterogenous Fenton process. However, iron residues may be produced and required cleaning action after the process. This process will be more expensive due to the requirement of cleaning and disposing of iron residues. Heterogenous Fenton process involves catalysts and substrate in a different phase. For example, Fe_3O_4 which is a solid is placed inside water. The iron will be suspended inside the liquid by using a structure to support it. By using heterogenous Fenton process, the large surface area of the catalysts will enable a more efficient reaction on the surface. However, the iron catalysts are not soluble in the water leading to formation of iron sludge. Moreover, heterogenous Fenton reaction is known to be more environmental friendly process because they require lower concentration of Fenton reagents during the process. The catalyst can also be easily extracted and reused.

Cruz, et al. (2017) found out that the heterogenous Fenton process will become more homogenous when the pH of the solution goes lower than the pKa of the alginate support. Some of the iron will be released to the solution when the pH falls lower than 3.0. Cruz, et al. (2017) also stated that the contribution of the homogenous process will be greater in pH value of 5.0 or less.

2.4.1 Iron Oxide (Fe₃O₄)

Nanoparticles exhibit great potential in advanced wastewater treatment industry due to its large specific surface area and high reactivity (Li, et al., 2018). Fe₃O₄ is one of the most found metal oxides and can easily manufactured at industrial scale using ambient conditions. Researchers have much interest in magnetic Fe₃O₄ because it can be applied widely in industries such as catalysis, pigments, biomedical, magnetic resonance image and so on (Singh, et al., 2019). Magnetic Fe₃O₄ will be fabricated in different sizes and morphology due to their significance in environmental research. Li, et al., (2016) reported that the size of magnetic Fe₃O₄ has to be less than 20 nm to exhibit superparamagnetic properties. Surface of magnetic Fe₃O₄ can be easily modified by adding atomic layers of organic or inorganic surfaces. These surfaces can be further functionalized by using different bioactive molecules (Businova, et al., 2011b).

In addition, Fe₃O₄ gained a lot of attention in the field of photocatalysis due to its magnetic properties, high absorbing properties (Li, et al., 2018), environmental friendly nature and stability (Singh, et al., 2019). By using external magnetic source, Fe₃O₄ nanoparticles can be easily separated from the suspension of reaction (Singh, et al., 2019; Tong, et al., 2019). The use of Fe₃O₄ nanoparticles can eliminate the use of filtration and centrifugation to extract the catalysts after the reaction. Moreover, Fe₃O₄ nanoparticles also show good redox recycling in the presence of H₂O₂ and hence can be a good catalyst in Fenton reaction. Fe₃O₄ can be an excellent alternative to replace the conventional iron salt catalysts in Fenton reaction because there will not be iron sludge produced (La Obra Jiménez, et al., 2020). In Fenton process, the amount of reagents such as Fe₃O₄ and H₂O₂ will be used to increase the amount of hydroxyl radical products. To improve the redox recycling of Fe³⁺/Fe²⁺, a lot of co-catalysts will be used to improve the generation of hydroxyl radicals (Liu, et al., 2018; Tong, et al., 2019).

To synthesis Fe₃O₄ nanoparticles, two main techniques can be employed, which include co-precipitation and thermal decomposition. Pyrolysis, hydrothermal reaction and sol-gel synthesis is the less commonly used method for synthesizing polymer coated Fe₃O₄ nanoparticles. For co-precipitation method, stoichiometric amount of aqueous Fe²⁺ and Fe³⁺ salts

will be used to control precipitation of Fe_3O_4 . At the same time, this process is done by using stabilizing agents and alkaline solution in non-oxidative situation. Magnetite will be synthesized from this reaction. This is the most promising and easy way to synthesis Fe_3O_4 nanoparticles in a large quantity with high purity (Businova, et al., 2011b). However, Fe_3O_4 nanoparticles produced from this way will have a larger range of particles sizes. This shortcoming can be overcome by controlling reaction temperature, stirring rate (Businova, et al., 2011b), ferrous salt concentration, stabilizing agents, time of reaction and pH (Barrow, et al., 2015). Reactants will undergo thermal decomposition in the presence of organic solvents containing surfactants of high boiling point. A narrower particle size range and crystallinity can be obtained by using thermal decomposition method. This can be done by changing the ratio of reagents used during reaction.

2.4.2 Polydimethyldiallyl ammonium chloride (PDDA) coated Fe_3O_4

The surface of the coating of Fe_3O_4 nanoparticles will be a key aspect that affect the colloidal stability, toxicity and magnetism of the nanoparticles (Barrow, et al., 2015). Fe_3O_4 nanoparticles that is coated with polymers or supported by matrices can prevent the iron ions from leaking to the treated water (Fernández, et al., 2020). Polymers are often used as coating for the Fe_3O_4 nanoparticles because it can enhance the colloidal stability in aqueous condition and prevent the iron core from degradation. The colloidal stability of polymer coating is given through electrostatic or steric repulsion. The polymer can be coated on Fe_3O_4 nanoparticles by using living radical polymerization techniques. Two types of polymerization process including atom transfer radical as well as reversible addition fragmentation chain transfer can be used.

Besides, there are many alternative ways to coat polymer on Fe_3O_4 core as well. The possible coating mode includes attach the polymer end group directly to the core, grafting of polymer on the core, diblock copolymer grafted on core, polymer with grafting groups wrapped around the core, interaction between opposite charge of core and polymer and interactions between amphiphilic polymer with hydrophobic Fe_3O_4 cores (Barrow, et al., 2015). The most favourable pathway to produce polymer coated Fe_3O_4 is the direct attachment to Fe-OH group of the nanoparticles. Polymer coated Fe_3O_4

synthesized this way can have colloidal stability for a longer time, owing to the permanent covalent bond between them.

The Fe_3O_4 isolated with matrices can give a uniform size and well dispersion. Polymers with different functional groups including hydroxyl, carboxyl, styrene, carboxylate and vinyl alcohol groups have been widely used in coating of magnetic Fe_3O_4 nanoparticles (Businova, et al., 2011b). PDDA is a water soluble cationic polyelectrolyte which used in different type of industries include biological, food, wastewater treatment, medical and so on (Li, et al., 2016). PDDA, which is positively charged, can enhance the dispersion of negatively charged particles by electrostatic interaction. Owing to the high surface energy, Fe_3O_4 nanoparticles contain a lot of -OH groups when dispersed in water. Hence, PDDA coating is expected to reduce the aggregation of the Fe_3O_4 nanoparticles.

2.5 Characterization Study

2.5.1 Scanning Electron Microscopy (SEM)

A SEM is a strong magnification tool that utilize the same basic principles as light microscope to obtain the topographical, morphological, and compositional information of a sample. The thing that SEM differs with light microscope is that instead of photons, beams of high-energy electrons are focused to magnify the sample. The basic configuration of a SEM is illustrated in Figure 2.10.

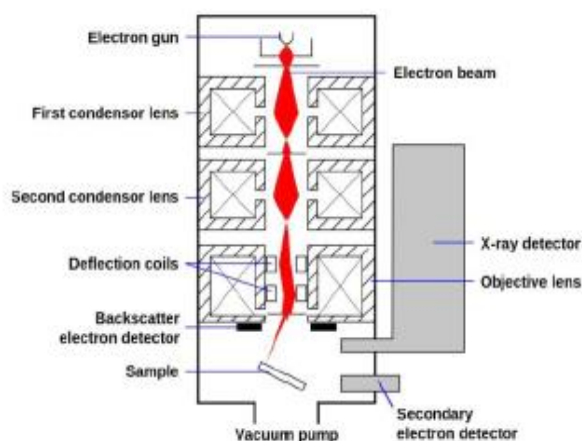


Figure 2.10: Configurations of SEM (Choudhary and Priyanka, 2017)

In SEM, the electron gun will generate a beam of high-energy electrons into the chamber onto a series of electromagnetic lenses. The electromagnetic lenses will be adjusted in a way that they will be focused onto the sample on the other side of the chamber. Pre-treatment of samples are usually required before placing into the sample holder. The two commonly used pre-treatment methods are sputter coating of non-conductive samples and dehydration of biological samples.

The sample will be handled in low pressure inside the chamber. The incident electron beams that come in contact with the sample will cause the reflect and release of electrons from the surface of the sample. The scattering electrons will provide information of the size, shape, texture and composition of the sample. A series of detectors will be inside the chamber to differentiate the scattered electrons, which includes secondary electrons, backscattered electrons, and X-rays. These scattered electrons provide information about sample such as the compositional data, topographic and so on.

SEM provides three dimensional black and white images. The magnification of the image can be up to 10 nm. It is very easy to operate SEM and the result can be obtained in just less than 5 min. However, SEM is a very large instrument, and it is very costly. SEM should be placed in an area which is free from any possible interference, including electric, magnetic as well as vibration. Moreover, SEM is limited to solid and inorganic samples with small sizes which can be fitted into the sample holder (Choudhary and Priyanka, 2017).

2.5.2 Transmission Electron Microscopy (TEM)

TEM also utilizes energetic electron beams to study the morphological, compositional, and crystallographic information of the sample. TEM is known as the most powerful microscopes as it abled to produce high resolution and two-dimensional images up to a magnification of 1 nm (Priyanka and Choudhary, 2018). The major difference between SEM and TEM is that TEM uses transmitted electrons instead of reflected electrons to create the image.

In TEM, the electron beams generated will be focused inside the column. The electron beam is focused directly onto the specimen placed on sample holder. The specimen used for TEM analysis is usually around 100 nm

so that the electron beams able to pass through. The schematic diagram of TEM is illustrated in Figure 2.11 below.

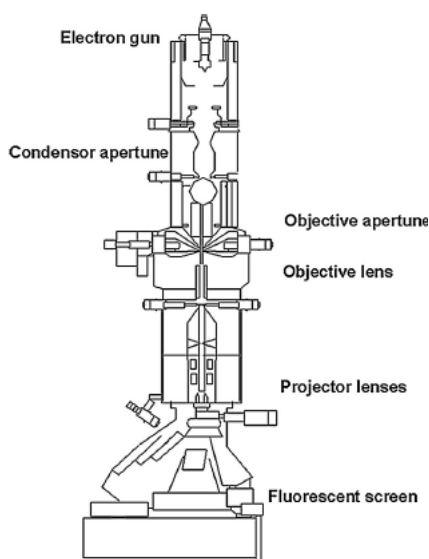


Figure 2.11: Schematic Diagram of TEM (Tang and Yang, 2017)

TEM is advantageous over the other characterization method due to its power of magnification up to one million times or more. High quality and detailed image regarding the structure, shape and size of the sample can be obtained. TEM can be easily operated with proper training. However, TEM has its own limitations which special housing and maintenance are required and TEM equipment is very large as well as costly. Moreover, the sample preparation is tedious, and sample may be affected during preparation leading to inaccuracy of the analysis. Similar to SEM, TEM has to be placed in an area where it is not exposed to any vibration and electromagnetic field.

2.5.3 Fourier Transform Infrared Spectroscopy (FTIR)

Infrared (IR) spectroscopy is commonly used to identify and analyse the structure of a chemical compound (Ismail, van de Voort and Sedman, 2007). The peaks formed during the excitation of vibrational modes of the sample will represent the chemical bonds and functional groups present in the molecules. Hence, IR spectrum is also known to be the fingerprint of the molecules due to this unique physical property. Table 2.1 below shows some absorption bands of some common functional groups.

Table 2.1: Absorption Bands of Common Functional Groups (Guerrero-Pérez and Patience, 2019)

Functional Group	Absorption Bands (cm⁻¹)
Alcohol O-H stretch	3550-3200
Water O-H stretch	3700-3100
Carboxylic acid O-H stretch	3000-2500
Alkyl C-H stretch	2950-2850
Alkenyl C-H stretch	3100-3010
Alkenyl C=H stretch	1680-1620
Alkynyl C-H stretch	≈3300
Alkynyl C≡H stretch	2260-2100
Aromatic C-H stretch	≈3030
Aromatic C-H bending	860-680
Aromatic C=C bending	1700-1500
Nitrile C≡N stretch	2260-2220
N-H stretch	3500-3350
Aldehyde C=O	1740-1715
Ester C=O	1740-1715
NO_x stretch	1600
C-O-C stretch	1250-1050

FTIR is a more favourable method than the conventional IR spectroscopy. When IR spectrum is passed through a sample, a portion of the radiation will be absorbed while another portion of the radiation will be transmitted. The molecular structure of the sample will be revealed through the signal collected. Fourier transform gives spectra which can be used to identify the molecules. Molecules with different molecular structures will produce different spectrums. There are four main types of FTIR sampling techniques which includes transmission (TIR), attenuated total reflection (ATR), specular reflection (RAIRS) and diffuse reflection (DRIFTS) as shown in Figure 2.12.

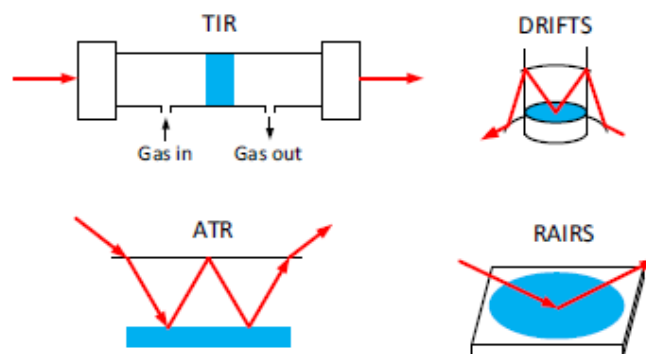


Figure 2.12: Different Types of FTIR (Guerrero-Pérez and Patience, 2019)

ATR-FTIR is commonly used in measuring the spectra of solids and liquid samples. The sample to be analysed will be placed onto the internal reflection element in the equipment. Infrared beam will be directed at an angle larger than the critical angle where internal reflection takes place (Schuttlefield and Grassian, 2008). The principle of ATR-FTIR is illustrated in Figure 2.13 where a high refractive index medium, such as ZnSe is used as an internal reflection element.

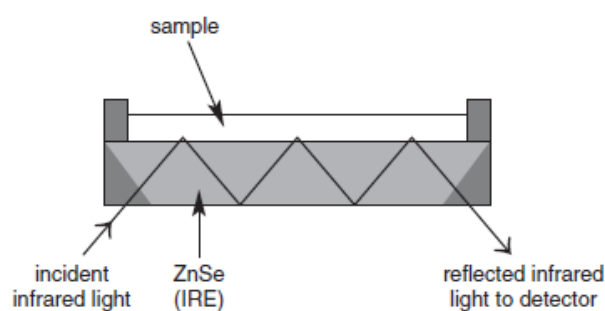


Figure 2.13: Pictorial Representation of ATR-FTIR (Schuttlefield and Grassian, 2008)

In ATR-FTIR, modified Beer-Lambert law (Equation 2.3) can be used to describe the relationship between the concentration, c , and the absorbance, A . The effective path length, b' is described in Equation 2.1 whereas the penetration depth per reflection, d_p is described in Equation 2.2.

$$b' = Nd_p \quad (2.1)$$

where

b' = effective path length

N = number of reflections

d_p = penetration depth per reflection

$$d_p = \frac{\lambda_1}{2\pi n_1 [\sin^2 \theta - n_{21}^2]^{\frac{1}{2}}} \quad (2.2)$$

where

n_1 = index of refraction of the internal reflection element

n_2 = index of refraction of the sample medium exposed to crystal

$$n_{21} = \frac{n_2}{n_1} = \frac{\lambda_{\text{vacuum}}}{n_1}$$

$$A = \epsilon cb' \quad (2.3)$$

where

A = absorbance

ϵ = molar absorptivity

2.5.4 X-ray Diffraction (XRD)

XRD is a strong non-destructive technique to characterize crystalline materials. The crystal structure and atomic spacing can be studied based on the constructive interference of the monochromatic X-rays and the sample. The basic configuration of XRD is illustrated in Figure 2.14. The X-rays will be generated by a cathode ray tube. The X-rays are then filtered to become monochromatic radiation. The radiation is concentrated and directed towards the sample.

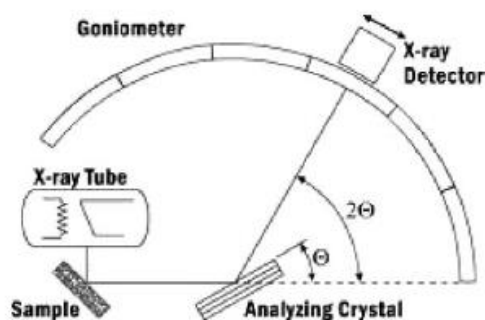


Figure 2.14: Schematic Diagram of XRD System (Bunaciu, Udriștioiu and Aboul-Enein, 2015)

The Bragg's law (Equation 2.4) can be used to describe the constructive interference due to the interaction between radiation and the sample.

$$n\lambda = 2d \sin \theta \quad (2.4)$$

where

n = integer

λ = wavelength of X-ray

d = interplanar spacing generating the diffraction

θ = angle of diffraction

The relationship between the wavelength of the electromagnetic diffraction and the diffraction angle as well as the lattice spacing of the crystalline sample can be described by using Equation 2.4 above. All the possible diffraction direction of the lattice can be obtained because the powdered samples are in a random orientation, when the sample is scanned at a range of 2θ angles.

By using XRD analysis, unknown sample can be identified in a very short time. The data generated by using XRD analysis requires relatively easy interpretation. The sample does not require complicated preparation before undergoing the analysis. However, XRD is more suitable for homogenous and single-phase material only. A standard reference file is required to identify the sample analysed (Bunaciu, Udriștioiu and Aboul-Enein, 2015).

2.5.5 Brunauer-Emmett-Teller (BET)

It is very important to measure the surface properties for a wide range of materials. One of the important surface properties is the surface area available for reactions. Surface area of a material can be increased by reducing particle size as well as making the material porous (Naderi, 2015).

There are few techniques in BET analysis including volumetric gas adsorption technique, gravimetric dynamic vapour sorption technique (DVS) and chromatographic adsorption technique (Naderi, 2015). In volumetric technique, the adsorbate gas, nitrogen will be admitted into the evacuated space at the top of the powdered sample. A defined equilibrium pressure, P of the gas will be given. Interfering effects of thermal diffusion can be avoided in this case since only pure adsorbate gas is used and no diluent gas is involved. DVS is a method to determine vapour sorption isotherms. A very accurate gravimetric system will give a clear representation of the adsorption and desorption of probe molecules. The differences between volumetric gas adsorption technique and DVS are tabulated in Table 2.2. Materials will behave according to temperatures. The operation of volumetric BET is limited since the experiments are to be carried out 77 K. To study the sorption under desired conditions, chromatographic adsorption technique is a good way.

Table 2.2: Comparison between Volumetric Gas Adsorption Technique and DVS (Naderi, 2015)

	Volumetric BET	Gravimetric BET
Adsorbing species	Nitrogen, argon, krypton	Liquid vapours at 300 K
Temperature	Low temperature (77 K)	Ambient temperature
Sample size	1 g	100 mg
Surface area	Given the surface area seen by small molecules	Given the surface area as seen by a real-world molecule
Experimental conditions	Low temperatures and vacuum	Ambient temperature and pressure

BET is an important analysis in the characterization because it can measure the specific surface area of the sample as well as the distribution of pore size. Specific surface area plays an important role in catalytic reaction because it will affect the rate of reaction. Basically the specific surface area of the sample will be obtained when a gas is adsorbed physically on the solid surface. Physical adsorption occurs in the presence of the weak intermolecular forces between the adsorbent surface area of sample and adsorbate gas. The analysis will be carried out in the temperature of liquid nitrogen to get measurable amounts of adsorption. The BET adsorption isotherm equation (Equation 2.5) will be used to explain the relationship between the amount of gas adsorbed and the pressure.

$$\frac{1}{\left[V_a \left(\frac{P_0}{P} - 1\right)\right]} = \frac{C - 1}{V_m C} \times \frac{P}{P_0} + \frac{1}{V_m C} \quad (2.5)$$

where

P = equilibrium partial vapor pressure of adsorbate gas at 77.4 K in Pascals

P_0 = saturated pressure of adsorbate gas in Pascals

V_a = volume of gas adsorbed at 273.15 K and 101.3 kPa in milliliters

V_m = volume of gas adsorbed to form monolayer in milliliters

C = dimensionless constant

2.5.6 Thermogravimetric Analysis (TGA)

TGA is a technique which is used to study the thermal stability of a substance. The mass of the substance will be monitored in terms of temperature and time. The substance will be heated or cooled at a constant rate to a pre-set temperature under controlled atmosphere by inert purge gas. The mass change of the substance in the furnace will be monitored and eventually thermogravimetric curve will be produced for analyse purpose. A thermogravimetric curve is a graph of mass against temperature and/or time (Gabbott, 2010). Nowadays, mainly compensation balances are used in TGA analysis. Even when mass changes during the analysis, the position of the sample will remain the same inside the furnace.

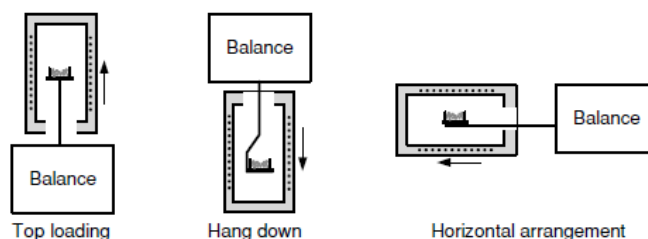


Figure 2.15: Thermobalances Design of TGA

There are three variations of TGA analysis which includes dynamic TGA, static TGA and quasistatic TGA. In dynamic TGA, temperature increases over time and the mass will be recorded at the same time. This will help to identify the amount of gas removed and at which temperature it occurs. In static TGA, temperature will be kept constant when mass is recorded. With this variation, the decomposition of a compound at a specified temperature can be observed and the material's ability to withstand certain temperature can be known. For quasistatic TGA, sample will be heated and held at different temperature intervals, until the mass stabilizes. This will help to observe the substances that are known to decompose in different ways at different temperatures. The way that they decompose can be characterized (Garcia-Herrera and Price, 2020).

One of the limitation of TGA is that it is not suitable for particles with larger size which is more than 50 mg (Saadatkah, et al., 2020). This is due to the heating rate is not fast enough to reach isothermal condition within the particles. This will cause deviation from the kinetic parameters. In thermogravimetry, the change in mass can relate to the extent of conversion as shown in Equation 2.6.

$$\alpha = \frac{W_0 - W(t)}{W_0 - W_\infty} \quad (2.6)$$

where

α = extent of conversion

$W(t)$ = mass of sample at time, t

W_0 = initial mass

W_∞ = residual mass

2.6 Reusability Test

In a report by Fernández, et al. (2020), the reusability of Fe_3O_4 was studied for 10 consecutive times. After each experiment, the nanoparticles will be separated from the suspension using magnet. The suspension will be removed, and fresh wastewater will be added to perform another disinfection cycle. It was stated that the catalysts showed a good performance for all the cycles for *E. coli* disinfection. However, it was stated that the possibility of the reusability of the Fe_3O_4 catalysts had not been studied in a real scale (Fernández, et al., 2020).

Apart from that, Tong, et al. (2019) investigated the reusability test of the Fenton-like reaction by using MoS_2 as co-catalyst in *E. coli* degradation for four cycles. First, the used materials were separated with magnet. The materials were then washed with ultrapure water and absolute ethanol, respectively. The materials were dried in vacuum before the next cycle. Tong, et al. (2019) proved that the reused materials showed a high disinfection performance for all the four cycles. In the fourth cycle, there were more than 99% of *E. coli* inactivation in 40 minutes.

One of the important elements in practical application is the reusability of the catalyst. In a study by Cruz, et al. (2017), the reusability of the catalysts were studied through four successive experiments with the initial condition as previous experiment for degradation of sulfamethoxazole. The catalysts were filtered after each experiment and washed with milliQ water. Every degradation had similar profile for each successive degradation, with only slight reduction observed for each successive run.

CHAPTER 3

METHODOLOGY

3.1 Framework for the Methodology of Literature Review

Literature review is an important tool to build up one's research on and correlate with one's knowledge, irrespective of discipline (Snyder, 2019). Literature review is also known as data collection tool, where one collects information relevant to the area of interest. Basically, literature review consists of tasks such as problem identification, data documentation, comprehensive interpretation of data and transferring the data collected to others. In literature review, data was collected in a formal way and be presented to others in comprehensive way (Onwuegbuzie and Frels, 2016).

Literature review can be done to study the background for an empirical research or as an independent piece of research which serve as a precious contribution on its own (Templier and Paré, 2015). The first type of literature review was the most common where a section in a journal was extracted to help researcher to understand the background of the topic. This project employed the second type of literature review where the review will serve as a standalone literature review. This will be a journal-length article which solely review the literatures related to the title proposed, without producing any empirical data.

As reported by Pillai N (2020), the main purposes of a literature review includes identification of data which existed in the research field, finding out the main ideas and theories of the research field, getting a context for the research, finding out relationships between the studies carried out by various researchers and identification of gaps between literature and current situation.

Figure 3.1 illustrates the overall flow chart to conduct a literature review. The detailed procedure will be explained in sub-sections below.

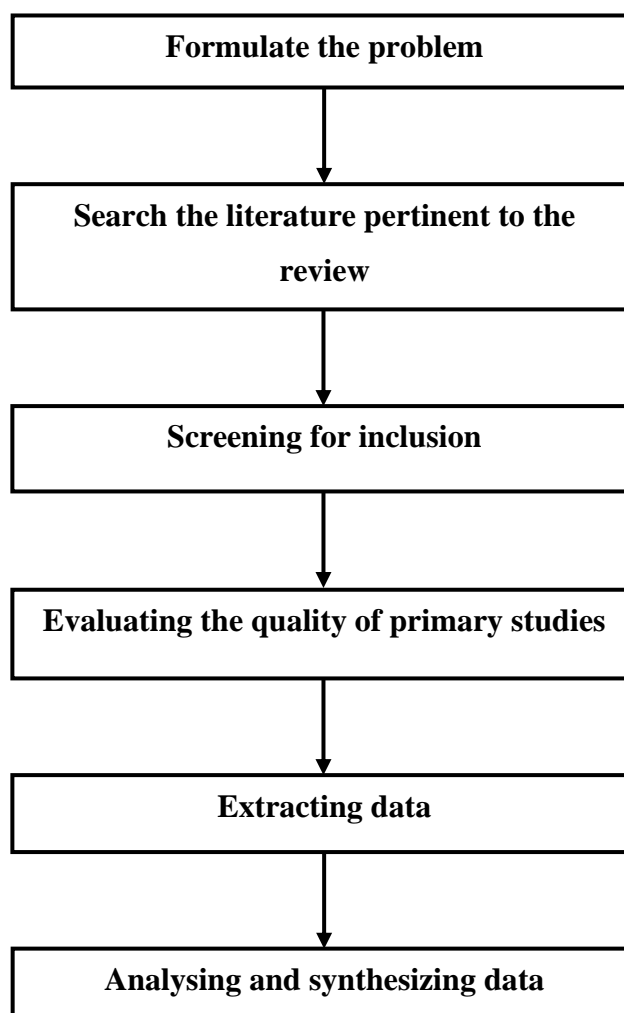


Figure 3.1: Overall Flowchart to Conduct Literature Review

3.1.1 Formulate the Problem

Before conducting the literature review, the first question to be asked was why the reason for the review to be conducted (Snyder, 2019). It is important to justify the need of the standalone review, as this helped to find out the type of information required and ease the selection of related literature (Templier and Paré, 2015).

Before conducting this review, discussion was carried out with project supervisor to have a better understanding of the background of this review. The background of the disinfection of bacteria via Fenton reaction and its applicability of this in water treatment field was discussed. After that, the problem statement and objectives of this review were formulated.

In short, the main problem of this review was to review the synthesis and characterization of PDDA coated Fe_3O_4 , effects of parameters affecting the degradation of *E. coli* using PDDA coated Fe_3O_4 via Fenton reaction as well as compare the effectiveness of this method with other disinfection methods. By conducting this review, more understanding was obtained in the effectiveness of PDDA coated Fe_3O_4 in degradation of *E. coli* as compared to other disinfection methods.

3.1.2 Search the Literature Pertinent to the Review

The next step was the start of the data collection phase. In this stage, all the related information was searched, and a range of information sources was identified. There were few approaches to search the literatures where one was to read each literature appearing in the search in full. This approach was beneficial to the researcher, but it was time consuming. Another approach was to conduct the review in stages where one read the abstract to make selection, and only those selected required readings in full-text articles (Snyder, 2019).

In this stage, keywords such as “Fenton reaction”, “disinfection of bacteria”, “PDDA coated Fe_3O_4 ” were used to search for literatures pertinent to the review. Main sources used in this review were from online journal websites or e-books. Some of the online sources used for this review to find out literatures pertinent to the review are listed below:

- i. UTAR Library E-Journals Database
(<https://library.utar.edu.my/>)
- ii. ScienceDirect (<https://www.sciencedirect.com/>)
- iii. Google Scholar (<https://scholar.google.com/>)
- iv. ResearchGate (<https://www.researchgate.net/>)
- v. SpringerLink (<https://link.springer.com/>)

3.1.3 Screening for Inclusion

After collecting all relevant literatures, a screening was required to be done to determine their relevance. This was to decide whether to include or exclude all the related literatures to ensure objectivity and reduce biases during the review. Full length articles were to be scanned to ensure that they fulfil the inclusion

criteria. Moreover, references of each articles were scanned to identify other possible relevant articles.

In this project, the obtained related literatures were grouped and organized by using Citavi software. This software eased the process of creating the citations and references, and the grouped literatures were screened and reviewed through more easily. In this stage, all the literatures found were screened through to obtain their year published. Only literatures published in recent years, especially in the latest 5 years (2016-2021) were reviewed while literatures published earlier than year 2010 were screened through another time to ensure that the data are not outdated. Figure 3.2 below shows the interface of Citavi software where the left column showed the lists of journals and the middle column showed the information such as author's name, year published as well as abstract of the journals.

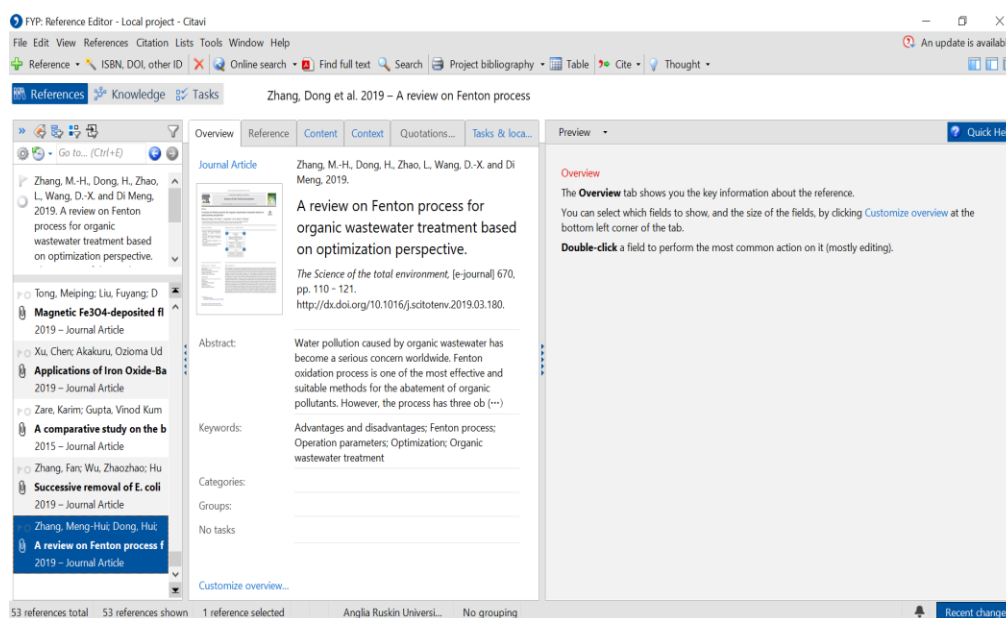


Figure 3.2: Citavi Program

3.1.4 Evaluating the Quality of Primary Studies

Other than screening for inclusion, the quality of all the related literatures were required to be evaluated. The quality of the design and methods used in the primary studies of the literatures must be accessed (Templier and Paré, 2015). Recognized methodological standards were required to be used in the literatures and only literatures from reputable sources were reviewed.

In this project, the evaluation of quality of the literatures were done at the same time with screening for inclusion. While screening for inclusion, the quality of the obtained literatures was evaluated. For example, given one literature was not from a reputable source but the contents met the inclusion criteria, the literature was not going to be reviewed. Literatures that were going to be reviewed must fulfil both criteria which is good quality and meet the inclusion criteria.

3.1.5 Extracting Data

The appropriate information that obtained from each literature selected must be standardized. Data extracted can be in the form of descriptive information, which describe type of study or findings. Data extracted can also be in the form of conceptualizations which consists of the theoretical idea (Snyder, 2019). The form of data extracted depended on the purpose of the research or the objective of the review. In this stage, the ideas of the content of the selected literatures were grouped into each category consisting of different topics. The significant findings of the literatures were identified and grouped into different categories. The information that was extracted include research design and methods, as well as the statistical results of the removal efficiency of bacteria of different disinfection methods.

3.1.6 Analysing and Synthesizing Data

The final step of a literature review will be categorize, summarize, organize and compare the findings extracted from the fundamental studies (Templier and Paré, 2015). The information extracted and compiled must be clear and allow good understanding to the others. The general trend of the studies can be made but the inconsistencies between the studies must be taken note. There are many types of literature reviews including narrative, theoretical, critical, descriptive, comprehensive, systemic as well as meta-analysis (Templier and Paré, 2015).

In this review, narrative review were employed where the research on the topic of interest that published formerly were summarized. The concept and theories behind the topic of interest, the method to carry out the research and the result of the research were focused on. Since the topic of interest of

this review was still under investigation, narrative review was a good method to compile and synthesize the existing literature to provide a complete overview to the readers. Narrative review will not propose conceptualizations or validate a theory. Moreover, narrative review also will not criticize a literature. Narrative review mainly acts as a bridge of huge amounts of published literatures to provide an overview for those who do not have time to track all the related literatures. After constructing a narrative review, the gaps of the current research which require further analysis or development can be identified (Templier and Paré, 2015).

CHAPTER 4

4.1 Synthesis of PDDA coated Fe₃O₄

Several ways are developed to functionalize the Fe₃O₄ using polymer, which include in situ coating and post-synthesis coating. In in-situ coating method, the conventional methods are mini/micro-emulsion polymerization and the sol-gel process to functionalize Fe₃O₄ using polymer. For emulsion polymerization, the polymer will cover the Fe₃O₄ which develops a capping layer to form a core-shell structure or matrix dispersed structure. The shortcomings of these direct surface modification are the difficulties in maintaining colloidal stability and controlling shell thickness.

Another common way to coat polymer on Fe₃O₄ is via post-synthesis coating where Fe₃O₄ is functionalized using one-pot route, self-assembly and heterogenous polymerization. One-pot route is one of the facile ways to coat polymer on Fe₃O₄. This synthesis method works by the physical adsorption and anchoring of functional groups on Fe₃O₄ surface, where a core-shell structure is formed. In addition, the polymer is coated on Fe₃O₄ using covalent bonding functional technique in which the cross-linking is made by hydrogen bonding and alkyl chain or carboxylic acid functionalized thiol. As mentioned by Wei Wu, et al. (2015), the presence of polymer layer on iron oxide nanoparticles (IONPs) may affect the magnetic properties. Hence, one must be careful while selecting the polymeric materials to coat on the IONPs.

Businova, et. al (2011) synthesized Fe₃O₄ nanoparticles by using coprecipitation method as well by using peristaltic pump. The materials used in the synthesis of Fe₃O₄ nanoparticles was Fe²⁺, Fe³⁺ salts solution and NaOH solution. 25 mL of 1.25 M of Fe²⁺ and Fe³⁺ salts solution was mixed with 25 mL of 5 M NaOH solution. The mixture was then added dropwise into 35 mL of water at 80 °C and stirred for 2 hr. 1.7 mL of 25 % tetramethylammonium hydroxide (TMAOH) was used to stabilize the Fe₃O₄ nanoparticles. Emulsion polymerization was used to coat polymer onto the prepared Fe₃O₄ nanoparticles at a high surfactant to monomer ratio. In the report of Businova, et. al (2011), 9.33 wt % of surfactant and 6.34 wt % of monomers were used. Apart from that, methyl methacrylate (MMA) and acrylic acid (AAc) were

used as comonomers at a weight ratio of 9 to 1. To coat the polymer onto Fe_3O_4 nanoparticles, 50 mL of 2 wt % of Fe_3O_4 nanoparticles suspension were ultrasonicated for 10 min before adding the surfactant. After that, the comonomer mixture was added and ultrasonicated for 40 min to ensure even dispersion. Potassium persulfate (KPS) was added as an initiator and the mixture was mixed in shaker at 65 °C for 1 day. Next, the polymer coated Fe_3O_4 was washed using water-methanol mixture to remove surfactant and unreacted monomers. The washed polymer coated Fe_3O_4 was washed again using pure water. After that, the polymer coated Fe_3O_4 was immersed in 0.1 M of sulphuric acid (H_2SO_4) to remove Fe_3O_4 nanoparticles which is not coated with polymer. Finally, polymer coated Fe_3O_4 can be obtained by washing with milli-Q water which had been deionized to remove all life forms.

In a report by Li, et al. (2016), Fe_3O_4 nanoparticles were synthesized by using initial materials, $\text{FeCl}_2 \cdot 4\text{H}_2\text{O}$ and $\text{FeCl}_3 \cdot 6\text{H}_2\text{O}$ using co-precipitation method. In co-precipitation method, alkaline precipitator was added drop-by-drop into the solution of initial materials under magnetic stirring. Excess alkaline precipitator was added to ensure that complete reaction occurred. Vacuum drying was then used to obtain the Fe_3O_4 nanoparticles. Next, 0.3 g of Fe_3O_4 nanoparticles was dispersed in 50 ml of distilled water to form an aqueous solution. 20 % of PDDA solution were added to the prepared aqueous solution. The mixture was ultrasonicated for 30 min to ensure homogenous mixture was obtained. Finally, the homogenous emulsion was dried and washed to obtain the Fe_3O_4 nanoparticles coated with PDDA.

In a study done by Al-Mashhadani and Hassen (2016), 20 mL of deoxygenated solution including 2.16 g of $\text{FeCl}_3 \cdot 6\text{H}_2\text{O}$, 0.8 g of $\text{FeCl}_2 \cdot 4\text{H}_2\text{O}$ and PDDA was heated gradually to 80 °C. Next, ammonium hydroxide (NH_4OH) was added rapidly into the heated solution. The mixture was then left stirring for 1 h. After stirring, the mixture was left to cool to room temperature before the PDDA coated Fe_3O_4 was recovered using magnet. Deionized water was used to wash the recovered PDDA coated Fe_3O_4 and the nanocomposites was dried at room temperature.

In the journal published by Qu, et al. (2015), 100 mL of solution containing 2.7031 g of $\text{FeCl}_3 \cdot 6\text{H}_2\text{O}$, 1.3901 g of $\text{FeCl}_2 \cdot 4\text{H}_2\text{O}$ and 1.0 % v/v of

PDDA was deoxygenated using vigorous stirring with nitrogen gas (N_2) for 20 min. The deoxygenated solution was then heated to 80 °C. 10 mL of 28 % ammonia aqueous solution was added drop-by-drop into the heated solution and the mixture was left for reaction to occur for 1 h at 80 °C. The mixture was left to cool to room temperature before the precipitate was collected by centrifugation. The collected precipitate was washed several times distilled water. The precipitate was dried using vacuum at 65 °C for 7 h to obtain the PDDA coated Fe_3O_4 .

To functionalized Fe_3O_4 using PDDA, the method on a published work by Low, Ng and Tan (2019) is reviewed. In this paper, 1000 mg of Fe_3O_4 was dispersed into 1 L of deionized water. The suspension was ultrasonicated for 1 h to break the aggregates. Next, PDDA solution of 0.02 g/mL was prepared and ultrasonicated for 1 h. After 1 h, the PDDA solution was kept in a water bath of 40 °C for 16 h. After that, the pH of both Fe_3O_4 suspension and PDDA solution was adjusted to 7.8. The Fe_3O_4 suspension was added dropwise into the PDDA solution after pH adjustment. The mixture of Fe_3O_4 suspension and PDDA solution was left in orbital shaker for 24 h to allow physisorption of the PDDA onto Fe_3O_4 . The PDDA coated Fe_3O_4 was separated from the suspension by using magnet bar. Finally, the PDDA coated Fe_3O_4 was washed with distilled water and dispersed in deionized water (Low, Ng and Tan, 2019).

As described by Yu, et. al (2010), to kick start the synthesis of PDDA coated Fe_3O_4 , 20 mL of solution containing 2.16 g of $FeCl_3 \cdot 6H_2O$, 0.8 g of $FeCl_2 \cdot 4H_2O$ and 1.0 % v/v of PDDA was deoxygenated under nitrogen atmosphere for 10 min. The deoxygenated solution was then heated to 80 °C. After that, 10 mL of 8 M NH_4OH solution was added into the solution and the mixture was left in orbital shaker for 1 h. The mixture was then cooled to room temperature before the PDDA coated Fe_3O_4 were isolated using magnet. The synthesized PDDA coated Fe_3O_4 was washed three times with deionized water before they were resuspended in 100 mL of N_2 saturated deionized water.

60 mL of deionized water associated with magnetic stirring were used to dissolve 1.95 g of $FeCl_3 \cdot 6H_2O$ and 0.716 g of $FeCl_2 \cdot 4H_2O$. Then, 20 mL of PDDA solution containing 2.5 g of 20 wt% PDDA solution was added drop by drop into the dissolved solution. The mixture was ultrasonicated for 15 min before the mixture was heated to 60 °C with mechanical agitation under nitrogen

atmosphere. To adjust the pH to 9-10, NH_4OH was added dropwise into the mixture under continuous stirring for 4 h. Lastly, the PDDA coated Fe_3O_4 was recovered using magnet and washed several times using deionized water until the supernatant was neutral. The PDDA coated Fe_3O_4 was dried for 6 h under vacuum condition (Chen, Ju and Chen, 2018).

For synthesis method, there are two distinct ways to synthesis PDDA coated Fe_3O_4 . One of the ways is to synthesize by in-situ coating as described by Yu, et al. (2010), Qu, et al. (2015) and Al-Mashhadani and Hassen (2016). They shared similar ways to synthesize PDDA coated Fe_3O_4 where all deoxygenated starting materials were mixed, and ammonium aqueous solution was added for reaction. Lastly the PDDA coated Fe_3O_4 was collected by using magnet. The main difference is that Yu, et al. (2010) and Al-Mashhadani and Hassen (2016) allowed the reaction to occur with stirring while Qu, et al (2015) did not. The reaction occurred with stirring may form a more homogenous solution and the PDDA can mix more evenly with Fe_3O_4 . Another way to synthesize PDDA coated Fe_3O_4 is post-synthesis coating as performed by Li, et al. (2016), Chen, Ju and Chen (2018) and Low, Ng and Tan (2019). Chen, Ju and Chen performed the mixing of PDDA and Fe_3O_4 under nitrogen atmosphere, to eliminate the presence of oxygen that will inhibit polymerization reaction to get a higher yield of product.

4.2 Characterization of PDDA coated Fe_3O_4

As reported by Businova, et al. (2011), the Fe_3O_4 nanoparticles have particle size of less than 20 nm and there was negligible difference for Fe_3O_4 nanoparticles before and after polymer coating. Moreover, the Fe_3O_4 nanoparticles are spherical in shape for both coated and uncoated Fe_3O_4 and the nanoparticles tended to form aggregates.

Li, et al. (2016) obtained the TEM image of PDDA coated Fe_3O_4 using JEM-2100 TEM operating at 23 °C. The sample was prepared by dispersing the PDDA coated Fe_3O_4 into alcohol under ultrasonication or absorbing directly from the PDDA and Fe_3O_4 mixture. Then one drop of sample will be evaporated in the carbon coated copper grid. Figure 4.1 below shows the TEM image of the PDDA coated Fe_3O_4 in suspension and in powder. As in Figure 4.1 (a) below under the magnification of 800000, the lattice spacing can be

observed and it indicated two different materials in the sample. The darker image was Fe_3O_4 nanoparticles whereas the grey image was PDDA microspheres. The PDDA coated Fe_3O_4 was spherical in shape and had a particle size of approximately 20 nm. The TEM image of powdered PDDA coated Fe_3O_4 showed that the Fe_3O_4 nanoparticles were dispersed evenly in PDDA matrix.

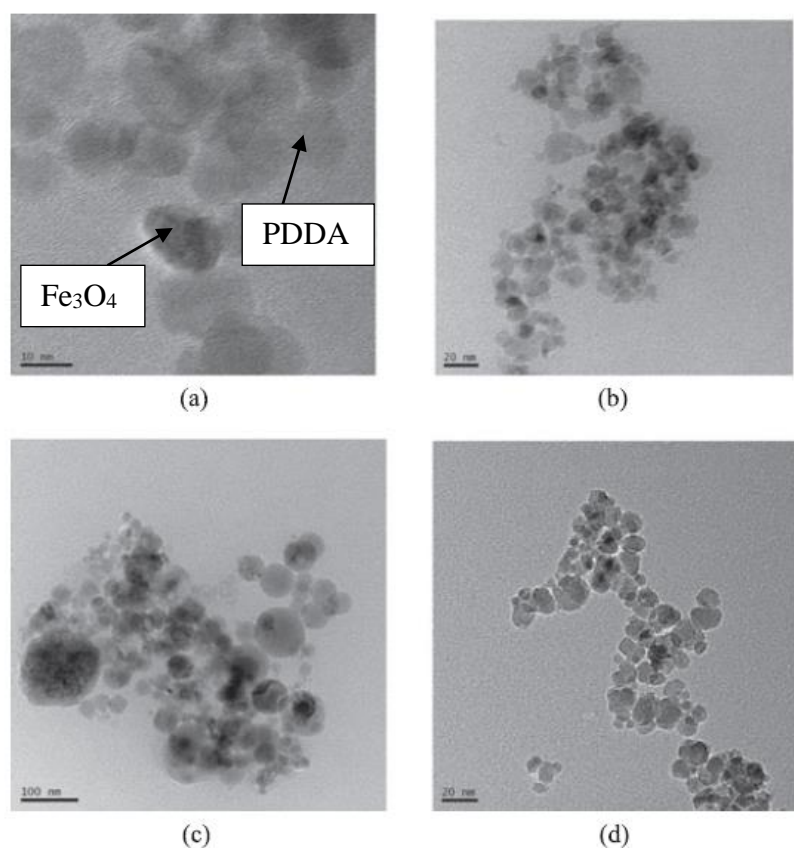


Figure 4.1: TEM Image of PDDA Coated Fe_3O_4 (a)-(c) in Suspension and (d) in Powder (Li, et al., 2016)

As reported by Li, et al. (2016), FTIR spectrum were collected using a Bruker TENSOR37, Germany with wavenumber ranging from 800 cm^{-1} to 4000 cm^{-1} . The samples were prepared in pellet form with spectroscopic grade potassium bromide (KBr). The FTIR spectrum of pristine PDDA and PDDA coated Fe_3O_4 was compared as shown in Figure 4.2. The peaks at about 3400 cm^{-1} indicated the presence of -OH vibration group in PDDA molecules. The presence of C=C groups were represented by the peaks at 1635 cm^{-1} and 1474 cm^{-1} . By comparing the spectra of pristine PDDA and PDDA coated Fe_3O_4 ,

additional peaks at 616 cm^{-1} and 472 cm^{-1} were observed. These peaks were due to the Fe-O stretching vibration of Fe_3O_4 nanoparticles. The wavenumber of characteristic peaks shifted slightly in the spectra of PDDA coated Fe_3O_4 indicated the complex electrostatic interaction between PDDA and Fe_3O_4 nanoparticles.

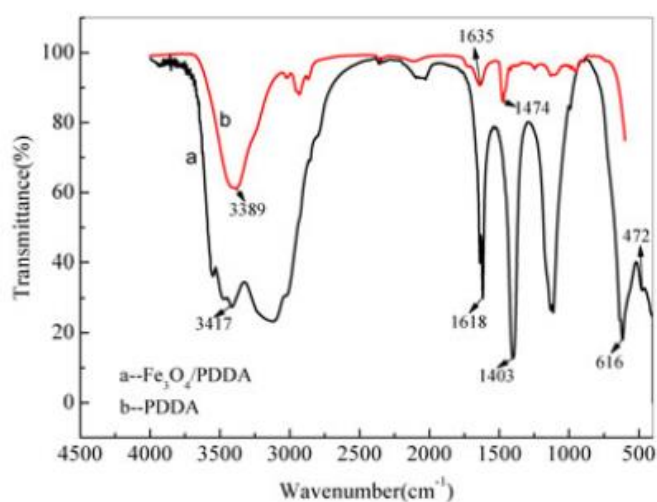


Figure 4.2: FTIR Spectrum of Pristine PDDA and PDDA Coated Fe_3O_4 (Li, et al., 2016)

In a report by Qu, et al. (2015), the TEM of Fe_3O_4 nanoparticles and PDDA coated Fe_3O_4 was compared as shown in Figure 4.3 below. It was found that the Fe_3O_4 coated with PDDA had a larger average diameter as compared to Fe_3O_4 nanoparticles.

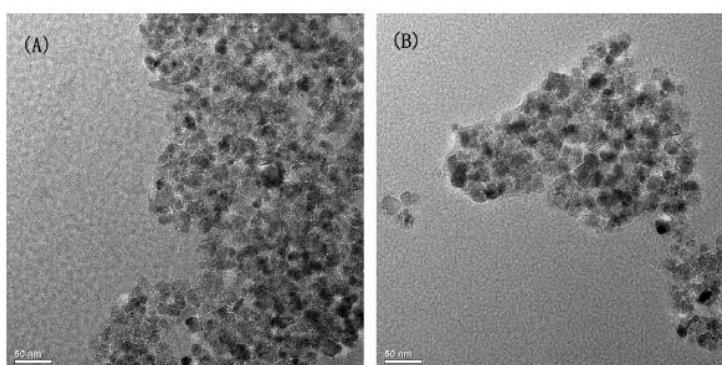


Figure 4.3: TEM Images of (A) Fe_3O_4 Nanoparticles (B) PDDA Coated Fe_3O_4 (Qu, et al., 2015)

Qu, et al. (2015) examined and compared the XRD patterns of Fe_3O_4 nanoparticles and PDDA coated Fe_3O_4 nanocomposites. The diffraction peaks at 2θ angles of 30.5° , 35.5° , 43.0° , 53.8° , 57.0° and 62.7° were shown. As shown in Figure 4.4, the characteristic peaks of PDDA coated Fe_3O_4 is similar to those of Fe_3O_4 nanoparticles. This implies that the PDDA added to Fe_3O_4 did not perturb the formation of Fe_3O_4 nanoparticles.

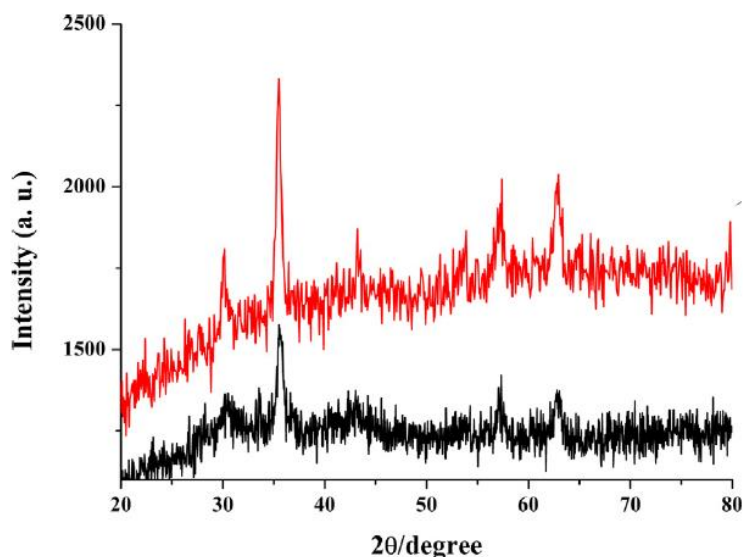


Figure 4.4: XRD Patterns of Fe_3O_4 Nanoparticles (Red) and PDDA Coated Fe_3O_4 (Black)

Yu, et al. (2010) reported that Fe_3O_4 nanoparticles showed diffraction peaks at $2\theta = 30.3^\circ$, 35.7° , 43.2° , 53.3° , 56.9° and 62.5° , which was in agreement to those in PDDA coated Fe_3O_4 . This indicated that the addition of PDDA into Fe_3O_4 did not perturb the formation of Fe_3O_4 nanoparticles.

Chen, Ju and Chen (2018) investigated the morphology of bare Fe_3O_4 and PDDA coated Fe_3O_4 using Hitachi S-4800 SEM. The SEM images showed that the as-prepared Fe_3O_4 were a group of spherical particles with average diameter of 30 nm. It can also be seen that the PDDA coated Fe_3O_4 had a better dispersion due to the electrostatic repulsion of PDDA coating as shown in Figure 4.5 below.

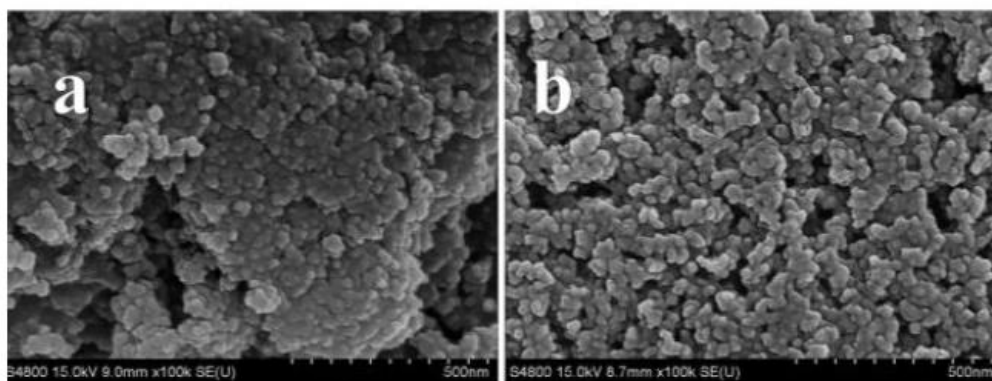


Figure 4.5: SEM Images of (a) Fe_3O_4 and (b) PDDA Coated Fe_3O_4 (Chen, Ju and Chen, 2018)

As shown in TEM images as shown in Figure 4.6, PDDA exists as a dense and transparent layer coating on the black Fe_3O_4 core (Chen, Ju and Chen, 2018). It can be seen that the Fe_3O_4 core is well wrapped by PDDA from the TEM images.

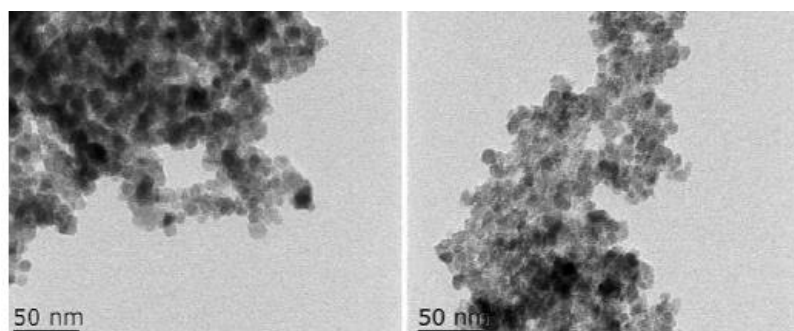


Figure 4.6: TEM Images of Fe_3O_4 Nanoparticles (Left) and PDDA Coated Fe_3O_4 (Chen, Ju and Chen, 2018)

Chen, Ju and Chen (2018) compared the FTIR spectrum of bare Fe_3O_4 , PDDA coated Fe_3O_4 as well as pristine PDDA using KBr pellet technique as illustrated in Figure 4.7 below. The FTIR was performed at a resolution of 4 cm^{-1} from 4400 cm^{-1} to 400 cm^{-1} on WQF-510A infrared spectrum analyser. Vibrations of O-H resulted in a peak at approximately 3400 cm^{-1} . The presence of C=C was confirmed from the peak at about 1630 cm^{-1} and 1470 cm^{-1} . A broad adsorption peak at 580 cm^{-1} indicated Fe-O stretching of Fe_3O_4 . Comparing PDDA and PDDA coated Fe_3O_4 , the characteristic peak of C=C in PDDA coated Fe_3O_4 shifted slightly in the wavenumber as compared

to pristine PDDA. This indicated that the PDDA was coated onto the Fe_3O_4 nanoparticles and complex electrostatic interaction exists between Fe_3O_4 and PDDA.

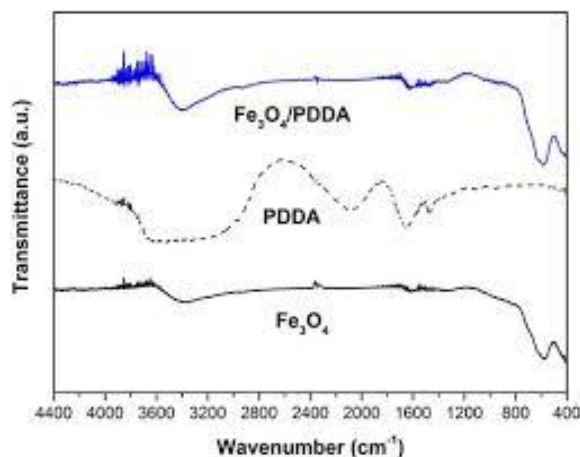


Figure 4.7: Comparison of FTIR Spectrum of PDDA Coated Fe_3O_4 , PDDA and Fe_3O_4 (Chen, Ju and Chen, 2018)

The XRD patterns of the bare Fe_3O_4 and PDDA coated Fe_3O_4 was obtained using D8 Advance diffractometer with $\text{CuK}\alpha$ radiation with $\lambda=1.540 \text{ \AA}$ (Chen, Ju and Chen, 2018). The molecules were scanned at $8^\circ/\text{min}$ from 10° to 80° . As observed from the XRD patterns, the peaks of PDDA coated Fe_3O_4 at $2\theta=30.06^\circ$, 35.60° , 43.14° , 57.04° and 63.56° were consistent with the face-centered cubic lattice of bare Fe_3O_4 . The crystalline structure of bare Fe_3O_4 was proven unchanged due to the similar diffraction patterns of bare Fe_3O_4 and PDDA coated Fe_3O_4 . The main difference is PDDA coated Fe_3O_4 had a broad peak at $2\theta=25^\circ$ due to its amorphous nature.

To find the specific surface area, BET analysis was used to determine the adsorption desorption of ultrapure N_2 of PDDA coated Fe_3O_4 (Chen, Ju and Chen, 2018). The total pore volume and the average pore diameter can be found as well. The PDDA coated Fe_3O_4 had pore diameters between 2 nm to 50 nm, proven that the prepared nanocomposites had mesopore in the structure. Comparing bare Fe_3O_4 and PDDA coated Fe_3O_4 , the specific surface area of PDDA coated Fe_3O_4 was larger, but the total pore volume and average pore diameter decreased. This may be due to the smaller grain agglomeration formed smaller channels.

Chen, Ju and Chen (2018) performed TGA analysis using Shimadzu DTG-60H to investigate the thermal stability by heating the sample from 30 to 800 °C with 5 °C/min under nitrogen atmosphere. From 30 °C to around 150 °C, the weight loss is due to the physically absorbed water while from 200 °C onwards, the weight loss is due to the decomposition of the organic components. According to the TGA curves as shown in Figure 4.8 below, the increase in weight loss of PDDA coated Fe_3O_4 indicated that the PDDA was coated successfully on Fe_3O_4 .

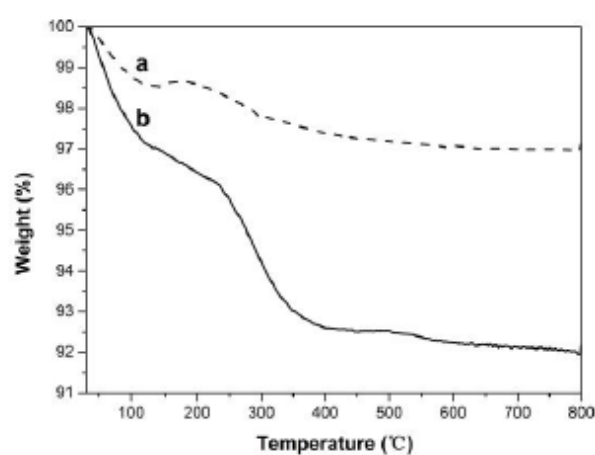


Figure 4.8: TGA Curves of (a) Fe_3O_4 and (b) PDDA Coated Fe_3O_4 (Chen, Ju and Chen, 2018)

Jang, et al. (2014) synthesized Prussian blue coated PDDA@ Fe_3O_4 to remove radioactive caesium in water. TEM image of PDDA coated Fe_3O_4 was as shown in Figure 4.9 below. Similar to Figure 4.1(d) above, the PDDA was dispersed evenly in Fe_3O_4 nanoparticles.

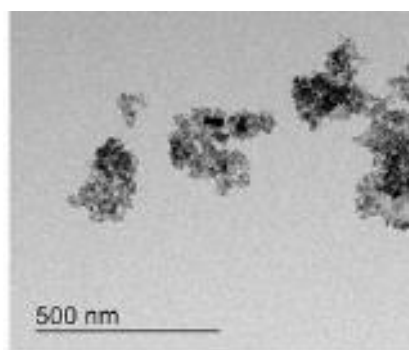


Figure 4.9: TEM Image of PDDA Coated Fe_3O_4 (Jang, et al., 2014)

In a nutshell, most of the TEM images showed successful coating of PDDA on Fe₃O₄ nanoparticles. These can be observed from the images where the PDDA in lighter colour coating on the Fe₃O₄ core with darker colour. The TEM images also show that the synthesized PDDA coated Fe₃O₄ is nano-sized particles in spherical shape. Both characterizations using FTIR performed by Li, et. al (2016) and Chen, Ju and Chen (2018) showed similar results in terms of wavelengths at which peaks appeared as well as the slight shift of peaks PDDA coated Fe₃O₄ when comparing with pristine PDDA. Most studies proved that the coating of PDDA onto Fe₃O₄ nanoparticles will not affect the original crystalline structure of Fe₃O₄ nanoparticles as similar diffraction peaks of bare Fe₃O₄ nanoparticles and PDDA coated Fe₃O₄ can be obtained.

4.3 Effect of Parameters in the Fenton Degradation of Microorganisms

4.3.1 Effect of pH

pH is an important parameter which affect the solubility of iron in water as well as the amount of ·OH in water (Moradi, et al., 2017). It was found that Fenton process was suitable to be conducted in acidic environment (Polo-López, Nahim-Granados and Fernández-Ibáñez, 2018; Tong, et al., 2019; Fernández, et al., 2020) with pH between 2.0 to 4.0 (O'Dowd and Pillai, 2020) regardless the targeted substrate. Giannakis, et al. (2017b), Soares, et al. (2015) and Rodríguez-Chueca, et al. (2013) stated that the optimum pH for Fenton process is pH 2.8 to prevent the occurrence of iron precipitation (O'Dowd and Pillai, 2020).

Figure 4.10 below shows the effect of pH on iron catalysts for Fenton reaction. At low pH, H⁺ ions act as a scavenger of ·OH where oxonium ions, [H₃O₂]⁺ will be formed. This will cause H₂O₂ to be electrophilic and reduce their reactivity with iron. At pH below pH 1.0, the overall efficiency of the reaction will be greatly reduced because only Fe²⁺ oxidation taking place from H₂O₂. The iron ions will be oxidized by H₂O₂ and this will decrease the amount of available iron for the process. Meanwhile for pH lower than 2.0, the number of iron available for reaction with H₂O₂ will decrease due to the formation of hexaaquairon ion, Fe(H₂O)₆³⁺. The iron will combine with the [H₃O₂]⁺ to form Fe(H₂O)₆³⁺. Moreover, H₂O₂ will become more stable due to

solvation and hence the reactivity towards iron will decrease (Litter and Slodowicz, 2017; O'Dowd and Pillai, 2020). $\cdot\text{OH}$ formation still occurs at higher pH value at a much slower rates (Fernández, et al., 2020). At higher pH, there will be formation of iron oxohydroxides, precipitation of ferric hydroxide (O'Dowd and Pillai, 2020) and H_2O_2 decomposition will occur (Wang, et al., 2020). All these scenarios will decrease the efficiency of the Fenton reaction (Fernández, et al., 2020). At pH above 5.0, ferryl ions will be formed but they are not as reactive as $\cdot\text{OH}$. The narrow operating pH range of Fenton reaction will be one of the greatest disadvantages of Fenton reaction.

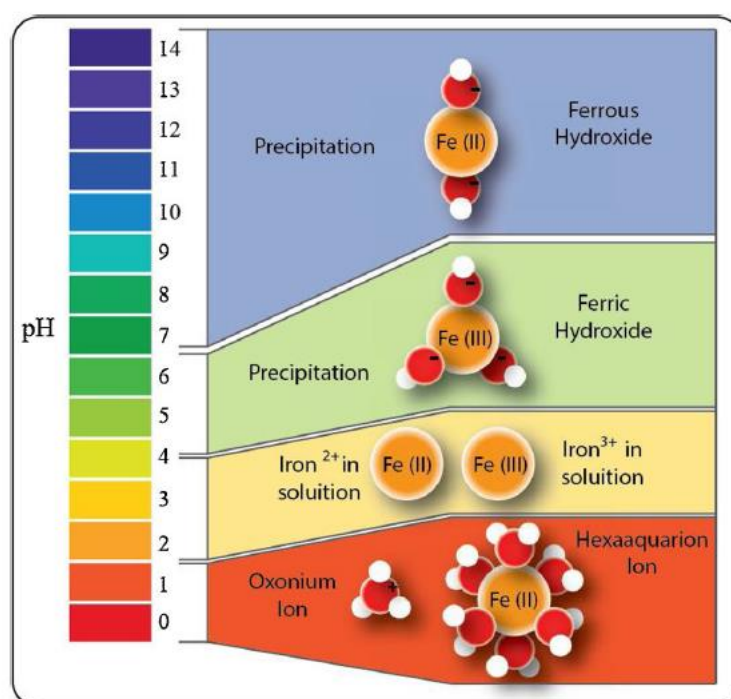


Figure 4.10: Effect of pH on Iron Catalysts in Fenton Process (O'Dowd and Pillai, 2020)

However, more recent researches were conducted in pH near neutral of naturally occurring or prepared Fe_3O_4 for the disinfection of wastewater (Giannakis, et al., 2017b; García, et al., 2018; Polo-López, Nahim-Granados and Fernández-Ibáñez, 2018; Fernández, et al., 2020; La Obra Jiménez, et al., 2020; O'Dowd and Pillai, 2020). It is very important to select an optimum pH for a reaction because it will affect the rate of reaction. The use of Fe_3O_4 instead of iron salts can eliminate iron precipitation and suitable to be used in

wide range of pH in Fenton reaction (Fernández, et al., 2020). The precipitation of iron salts and the use of stabilizing agents can be avoided by using Fe_3O_4 in heterogenous Fenton reaction (Wang, et al., 2020). Some studies proved that near neutral pH is the optimum pH value for heterogenous photo-Fenton process. This is because the near neutral pH can preserve $\text{O}_2^{\cdot-}$ to facilitate the Fenton process. This can reduce to cost of chemicals to reduce the pH of the wastewater that required treatment (Rodríguez-Chueca, et al., 2013; García, et al., 2018; O'Dowd and Pillai, 2020). This will be more beneficial for the process to provide clean drinking water in rural communities. The need to undergo few processing steps to reduce the pH for disinfection can be avoided. Time and cost will be saved by operating in near neutral pH.

E. coli is usually be degraded using two types of Fenton processes, including Fenton-like reaction and photo-Fenton reaction. Fenton-like reaction utilizes Fe^{3+} and H_2O_2 as reagents to initiate the reaction while photo-Fenton reaction utilizes Fe^{2+} and H_2O_2 as well as light to initiate the reaction.

Fernández, et al. (2020) studied and compared the efficiency of bacteria inactivation using Fenton process at pH 3, 5, 6.6 and 8 using the same dose of H_2O_2 and concentration of catalyst, Fe_3O_4 covered by polyethyleneimine and supported by mesoporous silica, $\text{Fe}_3\text{O}_4@\text{PEI}/\text{SBA15}$. The concentration of *E. coli* became zero after 30 min of the Fenton reaction at pH 3 and 5. However, the inactivation rate became significantly slower at pH 8. The kinetic parameters of the inactivation of *E. coli* were as shown in Table 4.1 below. It can be observed that there is no significant difference of *E. coli* inactivation from pH 3 to pH 6.6. This enhances the possibility to develop the use of Fe_3O_4 as catalyst in Fenton process in large scale at near neutral pH to reduce to cost to acidify and neutralize the wastewater.

Table 4.1: Kinetic Parameters and Time Required to Achieve log-3 Activation of *E. coli* (Fernández, et al., 2020)

Microorganisms	pH	k (h ⁻¹)	σ (h ⁻¹)	R ²	T _{3-log} (min)
<i>E. coli</i>	3.0	9.71	0.72	0.98	43
	5.0	9.32	0.80	0.97	44
	6.6	7.77	0.58	0.98	53
	8.0	1.17	0.30	0.80	353

Moradi, et al. (2017) investigated the effect of pH in *E. coli* degradation of pH 6, 7 and 8. Figure 4.11 below shows the comparison of the *E. coli* degradation rate of different pH. As shown in the figure, the bacteria inactivation rate decreased from 0.17 min⁻¹ to 0.11 min⁻¹ when the pH is increased from pH 6 to pH 8. This indicated that the inactivation rate decreased with increasing pH. However, complete inactivation of *E. coli* still can be achieved at neutral or even alkaline condition, with longer treatment time required.

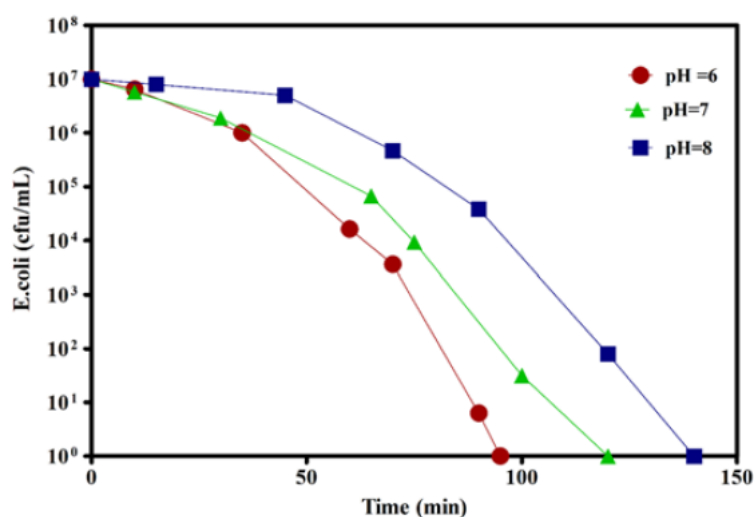


Figure 4.11: *E. coli* Degradation Rate at Different pH Values (Moradi, et al., 2017)

Tong, et al. (2019) investigated the efficiency of bacteria disinfection of magnetic Fe₃O₄-deposited MoS₂ flower-like spheres (MF) with 5 mM of H₂O₂ at pH 3.5, 6.0, 7.5 and 9.5. *E. coli* initial concentration of 1.2×10^6 CFU/mL was used to perform the experiment. At pH 3.5, complete disinfection of *E. coli* can be achieved within 20 min. When the pH is increased to pH 6 and pH 7.5, the *E. coli* is disinfected completely in 30 min and 40 min respectively. When pH is increased to pH 9.5, *E. coli* is fully disinfected in 75 min. When pH increases, the time required to completely disinfect *E. coli* increases. However, complete disinfection of *E. coli* can still be achieved with small amount of H₂O₂ even in alkaline condition. Figure 4.12 below shows the graph of time required to disinfect *E. coli* for different pH.

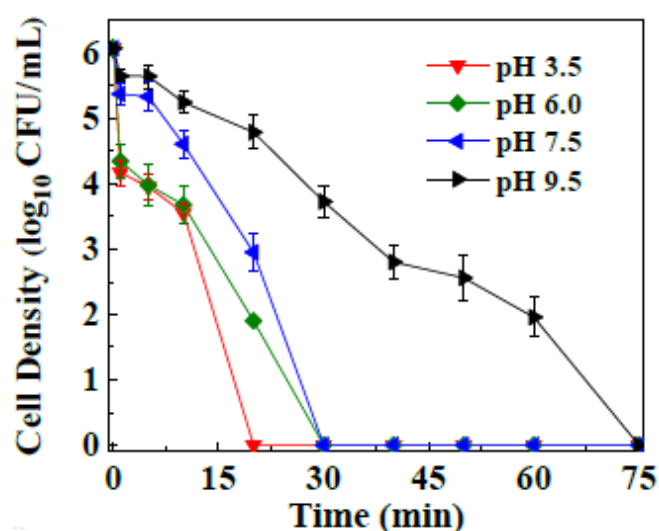


Figure 4.12: Graph of Time Required for *E. coli* Disinfection at Different pH (Tong, et al., 2019)

Apart from the Fenton-like degradation using H₂O₂, more studies had proven that *E. coli* can be successfully disinfected in near neutral pH via photo-Fenton and Fenton-like reaction. Moncayo-Lasso, et al. (2009) inactivated *E. coli* in river water via photo-Fenton process at pH of about pH 6.5 in a solar compound parabolic collector reactor. *E. coli* was completely inactivated with 11.0 kJL⁻¹ of accumulated energy at pH around 6.5 to pH 7. To ensure the accuracy of the result, the experiment was repeated thrice under same operating conditions and it was found that *E. coli* was inactivated completely with 10 kJL⁻¹ to 17 kJL⁻¹ of accumulated energy. A study was

carried out by using hybrid alginate montmorillonite iron enriched beads (Fe-MABs) as catalysts for heterogenous photo-Fenton reaction to investigate the effect of pH on the reaction (Barreca, et al., 2015). The experiment was carried out by using an initial bacterial concentration of 10^7 CFU/mL to demonstrate the *E. coli* loads in natural well water. It was proven that complete disinfection could be achieved in 60 min by photo-Fenton reaction at pH 7. In addition, López, et al. (2017) investigated the effect of type of reactor materials used in *E. coli* inactivation at pH 7. It was found that *E. coli* was disinfected completely after 120 min and 180 min. It was stated that the type of reactors used contributed to the difference in time taken to remove *E. coli* completely. Feng, et al. (2019) reported that the use of $\text{Fe}_3\text{O}_4/\text{SiO}_2/\text{C}$ nanocomposites (FSCNC) as a catalyst for Fenton like reaction to disinfect *E. coli* showed highest disinfection at pH 4.5. However, good performance was also shown in the neutral pH.

In conclusion, pH plays an important role in Fenton reaction as it affects the generation of $\cdot\text{OH}$ as well as the possibility of iron precipitation. Although literatures proved that the most effective range of pH was still in acidic condition, there were more recent research proved the disinfection of *E. coli* could be conducted at neutral pH especially using heterogenous Fenton reaction. Most of the literatures comparing acidic to alkaline pH found that a high disinfection rate was achieved in acidic condition. Complete disinfection still could be achieved at alkaline condition with a longer treatment time required. It is very important to ensure that the reaction can be carried out at near neutral pH to reduce the need and cost to acidify and neutralize the wastewater before treatment.

4.3.2 Effect of Temperature

Temperature will affect the catalytic effect of the process more than catalysts do. Temperature seemed to exert a catalytic effect on a process (O'Dowd and Pillai, 2020). O'Dowd and Pillai (2020) stated that increase in temperature will cause an increase in degradation of *E. coli*. It was reported that the increase in temperatures from 30 °C to 55 °C will ease the disinfection process. However, Ortega-Gómez, et al. (2012) reported that 37 °C is the optimum temperature for the process, in which this temperature will be optimum for bacterial growth

and metabolism. The increasing metabolism of microorganism enable the access of reagents or radicals into the cell more easily. However, at high temperatures above 90 °C, the iron precipitation will increase, and this will decrease the efficiency of the process.

Some of the studies showed that high temperature will decrease the rate of Fenton reaction due to the decomposition of H₂O₂ into H₂O and O₂. There are also some studies showed temperature between 40 °C to 90 °C favoured the reaction by increasing the rate of ·OH generation. However, Fenton reaction carried out at ambient conditions can sufficiently achieved the targeted efficiency of the process (Leonel, Mansur and Mansur, 2020).

4.3.3 Effect of Fenton Reagent Concentration

Concentration of reagents including H₂O₂ and Fe₃O₄ or Fe²⁺ play an important role in the degradation of bacteria in Fenton-like or Fenton reaction. Throughout the literatures reviewed, most of them show great variability of the concentrations of iron and H₂O₂ used even these are the key parameters in Fenton process. One general observation was that the H₂O₂ concentration used was equal or higher than iron concentration. Different microorganism or compound being disinfected required a different concentration or ratio of Fenton's reagent used. It was found that continuous reaction gave a more effective disinfection as compared to batch reaction (O'Dowd and Pillai, 2020).

As reported by O'Dowd and Pillai (2020), there are high variability of the ratio of iron to H₂O₂ used in Fenton process with the most common ratio of 1:2. Kim, et al. (2010) examined the different ratios of H₂O₂ and Fe²⁺ concentration in inactivation of MS2 coliphage using Fenton reaction. After 60 min, ratio of H₂O₂ to Fe²⁺ of 1:1 show the highest efficiency in the inactivation. In another study by Giannakis, et al. (2017a), it was shown that H₂O₂ to Fe²⁺ ratio of 1:1 gives an effective disinfection in homogenous and heterogenous catalyst. However, it was worth to take note that Giannakis, et al. (2017a) used a relatively high irradiation to complete the disinfection which was 300 Wm⁻². When Rubio, et al. (2013) investigated the inactivation of *E. coli* in artificial seawater, it was found that concentration of Fe²⁺ and concentration of H₂O₂ set at 1 mgL⁻¹ and 10 mgL⁻¹, which was at a ratio of 1:10, gave an effective disinfection of *E. coli* at this ratio. Salgado, Frontela and Vidal (2020) studied

the individual and interactive effect of molar ratio of H_2O_2 and Fe^{2+} on Fenton process. Concentrations of H_2O_2 and Fe^{2+} was studied at a molar ratio of 1:1, 2:1 and 3:1. The value of molar ratio of H_2O_2 and Fe^{2+} do not affect the disinfection of *E. coli* significantly. Selvakumar, et al. (2009) stated that regardless the amount of Fe^{2+} and H_2O_2 used, *E. coli* fell below detection limit almost instantly at pH 6.

4.3.3.1 Effect of H_2O_2 Concentration

H_2O_2 concentration is an important parameter in Fenton process because it indicates the amount of $\cdot\text{OH}$ produced to oxidize the targeted substrate. The process proceeded more efficiently when the concentration of $\cdot\text{OH}$ is remained high. However, excess H_2O_2 caused a scavenging effect where the treatment efficiency is decreased, and it is toxic to plenty of organisms. Hence, the amount the H_2O_2 used during the Fenton reaction must be controlled in a way that most of the H_2O_2 is reacted during the reaction (Leonel, Mansur and Mansur, 2020).

According to O'Dowd and Pillai (2020), higher H_2O_2 concentration led to an increase in kinetics of the reaction in the disinfection of *E. coli*. There was a high variation of H_2O_2 concentration proposed in the literature, ranging from 0.5 mg/L to 4000 mg/L. However, the most commonly seen concentration of H_2O_2 is between 10 to 20 mg/L.

Control tests was carried out by Fernández, et al. (2020) using H_2O_2 concentration of 5, 10, 20 and 100 mg/L to investigate the effect of this parameters over *E. coli* disinfection. In this study, lower than 16% and 40% of *E. coli* can be disinfected with 10 mg/L and 20 mg/L of H_2O_2 dosage, respectively. When 100 mg/L of H_2O_2 was used, complete disinfection of *E. coli* can be achieved. Figure 4.13 below shows the inactivation percentage of different H_2O_2 dosage.

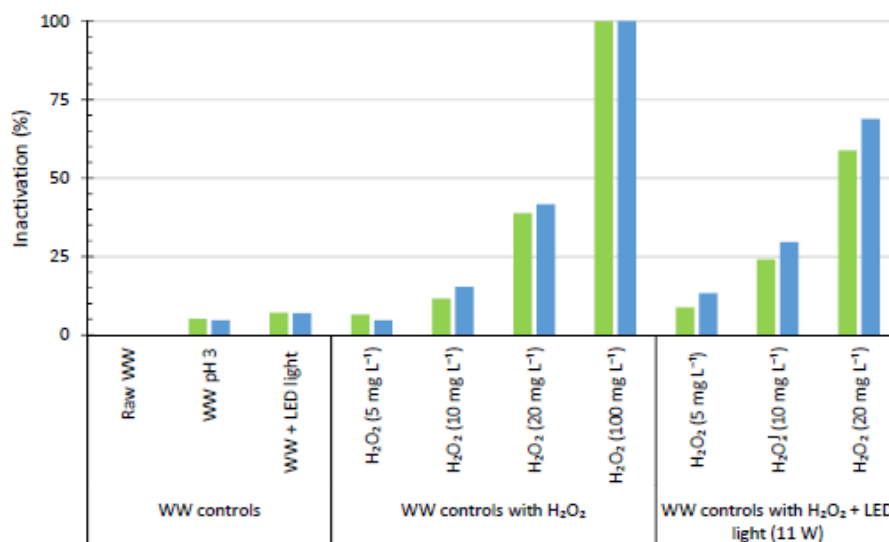


Figure 4.13: Inactivation Percentage of Different H₂O₂ Dosage (Middle Column) (Fernández, et al., 2020)

In a report by Gutiérrez-Zapata, et al. (2017), the disinfection of *E. coli* was done using the groundwater samples containing natural iron with concentration of 0.3 mg/L. When 10 mg/L of H₂O₂ is added in dark condition, Fenton reaction occurs and 99% of the *E. coli* was disinfected after 8 h. When the sample was only exposed to simulated sunlight without H₂O₂, 99.9% of *E. coli* was disinfected after 8 h. However, when the sample was exposed to simulated sunlight and 10 mg/L of H₂O₂, 100% of *E. coli* was disinfected after 6 h of treatment. This indicated that 0.3 mg/L of iron was enough to establish efficient disinfection of *E. coli* even without presence of H₂O₂ but in the presence of simulated sunlight.

Ortega-Gómez, et al. (2015) investigated the efficiency of photo-Fenton process for virus inactivation by changing the Fe³⁺ concentration of 0.1, 0.5 and 1 mg/L when the concentration of H₂O₂ was fixed at 1 mg/L at near neutral pH. When 1 mg/L of Fe³⁺ was used, the detection limit was reached after 20 min of treatment. Detection limit is defined as the lowest number of virus population which can be reliably distinguished from the baseline. Furthermore, the time taken to reach detection limit was doubled when the concentration of Fe³⁺ was 0.5 mg/L. When 0.1 mg/L of Fe³⁺ was used, only 2-log reduction was observed, which was the lowest among the three concentrations studied.

Nahim-Granados, Pérez and Polo-Lopez (2017) stated that when the concentration of H_2O_2 was increased from 5 mg/L to 20 mg/L, the kinetic constants of *E. coli* disinfection increased linearly. 20 mg/L of H_2O_2 showed the best efficiency of disinfection where the detection limit was obtained after 10 min of the disinfection process.

With only 2 mg/L of H_2O_2 , the inactivation rate constant of *E. coli* increased from 0.008 min^{-1} to 0.016 min^{-1} . When the concentration of H_2O_2 was further increased to 4 mg/L, all the *E. coli* had been successfully inactivated after 90 min of the treatment. The inactivation rate constants increased from 0.008 min^{-1} to 0.034 min^{-1} when H_2O_2 concentration increased from 0 mg/L to 10 mg/L (Ndounla, et al., 2014).

In a study by Ortega-Gómez, et al. (2012), when 120 mg/L of H_2O_2 was used, the detection limit was achieved after 80 min of the treatment time. However, when the concentration of H_2O_2 used was 20 mg/L and 70 mg/L, the detection limit was not achieved after 120 min of the treatment. The concentration of H_2O_2 chosen in this experiment was higher than most of the other literatures due to the different type of experimental system used where the efficiency of the process was decreased due to the flow conditions and dark volume.

Barreca, et al. (2015) used Fe-MABs to disinfect *E. coli* and it was found that no bacteria were inactivated in the dark Fenton reaction with low concentration (10 mg/L) of H_2O_2 . Experiments were carried out at pH7 and using 10 mg/L H_2O_2 to investigate the effect of catalyst amount for the Fenton reaction. It was observed that 230 mg/L of catalyst with 10 mg/L of H_2O_2 achieved the best efficiency of disinfection whereby complete disinfection was achieved in 60 min.

Moradi, et al. (2017) varied concentrations of H_2O_2 from 10 mg/L to 68 mg/L to investigate its effect on *E. coli* inactivation. It was found that the bacterial inactivation rate increased significantly from 0.192 min^{-1} to 0.355 min^{-1} with the increasing concentration of H_2O_2 . More H_2O_2 will create more $\cdot\text{OH}$ to damage the cell membrane of bacteria and hence inactivate them.

Liu, et al. (2018) reported that H_2O_2 is known to have a sterilization function in which the increase in H_2O_2 concentration will decrease the survival rate of *E. coli*. The significant effect of H_2O_2 on *E. coli* disinfection was

proved. When the amount of H₂O₂ was increased from 1 µL to 32 µL, the inactivation rate increased from 50 % to about 80 %.

A lot of research carried out on *E. coli* gave a huge number of different concentrations of H₂O₂ used to disinfect *E. coli* efficiently at near neutral pH. Table 4.2 below summarize some of the concentrations of H₂O₂ and its inactivation rate of *E. coli*. As shown from Table 4.2 below, most of the experiments was carried out in the presence of solar radiation or natural sunlight. The use of solar radiation can enhance the inactivation rate. Comparing the experiments in the absence of light, a higher concentration of H₂O₂ is required to achieve an effective inactivation rate. Experiments should be carried out to get an accurate concentration of H₂O₂ to be used under the designed condition.

Table 4.2: Concentrations of H₂O₂ and Inactivation Rate of *E. coli*

Concentration	Inactivation rate	Time	Light	Source
10 mg/L	99.9 %	120 min	✓	(Ruales-Lonfat, et al., 2014)
10 mg/L	100 %	-	✓	(Moncayo-Lasso, et al., 2009)
10 mg/L	99.99%	60 min	✓	(Valero, et al., 2017)
10 mg/L	99.99%	30 min	✓	(Alvear-Daza, et al., 2018)
10 mg/L	99.99%	2 min	✓	(Giannakis, et al., 2018)
10 mg/L	100 %	60 min	✓	(Barreca, et al., 2015)
10 mg/L	100%	60 min	✓	(Marjanovic, et al., 2018)
10 mg/L	100%	90 min	✓	(Kohantorabi, et al., 2018)
10 mg/L	100%	220 min	✓	(Gutiérrez-Zapata, Sanabria and Rengifo-Herrera, 2017)
10 mg/L	99.999%	10 min	✓	(García-Fernández, et al., 2012)
20 mg/L	100%	120 min	✓	(López, et al., 2017)
		180 min	✓	
20 mg/L	100%	60 min	✓	(Nahim-Granados, Pérez and Polo-Lopez, 2017)
20 mg/L	99.6 %	180 min	✓	(Rodríguez-Chueca, et al., 2012)
	42.46 %			

Table 4.2 (Continued)

20 mg/L	99.99999%	180 min	✓	(Porras, et al., 2018)
10 mg/L	99.99%	60 min	✓	(Topac and Alkan, 2016)
30 mg/L		45 min	(200 W/m ²)	
50 mg/L		28 min		
10 mg/L		41 min	✓	
30 mg/L		26 min	(500 W/m ²)	
50 mg/L		14 min		
30 mg/L	99.99%	60 min	✓	(Jímenez, et al., 2019a)
30 mg/L	99.9%	22.4 min	✓	(Jímenez, et al., 2019b)
1 mg/L	99.99%	30 min	✓	(Giannakis, et al., 2017a)
50 mg/L	100%	80 min	✓	(García, et al., 2018)
8.5 mg/L	99.999%	30 min	✓	(Ndounla, et al., 2014)
25 mg/L	99.987%	60 min	✓	(Rodríguez-Chueca, et al., 2015)
	99.997%	240 min	✓	
10 mg/L	99.99999%	26 s	✓	(Aguilar, et al., 2017)
30 mg/L		56s		

Table 4.2 (Continued)

5 mg/L	99.99%	40 min	✓	(Rodríguez-Chueca, et al., 2013)
10 mg/L	99.99%		✓	
20 mg/L	99.9999%		✓	
	90 %			
25 mg/L	99.9999%		✓	
50 mg/L	99.9999%		✓	
	99.999%			

4.3.3.2 Effect of Iron Concentration

In heterogenous photo-Fenton process, optimum iron content is a key parameter to achieve efficient disinfection process. High active sites availability could be achieved with increasing number of iron loading (Wang, et al., 2020). Even the concentration of iron catalyst is an important parameter affecting Fenton process, it cannot be added in an excessive amount (Zhang, et al., 2019). When there is too high concentration of iron in the process, the efficiency of the process may be decreased due to the saturation of radicals. Moreover, the excess Fe^{2+} may result in the formation of iron sludge (O'Dowd and Pillai, 2020).

Carra, et al. (2013) investigated the iron dosage on the performance of removing pollutants of mixture of five commonly used pesticides in demineralized water and real wastewater. It was demonstrated successfully that iron can be added into the reaction system in stages to obtain the similar reaction rate at neutral pH as compared to the optimum pH, pH 2.8. By dosing iron in stages, the pollutants could be removed by Fenton reaction but in a slower rate and occurrence of mineralization.

Cruz, et al. (2013) treated the wastewater from municipal wastewater treatment plant with initial iron content of 1.6 mgL^{-1} at near neutral pH of pH 6 to pH 7. An average degradation rate of 80 % was achieved in this experiment. The concentration of iron was varied at 0 mgL^{-1} , 2 mgL^{-1} and 4 mgL^{-1} . However, no significant effect was shown from the addition of iron as compared to the one with initial iron concentration in the wastewater. For example, when the concentration of H_2O_2 was fixed at 30 mgL^{-1} , the degradation rate for 0 mgL^{-1} , 2 mgL^{-1} and 4 mgL^{-1} was 83%, 83% and 84% respectively.

When Salgado, Frontela and Vidal (2020) investigated the concentration of Fe^{2+} at 33.50, 44.67 and 55.84 mg/L using Box-Behnken Design in Design Expert software, these increasing values of Fe^{2+} concentration showed a significant negative effect on the rate of disinfection of bacteria. Hence, it was proposed that the increasing Fe^{2+} could react with the $\cdot\text{OH}$ formed, decreasing the amount of $\cdot\text{OH}$ to oxidize the substrate.

The effect of nanoparticles dosage was also evaluated by using Fe^{2+} concentration of 0 mg/L, 750 mg/L, 1500 mg/L, 3000 g/L and 6000 g/L

(Moradi, et al., 2017). The bacterial inactivation rate for these concentrations of Fe^{2+} was 0.0011 min^{-1} , 0.048 min^{-1} , 0.1 min^{-1} , 0.13 min^{-1} and 0.0117 min^{-1} . The bacterial inactivation rate increased with increase in Fe^{2+} dosage up to 3000 g/L. However, the bacterial inactivation rate decreased when Fe^{2+} dosage increased further to 6000 g/L. This is due to the excess of Fe^{2+} will react with $\cdot\text{OH}$ hence reduce availability of $\cdot\text{OH}$ for reaction.

Liu, et al. (2018) investigated the concentration of Fe^{2+} from 1 mg to 8 mg. It was found that the inactivation rate increased from 70% to 80% when 2 mg of Fe^{2+} was used but started to decline to less than 60 % with the further increase in the amount of Fe^{2+} . This indicated that the optimum dosage of Fe^{2+} was required to be determined. An optimum dosage of Fe^{2+} will be beneficial for H_2O_2 to generate more $\cdot\text{OH}$. However, excessive of Fe^{2+} dosage will have a scavenging effect on $\cdot\text{OH}$ whereas too low dosage will not be capable to catalyze the decomposition of H_2O_2 to form $\cdot\text{OH}$.

Feng, et al. (2019) varied the weight of FSCNC from 0 mg to 20 mg to investigate its influence in the heterogenous Fenton-like reaction. As in Figure 4.14 below, it was shown that the inactivation rate increased with increasing FSCNC, up to a certain extend and the inactivation rate decreased with further increase of FSCNC. This result was tally with other literatures that an optimum dosage of iron should be employed where the dosage cannot be added in an excessive way.

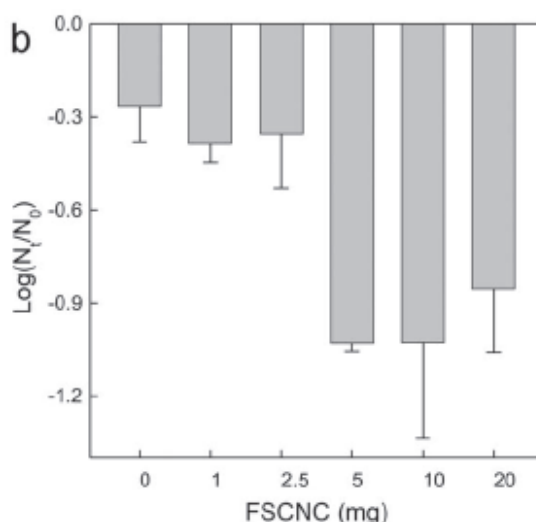


Figure 4.14: Effect of FSCNC in heterogenous Fenton-like reaction (Feng, et al., 2019)

Barreca, et al. (2015) used Fe-MABs to disinfect *E. coli*. Experiments were carried out at pH7 and using 10 mg/L H₂O₂ to investigate the effect of catalyst amount for the Fenton reaction. The catalyst amount was altered at 230, 450 and 900 mg/L of catalysts. It was observed that 230 mg/L of catalyst achieved the best efficiency of disinfection whereby complete disinfection was achieved in 60 min.

Table 4.3 below summarize some of the concentrations of iron and its corresponding inactivation rate of *E. coli*. As observed in Table 4.3 below, even a very small concentration of iron used is effective in disinfecting more than 99% of *E. coli* in the presence of light. Similar to concentration of H₂O₂ and its effect on disinfection rate, it can be observed that the presence of solar radiation or natural sunlight can enhance the Fenton process greatly.

Table 4.3: Concentrations of Iron and Corresponding Inactivation Rate of *E. coli*

Concentration	Inactivation rate	Required time	Light	Source
0.39 mg/L	99.998%	30 min	✓	(Alvear-Daza, et al., 2018)
0.07 mg/L	81.8 %	360 min		(Ndounla, et al., 2014)
	100 %	120 min	✓	
0.67 mg/L	100 %	30 min	✓	(Ndounla, et al., 2013)
0.07 mg/L	100 %	60 min	✓	
1 mg/L	99.99 %	30 min	✓	(Giannakis, et al., 2017a)
5 mg/L	99.999 %	10 min	✓	(García-Fernández, et al., 2012)
5 mg/L	99.6 %	180 min	✓	(Rodríguez-Chueca, et al., 2012)
	(Wastewater)			
	99.9998 %			
	(Simulated water)			
	42.46%	180 min		
(Wastewater)				
	97.43%			
(Simulated water)				
5.6 mg/L	99.99%	14 min	✓	(Topac and Alkan, 2016)

Table 4.3 (Continued)

2.5 mg/L	68.38 %	10 min		(Rodríguez-Chueca, et al., 2013)
10 mg/L	99 %			
	99.9 %	240 min		
20 mg/L	100 %	80 min	✓	(García, et al., 2018)
230 mg/L	100 %	60 min	✓	(Barreca, et al., 2015)

4.4 Comparison with Other Disinfection Methods

4.4.1 Cost

Rodriguez-Chueca, et al. (2015) compared the four disinfection methods based on economical aspect. The cost of treatment required per m³ of wastewater was tabulated in Table 4.4 below. In this paper, the effectiveness of the method was evaluated based on disinfection rate to cost ratio and the most effective selected was chlorination, followed by UVC irradiation, solar photo-Fenton and H₂O₂/solar treatment. However, it should be taken note that solar photo-Fenton at pH 5 also gave an effective level of inactivation. It was the cost associated to decrease the pH from neutral to slightly acidic causes the increase in cost of treatment.

Table 4.4: Comparison of Cost of Treatment for Four Different Methods

Method	Disinfection rate, Log (N _t /N ₀)	Cost of treatment, \$/ m ³
Chlorination	7.20	5.67×10^{-4}
UVC irradiation	3.80	1.76×10^{-1}
H ₂ O ₂ /sunlight	3.30	3.97×10^{-1}
Photo-Fenton	4.87	4.07×10^{-1}

Meng, et al. (2018) estimated and compared the cost to treat the wastewater in industrial applications using adsorption and Fenton-process. It was stated that the cost for the equipment for both processes did not have large difference and could be neglected. The energy and chemical consumption during the operation contributed most to the total cost analysis. Meng, et al (2018) analyzed the cost mainly based on these energy and chemical cost. It was found that adsorption and Fenton process required 3.57 US\$/m³ and 0.35 US\$/m³, respectively. The high cost of adsorption process was mainly due to the high chemical cost of granular activated carbon.

Krishnan, et al. (2017) suggested that the cost of ozonation was high in terms of capital cost while the operating and maintenance cost were relatively lower. This is because ozonation is energy intensive where energy required to generate ozone will be very high. The main cost arising from ozonation disinfection process is due to the cost to generate ozone. The cost for

ozonation ranged from \$0.09/m³ to \$0.96/m³. For H₂O₂/ UV, the operating cost was relatively lower since H₂O₂ can be obtained from the market easily. The capital cost for H₂O₂/ UV is the lowest but the operating and maintenance cost will be higher due to the high energy usage. The cost for H₂O₂/ UV ranged from \$0.08/m³ to \$1.08/m³. When estimating the cost of the process for Fenton, photo-Fenton and Fenton-like reaction, the cost to remove and dispose the iron sludge must be considered. The estimated costs were found to be US\$2.88/ m³. For TiO₂ photocatalysis, the raw materials are inexpensive. However, the recycling and recovery of the particles are difficult and increasing the cost for the process. TiO₂ photocatalysis was found to be least cost effective when compared to other AOPs with cost ranged from \$0.27/m³ to \$1.36/m³. However, the cost analysis relied on the treatment target hence it is suggested to carry out pilot testing to compare the costs.

Collivignarelli, et al. (2018) compared the costs required for different disinfection methods and disinfectants. The comparison was based on maintenance, investment as well as management only. The comparison is tabulated in Table 4.5 below. Comparing between the disinfection methods, chlorination possessed a relatively lower costs in terms of maintenance, investment, and management. Ozonation, UV radiation and AOPs possessed a comparable cost since exact value of the costs were not shown. However, the costs evaluated were similar to that of Rodriguez-Chueca, et al. (2015) where chlorination possessed lowest cost among all.

Table 4.5: Comparison of Costs for Different Disinfection Methods

Method	Disinfectants	Costs		
		Maintenance	Investment	Management
Chlorination	Chlorine gas	Low	Low	Low
	Sodium hypochlorite	Low	Low	Low
	Chlorine dioxide	Moderate	Moderate	Moderate
Ozonation	Ozone	Frequent	Very high	High
UV Radiation	UV	Moderate to frequent	High	Medium
AOPs		High	High	High

Comparing the cost evaluation from different literatures, chlorination requires lowest cost to implement for water disinfection. The cost required to generate ozone and UV are very high. However, the main reason that Fenton reaction required higher cost was due to the cost associated to acidify and neutralize the wastewater since the reaction is more effective at acidic pH. Recent advances to carry out the reaction at near neutral pH can eliminate this shortcoming of Fenton reaction. Hence, Fenton reaction can be considered as a promising approach to disinfect wastewater.

4.4.2 Disinfection By-Products (DBPs) Formation

Li (2014) compared the DBPs of chlorination, photo-Fenton and TiO₂ photocatalysis. It was found that a lot of DBPs were produced from the disinfection process using chlorination method. The DBPs produced included THMs, haloacetonitriles (HANs), chloral hydrate (CH) as well as 1,1-dichloro-2-propanone (1,1-DCP). These DBPs were found to be harmful to human and living organisms which may cause cancer or other health effects. In contrast with chlorination method, no DBPs were found from disinfection using photo-Fenton process and TiO₂ photocatalysis.

Ozonation is known to be one of the effective AOPs due to generation of ·OH and superoxide radical (O₂^{·-}) to oxidize the targeted substrate when

ozone is added to water (Krishnan, et al., 2017). However, ozonation have a potential to generate bromate as a DBPs during the disinfection. Next, it was reported that H_2O_2/UV also generated bromate as DBPs, but this only occurred at high pH value. For Fenton, photo-Fenton and Fenton-like reaction, they are known to be environmentally safe since no DBPs produced. TiO_2 photocatalysis was also known to be suitable for water treatment because they will not react chemically or biologically with the organic matters in the water.

Collivignarelli, et al. (2018) discussed some of the DBPs formation during the disinfection processes. When chlorine is used for the disinfection, it will react with the natural organic substances to form THMs and acetoacetic which is known to be carcinogenic. Moreover, many unwanted halogenated organic compounds such as haloacetic acids (HAAs), chlorophenols, CH and HANs will also be formed. When chlorine dioxide was used as disinfectant in chlorination, potentially toxic by-products such as chlorite and chlorate are formed. For ozonation, both organic and inorganic DBPs such as aldehydes, carboxylic acids and bromate will be formed. Recent research also suggested that ozonation will cause the formation of N-nitrosodimethylamine (NDMA) which is harmful to livers of living organisms. Next, the disinfection using UV radiation and AOPs are known to not produce any DBPs.

It is very clear to observe that chlorination and ozonation disinfection will produce a lot of toxic or unwanted DBPs which will be harmful to living organisms or aquatic life. Literatures suggested that both UV disinfection and AOPs will not produce any DBPs. UV will leave no footprints after disinfection while AOPs will release only harmless compounds such as CO_2 and H_2O only. Conventional Fenton reaction is known to produce iron sludge where further treatment and disposal of iron sludge make the process more complicated. Recent development for heterogenous Fenton reaction enabled the catalysts to be recovered and recycled easily using magnet. Hence, Fenton process will be a good approach to be utilized for water disinfection since lower energy requirement as compared to UV radiation.

4.4.3 Contact Time Required for Disinfection

In a report by Rodriguez-Chueca, et al. (2015), when 2 mg/L Cl_2 were used, a 6.15 log-reduction and 7.2 log-reduction were observed after 15 min and 30 min respectively. When UV radiation was used, only 2 and 10 s of treatment time required to get a lower than 1-log reduction of *E. coli*

. When 180, 300, 480 and 600s contact time was used, 3.80, 3.21, 3.61, 4.10 log reduction was observed, respectively. It can be observed that higher contact time can achieve better efficiency than that with lower contact time. When H_2O_2 and sunlight irradiation were used to disinfect *E. coli*, a 30 min treatment time was required to get 3.3-log reduction. Moreover, when Fe^{3+} , H_2O_2 and sunlight irradiation were used in the photo-Fenton process, 30 min treatment time was sufficient to achieve a 5.29 log-reduction. Comparing in terms of time required for disinfection in this paper, UV radiation was the fastest followed by chlorination, photo-Fenton and $\text{H}_2\text{O}_2/\text{UV}$.

From the experiments comparing Fenton reaction, ozonation and chlorination, it was observed that for all disinfection methods, higher treatment time resulted in higher disinfection rate (Diao, et al., 2004; Pereira, et al., 2011). Comparing different disinfection methods as shown in Table 4.6, ozonation gave the highest disinfection rate with lowest treatment time. Even chlorination required a longer treatment time, it gave a more effective disinfection rate than Fenton reaction. When Diao, et al. (2004) compared electrochemical disinfection with the above three methods, it was found that electrochemical disinfection was comparable with ozonation. Complete disinfection can be achieved in 0.5 min.

Table 4.6: Disinfection Rate of Fenton Reaction, Ozonation, Chlorination and Electrochemical disinfection

Method	Treatment time, min	Disinfection rate, %
Fenton reaction	10	99.4
	30	99.8
Ozonation	2.5	99.9
	5	100
Chlorination	30	99.94
	60	99.98
Electrochemical	2 (16 mA/cm ²)	99.98
	0.5 (25 mA/cm ²)	100

Li (2014) compared the required treatment time and the disinfection rate of chlorination, photo-Fenton reaction and TiO₂ photocatalysis. The treatment time and their respective disinfection rate were summarized and tabulated in Table 4.7 below. In terms of treatment time, chlorination able to achieve the highest disinfection rate in the shortest treatment time. However, similar disinfection rate was observed at longer treatment time.

Table 4.7: Treatment Time and Disinfection Rate for Different Disinfection Methods

Method	Disinfection time (min)	Disinfection rate (%)
Chlorination	5	99.9
	80	99.9999
Photo-Fenton	5	0
	60	99.999
TiO ₂ photocatalysis	5	0
	80	100

It can be concluded that in terms of contact time, UV radiation and ozonation give an efficient disinfection with shortest contact time. For UV radiation, 10 s of contact time was sufficient to get 90 % disinfection (Rodriguez-Chueca, et al., 2015) while ozonation only required 2.5 min to get

99.9% disinfection rate (Diao, et al., 2004). Although other disinfection methods required longer contact time, they could still achieve high and efficient disinfection rate within 30 min (Diao, et al., 2004; Rodriguez-Chueca, et al., 2015) to 60 min (Li, 2014). The contact time required still depends on many other parameters as Fenton reaction still able to achieve 99% of disinfection rate in 10 min (Rodríguez-Chueca, et al., 2013) or 99.99% in 2 min in the presence of solar radiation (Giannakis, et al., 2018).

4.4.4 Efficiency of Different Disinfection Processes

When UV-Vis radiation was provided, TiO_2 itself exhibit disinfection efficiency of *E. coli* as a photocatalyst (Dong, Xing and Zhang, 2020). When H_2O_2 was added, the disinfection efficiency was enhanced because the photoinduced charge transfer was effectively separated. H_2O_2 will act as electron acceptor which prevent the electron-hole pairs to recombine and generated more $\cdot\text{OH}$. It can be observed that in the presence of UV-Vis, $\text{TiO}_2/\text{H}_2\text{O}_2$ system exhibited a higher disinfection efficiency than $\text{Fe}^{3+}/\text{H}_2\text{O}_2$ system. However, when UV-Vis was absent, $\text{Fe}^{3+}/\text{H}_2\text{O}_2$ exhibited a higher disinfection efficiency than $\text{TiO}_2/\text{H}_2\text{O}_2$. The addition of TiO_2 could only increase the bactericide oxidation ability of H_2O_2 .

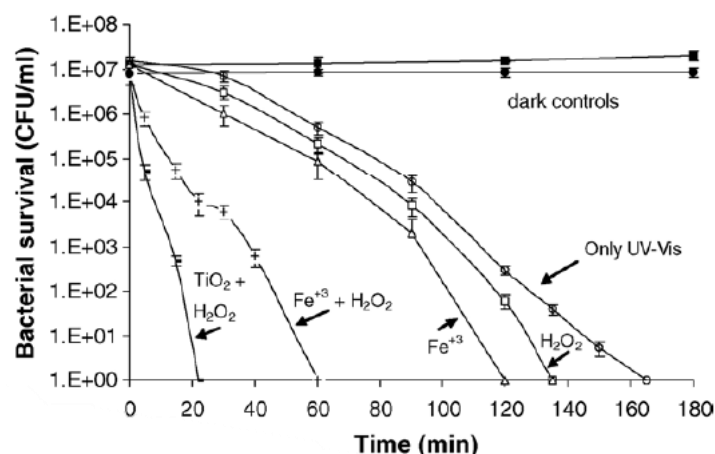


Figure 4.15: Efficiency of *E. coli* Inactivation under Different AOPs System with UV-Vis (Rincón and Pulgarin, 2006)

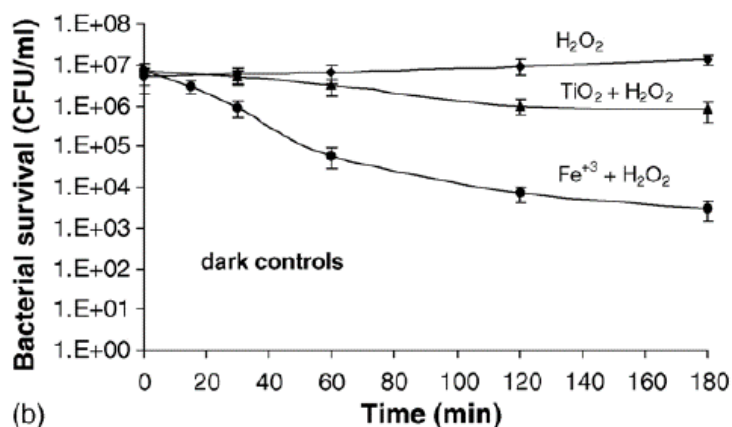


Figure 4.16: Efficiency of *E. coli* Inactivation under Different AOPs System Without UV-Vis (Rincón and Pulgarin, 2006)

The efficiency of the Fenton-like system using Fe₃O₄ and H₂O₂ was investigated by Feng, et al. (2019). In this report, FSCNC was synthesized to inactivate *E. coli* in simulated water via Fenton-like reaction. Effective disinfection was found at lower inoculation number, larger FSCNC dosage and high H₂O₂ concentration.

Giannakis, et al. (2015) reported that when no any reagents were added, the population of bacteria was observed increase. There was only 24.4% of disinfection rate achieved after 4 h when 1 ppm of Fe²⁺ and 10 ppm of H₂O₂ was added to initiate the Fenton reaction. When only ultrasound alone was added to the bacteria population, the disinfection rate was found to be 27.9%. When Fenton reagents was added concurrently with ultrasound treatment, the disinfection rate increased to 82.1%. It was observed that much higher disinfection rate was achieved due to the breakage of cavitation bubbles that formed a point-size heat source. These extreme conditions led to lysis of water molecules to produce more ·OH for the reaction.

Rodriguez-Chueca, et al. (2015) used different chlorine dosage to inactivate *E. coli* using chlorination process. From Figure 4.17 below, all the chlorine dosages shown similar trend in which a swift fall of logarithmic response was observed during the first 10 min of the treatment. An asymptotic region was observed after 20 min where bacteria inactivation was not observed. After 90 min of the treatment, all dosages of chlorine showed up to 6 log decrease in *E. coli*. Moreover, UV radiation wavelength of 254 nm which is

lethal for all microorganisms was used to disinfect *E. coli* (Rodriguez-Chueca, et al., 2015) However, concentration of *E. coli* was analyzed only after 6 h of treatment to include the possible regrowth of *E. coli*. The highest disinfection rate was 4.1 log-reduction as seen in Figure 4.18 below. When H₂O₂ and sunlight irradiation were applied for the treatment at the same time, it was found that highest inactivation rate of 3.30 log reduction with H₂O₂ concentration of 20 mg/L and sunlight irradiation of 500 W/m². A higher disinfection rate of 5.29-log reduction when Fe³⁺ was added to H₂O₂ and sunlight irradiation to initiate photo-Fenton process. Comparing four types of disinfection methods in this paper, it was found that chlorination followed by UV radiation gave the best disinfection rate as compared to H₂O₂/solar and photo-Fenton process.

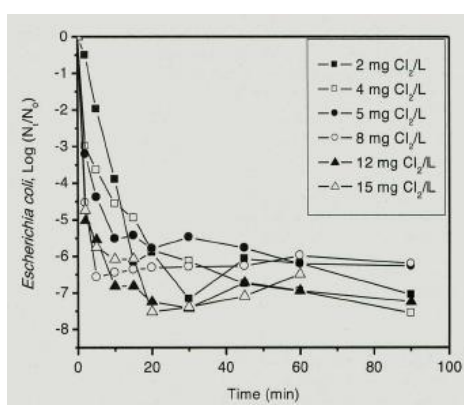


Figure 4.17: Inactivation of *E. coli* Using Different Chlorine Dosages (Rodriguez-Chueca, et al., 2015)

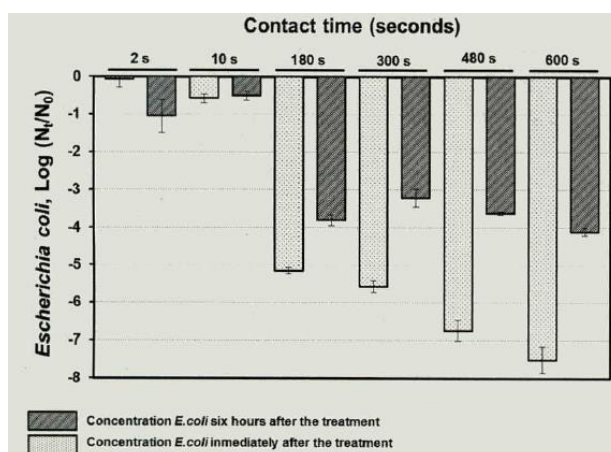


Figure 4.18: Inactivation of *E. coli* After Different Contact Time (Rodriguez-Chueca, et al., 2015)

Experiments to disinfect *E. coli* was carried out using chlorine, ozone and $\cdot\text{OH}$ (Pereira, et al., 2011). The Fenton reaction to produce $\cdot\text{OH}$ was carried out with concentration of Fe^{2+} and H_2O_2 of 8.5 mg/L and 0.85 mg/L, respectively in pH 4. It was found that ozonation gave the most effective disinfection rate as compared to others. However, Fenton's reagent still possessed disinfection rate high up to 99.8%. Table 4.8 below show the result of the experiment for different disinfection method.

Table 4.8: Disinfection Rate of Fenton Reaction, Ozonation and Chlorination

Method	Reagent Concentration, mg/L	pH	Disinfection rate, %
Fenton	Fe^{2+} : 0.85 H_2O_2 : 8.5	4	99.8
Ozonation	10	-	99.9
Chlorination	5	-	99.98

Cho, et al. (2004) compared the efficiency of different disinfection methods by using the CT value. CT value obtained from the product of concentration of $\cdot\text{OH}$ and the contact time which can be used to study the combination effect of the concentration of disinfectant as well as treatment time to disinfect *E. coli*. In this study, photo-ferrioxalate system was employed where solar light and oxalate ions were used to drive the Fenton reaction. Table 4.9 below summarize the comparison of CT values and oxidation potential for ozone, free chlorine, chlorine dioxide and photo-ferrioxalate Fenton system. The CT value obtained was to achieve a 2-log disinfection of *E. coli*. It can be observed that $\cdot\text{OH}$ had the smallest CT value among all other disinfectant. However, Cho, et al. (2004) stated that although this photo-ferrioxalate Fenton system did not achieve disinfection rate as high as others, it had great potential to treat microorganisms and organic pollutants in water due to its environmental friendly nature as compared to the other methods.

Table 4.9: Comparison of CT Values for Different Disinfection Methods

Disinfectant	CT (mg/liter/min)
Ozone	4.0×10^{-2}
Free Chlorine	1.3×10^{-1}
Chlorine dioxide	8.0×10^{-2}
$\cdot\text{OH}$	1.5×10^{-5}

Li (2014) stated that chlorination achieved the fastest inactivation rate of 99.9% in less than 5 min of the treatment as compared to photo-Fenton reaction and TiO_2 photocatalysis. AOPs such as photo-Fenton reaction and TiO_2 photocatalysis possessed a relatively slower disinfection rate where very low or no observable disinfection in the first 20 min of the treatment. However, 100% of disinfection rate was achieved after 80 min of the treatment which was a higher rate than chlorination. Li (2014) further stated that the difference in the disinfection rate might be due to the difference in reactive species involved in the reaction.

Rubio, et al. (2013) compared the inactivation rate of *E. coli* in Milli-Q water by using the simulated solar light, UV, UV/ H_2O_2 as well as photo-Fenton process. When only UV light was applied to disinfect *E. coli*, the treatment was efficient and fast with treatment time not higher than 5 min. Next, H_2O_2 was added to enhance the *E. coli* disinfection where the disinfection rate was increased 130% as compared to UV alone. Photo-Fenton system where Fe^{2+} and H_2O_2 was used as catalysts in the presence of UV showed a much higher disinfection rate as compared to the previous experiments. The rate of *E. coli* disinfection in 300 s was as shown in Figure 4.19 below.

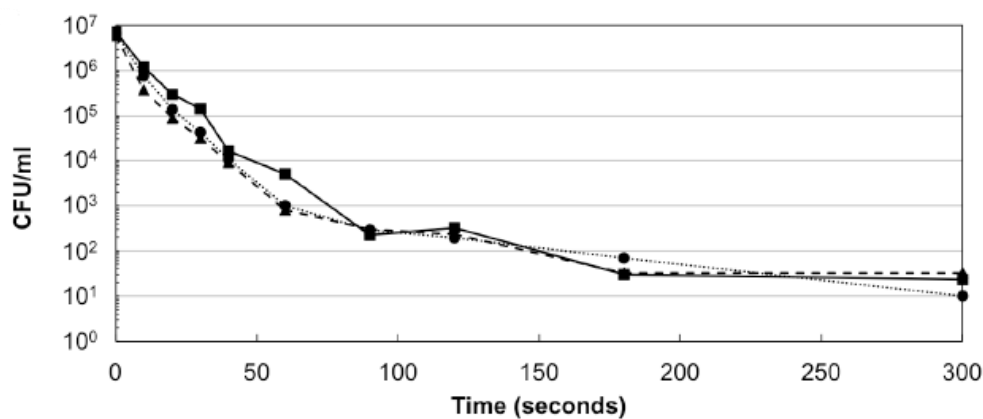


Figure 4.19: *E. coli* Inactivation in Milli-Q Water (■) UV (●) UV/ H₂O₂ (▲) Fe²⁺/ H₂O₂/UV (Rubio, et al., 2013)

A Fenton-like system of using H₂O₂ and copper with iminodisuccinic acid (Cu-IDS) as metal chelating agent in the presence of UV was compared with photo-Fenton process (Fiorentino, et al., 2018). It was found that the Fenton-like system using H₂O₂ and Cu-IDS was better than the conventional photo-Fenton process. Complete inactivation of *E. coli* was achieved in 10 min for the Fenton-like reaction while 20 min was required for the photo-Fenton reaction. When only UV alone or H₂O₂ alone was used, complete disinfection was not achieved.

Alkawareek, et al. (2019) compared the antibacterial activity using Fenton-like systems. The catalysts used in the system was H₂O₂ and silver nanoparticles (AgNP). Two types stabilizing agents was used where one was polyvinyl alcohol (PVA) and another was polyallylamine hydrochloride (PAH) and their capped silver nanoparticles was known as PVA-capped AgNP (PVA-AgNP) and PAH -capped AgNP (PAH-AgNP) respectively. Figure 4.20 and Figure 4.21 showed the *E. coli* survival rate after being treated with the Fenton-like system using H₂O₂ and PVA-AgNP as well as PAH-AgNP respectively. For both PVA-AgNP and PAH-AgNP, their combination with H₂O₂ showed higher bacteria disinfection rate than just applying the nanoparticles or H₂O₂ alone. Complete disinfection of bacteria can be observed by Fenton-like system using PVA-AgNP and PAH-AgNP in 45 min and 15 min respectively.

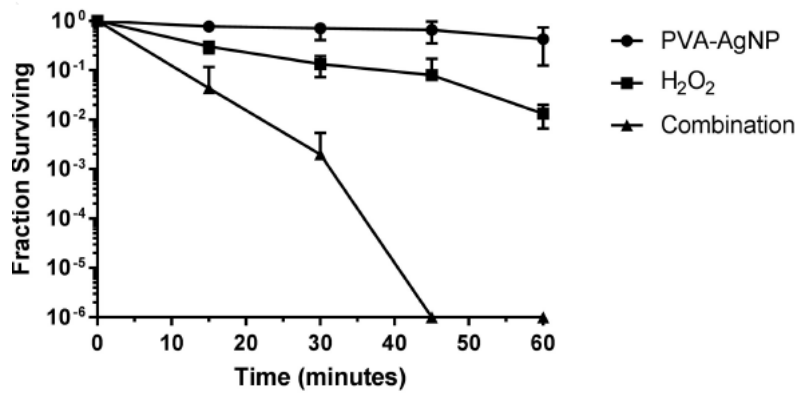


Figure 4.20: Disinfection Efficiency of PVA-AgNP (Alkawareek, et al., 2019)

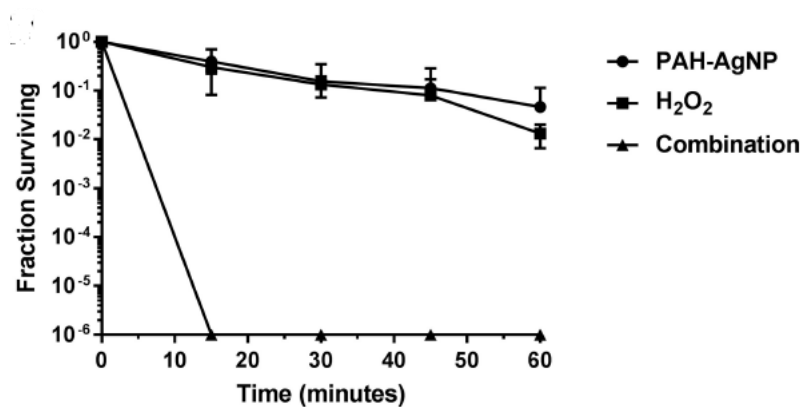


Figure 4.21: Disinfection Efficiency of PAH-AgNP (Alkawareek, et al., 2019)

Diao, et al. (2004) examined and compared different disinfection methods to disinfect *E. coli*. Table 4.10 tabulated the experimental conditions and efficiencies of the different disinfection method. In this experiment, Diao, et al. (2004) mentioned that Fenton reaction did not present as the most powerful disinfection methods due to the low Fenton reagents used as compared to other Fenton reactions conditions. Generally, all the disinfection methods examined showed a very high efficiency, which was all higher than 99.4%.

Table 4.10: Experimental Conditions and Efficiency of Different Disinfection Methods

Method	Testing conditions	Disinfection rate, %
Fenton reaction	Fe ²⁺ : 0.85 mg/L H ₂ O ₂ : 8.5 mg/L pH 4	99.8
Ozonation	10 mg/L	100
Chlorination	5 mg/L	99.98
Electrochemical disinfection	25 mA/cm ²	100

This literature also compared the SEM image of *E. coli* before and after disinfection by different type of disinfection methods (Diao, et al., 2004). No visible surface defects and cell lysis was observed for chlorination method. The cell surface became more rougher, and the integrity of cells were not affected. More obvious changes were observed for the *E. coli* that undergo ozonation where cellular constituents leaked from the cells due to cell lysis. More cellular constituents were released for the *E. coli* that was disinfected by Fenton reaction. The cell also deformed after being disinfected by Fenton reagents. Fenton reaction caused massive cell lysis and severe damage to cell. For the *E. coli* that undergo electrochemical disinfection, surface deformation was observed as well as large amount of cellular constituents were released. It was observed that the SEM image of electrochemical disinfection was similar to Fenton disinfection. Figure 4.22 below show the different SEM image of the *E. coli* treated by different disinfection methods.

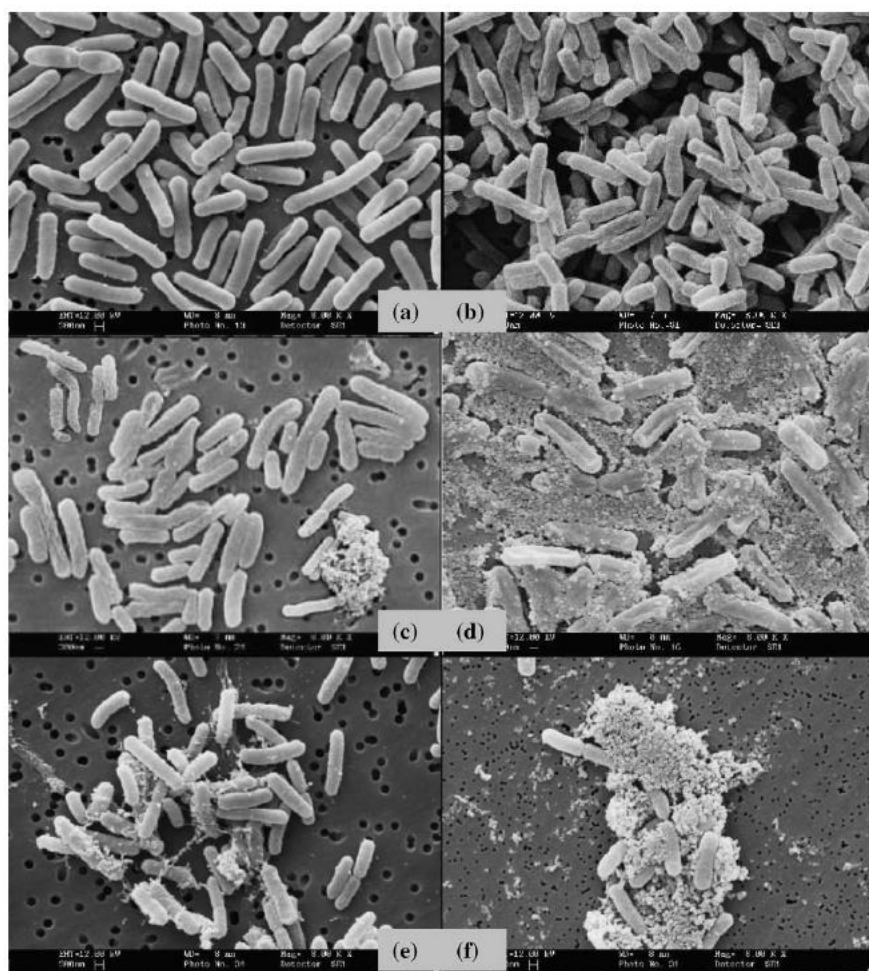


Figure 4.22: (a) Initial *E. coli*; (b) *E. coli* After Chlorination Disinfection; (c) *E. coli* After Ozonation Disinfection; (d) Fenton Treatment for 10 min; (e) Electrochemical Disinfection at 16 mA/cm²; (f) Electrochemical Disinfection at 25 mA/cm² (Diao, et al., 2004)

When electrochemical method was used to disinfect *E. coli*, 1.7-log reduction was observed after 120 min. In contrast, when Fe²⁺ was added for photo-Fenton process, the disinfection of *E. coli* was enhanced to 4.3-log reduction 120 min. Chen, et al. (2020) stated that electrochemical disinfection is an effective way to disinfect bacteria while electro-Fenton reaction is a more promising way to remove *E. coli* in water.

Generally, the efficiency of all the disinfection methods compared in literatures showed comparable results where more than 99% of disinfection rates could be achieved. The differences among them were the disinfectants or catalysts dosage as well as contact time. It is worth to take note that regrowth of bacteria was observed from the disinfection using ozonation. The residual

chlorine and H_2O_2 in water inhibit the regrowth of bacteria using chlorination and Fenton process respectively (Rodriguez-Chueca, et al., 2015). In recent years, Fenton process had emerged as a favorable disinfection method due to its environmental friendly nature. It does not require any special equipment to carry out the process and the catalysts can be easily removed by magnet. Moreover, the Fenton process can be initiated under ambient temperature and pressure.

CHAPTER 5

CONCLUSIONS AND RECOMMENDATIONS

5.1 Conclusions

In this report, the potential of PDDA functionalized Fe_3O_4 for the disinfection of bacteria had been reviewed. The review showed that Fenton reaction is a good alternative to remove pathogenic *E. coli* from wastewater. Moreover, heterogenous Fenton reaction is advantageous over the conventional homogenous Fenton reaction due to the ease in separation and removal of the catalysts from the treated water.

This report contained the reviews based on three main findings. First, it was found that PDDA functionalized Fe_3O_4 can be synthesized from two main routes, namely in-situ coating and post synthesis coating. In in-situ coating, ammonium aqueous solution was added to the heated and deoxygenated $\text{FeCl}_3 \cdot 6\text{H}_2\text{O}$, $\text{FeCl}_2 \cdot 4\text{H}_2\text{O}$ and PDDA. For post synthesis coating, Fe_3O_4 was dissolved before adding the PDDA for coating. All the characterization studies showed that the coating of PDDA onto Fe_3O_4 core did not perturb the original crystallinity of Fe_3O_4 nanoparticles.

The effect of parameters affecting the Fenton reaction were also reviewed. The conventional Fenton reaction was suitable to be carried out at acidic pH but recent research showed that Fenton reaction at near neutral pH showed a good disinfection efficiency as well. Moreover, literatures stated that Fenton reaction is suitable to be carried out at temperature between 30 °C to 90 °C, with optimum temperature of 37 °C. The range of H_2O_2 dosages mostly varied from 10 mg/L to 50 mg/L to achieve efficiency up to 100%. Large variation in iron dosages which was from 0.07 mg/L to 230 mg/L were reported. Only a general observation that both Fenton reagents cannot be added excessively and the optimum dosages depended on the experimental condition.

Fenton reaction was compared to other disinfection techniques. It was found that Fenton reaction required higher cost than the conventional chlorination disinfection method. However, the cost associated to acidify and

neutralize the wastewater can be reduced if it can be carried out at near neutral pH. Fenton reaction also required higher contact time to achieve the same efficiency as UV and ozonation disinfection method. However, Fenton reaction gave no DBPs and high efficiency in disinfection of bacteria.

5.2 Recommendations for future work

From the reviews, it can be observed that Fenton reaction had a high potential in wastewater treatment industry. There are a lot of studies carried out at lab scale to disinfect *E. coli* via Fenton reaction in lab scale. PDDA functionalized Fe_3O_4 may be a good choice of catalysts in heterogenous Fenton reaction due to its easy synthesis process. Hence, more studies can be done to discover the potential of Fenton disinfection techniques using PDDA functionalized Fe_3O_4 to disinfect *E. coli* in real conditions. Experiments were to be carried out to find the optimum dosages of catalysts and the working pH range for the disinfection via Fenton reaction using PDDA functionalized Fe_3O_4 .

REFERENCES

- Al-Badaii, F. and Shuhaimi-Othman, M., 2015. Water Pollution and its Impact on the Prevalence of Antibiotic-Resistant *E. coli* and Total Coliform Bacteria: A Study of the Semenyih River, Peninsular Malaysia. *Water Quality, Exposure and Health*, [e-journal] 7(3), pp. 319–330. <http://dx.doi.org/10.1007/s12403-014-0151-5>.
- Alkawareek, M. Y., Bahloul, A., Abulateefeh, S. R. and Alkilany, A. M., 2019. Synergistic antibacterial activity of silver nanoparticles and hydrogen peroxide. *PLoS ONE*, [e-journal] 14(8). <http://dx.doi.org/10.1371/journal.pone.0220575>.
- Al-Mashhadani, A. H. and Hassen, Z. A. A., 2016. DECONTAMINATED RADIOACTIVE WATER FROM RADIONUCLIDES BY MAGNETIC NANOPARTICLES. *International Journal of Latest Trends in Engineering and Technology*, [e-journal] 8(1), pp. 661–666. <http://dx.doi.org/10.21172/1.81.086>.
- Alvear-Daza, J. J., Sanabria, J., Rengifo Herrera, J. A. and Gutierrez-Zapata, H. M., 2018. Simultaneous abatement of organics (2,4-dichlorophenoxyacetic acid) and inactivation of resistant wild and laboratory bacteria strains by photo-induced processes in natural groundwater samples. *Solar Energy*, [e-journal] 171, pp. 761–768. <http://dx.doi.org/10.1016/j.solener.2018.07.026>.
- Barreca, S., Colmenares, J. J. V., Pace, A., Orecchio, S. and Pulgarin, C., 2015. Escherichia coli inactivation by neutral solar heterogeneous photo-Fenton (HPF) over hybrid iron/montmorillonite/alginate beads. *Journal of Environmental Chemical Engineering*, [e-journal] 3, pp. 317–324. <http://dx.doi.org/10.1016/j.jece.2014.10.018>.
- Barrow, M., Taylor, A., Murray, P., Rosseinsky, M. J. and Adams, D. J., 2015. Design considerations for the synthesis of polymer coated iron oxide nanoparticles for stem cell labelling and tracking using MRI. *Chemical Society reviews*, [e-journal] 44(19), pp. 6733–6748. <http://dx.doi.org/10.1039/c5cs00331h>.
- Bong, C. W., Chai, S. K., Chai, L. C., Wang, A. J. and Lee, C. W., 2020. Prevalence and characterization of Escherichia coli in the Kelantan River and its adjacent coastal waters. *Water Supply*, [e-journal] 20(3), pp. 930–942. <http://dx.doi.org/10.2166/ws.2020.018>.
- Bunaciu, A. A., Udriștioiu, E. G. and Aboul-Enein, H. Y., 2015. X-ray diffraction: instrumentation and applications. *Critical reviews in analytical chemistry*, [e-journal] 45(4), pp. 289–299. <http://dx.doi.org/10.1080/10408347.2014.949616>.
- Businova, P., Chomoucka, J., Prasek, J., Hrdy, R., Drbohlavova, J., Sedlacek, P. and Hubalek, J., 2011a. POLYMER-COATED IRON OXIDE MAGNETIC

NANOPARTICLES - PREPARATION AND CHARACTERIZATION, 9, pp. 21–23.

Businova, P., Chomoucka, J., Prasek, J., Hrady, R., Drbohlavova, J., Sedlacek, P. and Hubalek, J., 2011b. POLYMER-COATED IRON OXIDE MAGNETIC NANOPARTICLES - PREPARATION AND CHARACTERIZATION, 9, pp. 21–23.

Carra, I., Pérez, J.A. S., López, J.L. C., Santos-Juanes, L. and Malato, S., 2013. Iron dosage as a strategy to operate the photo-Fenton process at initial neutral pH. *Chemical Engineering Journal*, [e-journal] 224, pp. 67–74. <http://dx.doi.org/10.1016/j.cej.2012.09.065>.

Chen, J., Ju, Y. and Chen, H., 2018. One-pot synthesis of magnetic cationic adsorbent modified with PDDA for organic phosphonates removal. *NANO: Brief Reports and Reviews*, [e-journal] 1(1), pp. 1–13. <http://dx.doi.org/10.1142/S179329201950019X>.

Chen, L., Zhou, Z., Shen, C. and Xu, Y., 2020. Inactivation of antibiotic-resistant bacteria and antibiotic resistance genes by electrochemical oxidation/electro-Fenton process. *Water Science & Technology*. <http://dx.doi.org/10.2166/wst.2020.282>.

Cho, M., Lee, Y., Chung, H. and Yoon, J., 2004. Inactivation of *Escherichia coli* by Photochemical Reaction of Ferrioxalate at Slightly Acidic and Near-Neutral pHs. *Applied and Environmental Microbiology*, [e-journal] 70(2), pp. 1129–1134. <http://dx.doi.org/10.1128/AEM.70.2.1129-1134.2004>.

Choudhary, O. P. and Priyanka, 2017. Scanning Electron Microscope: Advantages and Disadvantages in Imaging Components. *International Journal of Current Microbiology and Applied Sciences*, [e-journal] 6(5), pp. 1877–1882. <http://dx.doi.org/10.20546/ijcmas.2017.605.207>.

Collivignarelli, M. C., Abbà, A., Benigna, I., Sorlini, S. and Torretta, V., 2018. Overview of the Main Disinfection Processes for Wastewater and Drinking Water Treatment Plants. *Sustainability*, [e-journal] 10(86). <http://dx.doi.org/10.3390/su10010086>.

Crini, G. and Lichtfouse, E., 2019. Advantages and disadvantages of techniques used for wastewater treatment. *Environmental Chemistry Letters*, [e-journal] 17(1), pp. 145–155. <http://dx.doi.org/10.1007/s10311-018-0785-9>.

Cruz, A., Couto, L., Esplugas, S. and Sans, C., 2017. Study of the contribution of homogeneous catalysis on heterogeneous Fe(III)/alginate mediated photo-Fenton process. *Chemical Engineering Journal*, [e-journal] 318, pp. 272–280. <http://dx.doi.org/10.1016/j.cej.2016.09.014>.

Cruz, N. D. I., Esquiús, L., Grandjean, D., Magnet, A., Tungler, A., Alencastro, L.F. d. and Pulgarín, C., 2013. Degradation of emergent contaminants by UV, UV/H₂O₂ and neutral photo-Fenton at pilot scale in a domestic wastewater

treatment plant. *Water research*, [e-journal] 47, pp. 5836–5845. <http://dx.doi.org/10.1016/j.watres.2013.07.005>.

Deng, Y. and Zhao, R., 2015. Advanced Oxidation Processes (AOPs) in Wastewater Treatment. *Current Pollution Reports*, [e-journal] 1(3), pp. 167–176. <http://dx.doi.org/10.1007/s40726-015-0015-z>.

Diao, H. F., Li, X. Y., Gu, J. D., Shi, H. C. and Xie, Z. M., 2004. Electron microscopic investigation of the bactericidal action of electrochemical disinfection in comparison with chlorination, ozonation and Fenton reaction. *Process Biochemistry*, [e-journal] 39, pp. 1421–1426. [http://dx.doi.org/10.1016/S0032-9592\(03\)00274-7](http://dx.doi.org/10.1016/S0032-9592(03)00274-7).

DOE, 2017. *Kualiti Air Sungai River Water Quality*. [online] Available at: <<https://www.doe.gov.my/portalv1/wp-content/uploads/formidable/5/Kualiti-Air-Sungai.pdf>> [Accessed 29 December 2020].

Dong, C., Xing, M. and Zhang, J., 2020. Recent progress of photocatalytic Fenton-like process for environmental remediation. *Frontiers in Environmental Chemistry*. <http://dx.doi.org/10.3389/fenvc.2020.00008>.

Feng, S., Yilihamu, A., Luo, J., Ma, Q., Wang, R., Yang, S., Yang, S.-T. and Bai, Y., 2019. Fe₃O₄/SiO₂/C nanocomposites for the fenton-like disinfection of Escherichia coli in water. *Materials Research Express*, [e-journal] 6. <http://dx.doi.org/10.1088/2053-1591/ab0585>.

Fernández, L., González-Rodríguez, J., Gamallo, M., Vargas-Osorio, Z., Vázquez-Vázquez, C., Piñeiro, Y., Rivas, J., Feijoo, G. and Moreira, M. T., 2020. Iron oxide-mediated photo-Fenton catalysis in the inactivation of enteric bacteria present in wastewater effluents at neutral pH. *Environmental pollution (Barking, Essex : 1987)*, [e-journal] 266(Pt 3), p. 115181–115181. <http://dx.doi.org/10.1016/j.envpol.2020.115181>.

Fiorentino, A., Cucciniello, R., Cesare, A. D., Fontaneto, D., Prete, P., Rizzo, L., Corno, G. and Proto, A., 2018. Disinfection of urban wastewater by a new photo-Fenton like process using Cu-iminodisuccinic acid complex as catalyst at neutral pH. *Water research*. <http://dx.doi.org/10.1016/j.watres.2018.08.024>.

Forney, L., 2008. Advances in disinfection techniques for water reuse. In: 2008. *Handbook of Water and Energy Management in Food Processing*: Elsevier, pp. 700–719.

Frederick, A., 2011. Escherichia Coli, it Prevalence and Antibiotic Resistant in Malaysia: A Mini Review. *Microbiology Journal*, [e-journal] 1(2), pp. 47–53. <http://dx.doi.org/10.3923/mj.2011.47.53>.

Gabbott, P., ed., 2010. *Principles and applications of thermal analysis*. Oxford: Blackwell Pub.

García, B. E., Rivas, G., Arzate, S. and Sánchez Pérez, J. A., 2018. Wild bacteria inactivation in WWTP secondary effluents by solar photo-fenton at neutral pH in raceway pond reactors. *Catalysis Today*, [e-journal] 313, pp. 72–78. <http://dx.doi.org/10.1016/j.cattod.2017.10.031>.

García-Fernández, I., Polo-López, M.I., Oller, I. and Fernández-Ibáñez, P., 2012. Bacteria and fungi inactivation using Fe³⁺/sunlight, H₂O₂/sunlight and near neutral photo-Fenton: A comparative study. *Applied Catalysis B: Environmental*, [e-journal] 121-122, pp. 20–29. <http://dx.doi.org/10.1016/j.apcatb.2012.03.012>.

Garcia-Herrera, L. F. and Price, H., 2020. *Thermogravimetric analysis (TGA)*. [online] Available at: <[https://chem.libretexts.org/Courses/Franklin_and_Marshall_College/Introduction_to_Materials_Characterization_CHM_412_Collaborative_Text/Thermal_Analysis/Thermogravimetric_analysis_\(TGA\)](https://chem.libretexts.org/Courses/Franklin_and_Marshall_College/Introduction_to_Materials_Characterization_CHM_412_Collaborative_Text/Thermal_Analysis/Thermogravimetric_analysis_(TGA))> [Accessed 6 January 2021].

Giannakis, S., Androulaki, B., Comninellis, C. and Pulgarin, C., 2018. Wastewater and urine treatment by UVC-based advanced oxidation processes: Implications from the interactions of bacteria, viruses, and chemical contaminants. *Chemical Engineering Journal*, [e-journal] 343, pp. 270–282. <http://dx.doi.org/10.1016/j.cej.2018.03.019>.

Giannakis, S., Liu, S., Carratalà, A., Rtimi, S., Bensimon, M. and Pulgarin, C., 2017a. Effect of Fe(II)/Fe(III) species, pH, irradiance and bacterial presence on viral inactivation in wastewater by the photo-Fenton process: Kinetic modeling and mechanistic interpretation. *Applied Catalysis B: Environmental*, [e-journal] 204, pp. 156–166. <http://dx.doi.org/10.1016/j.apcatb.2016.11.034>.

Giannakis, S., Liu, S., Carratalà, A., Rtimi, S., Talebi Amiri, M., Bensimon, M. and Pulgarin, C., 2017b. Iron oxide-mediated semiconductor photocatalysis vs. heterogeneous photo-Fenton treatment of viruses in wastewater. Impact of the oxide particle size. *Journal of Hazardous Materials*, [e-journal] 339, pp. 223–231. <http://dx.doi.org/10.1016/j.jhazmat.2017.06.037>.

Giannakis, S., Papoutsakis, S., Darakas, E., Escalas-Canellas, A., Petrier, C. and Pulgarin, C., 2015. Ultrasound enhancement of near-neutral photo-Fenton for effective *E. coli* inactivation in wastewater. *Ultrasonic Sonochemistry*, [e-journal] 22, pp. 515–526. <http://dx.doi.org/10.1016/j.ultsonch.2014.04.015>.

Guerrero-Pérez, M. O. and Patience, G. S., 2019. Experimental methods in chemical engineering: Fourier transform infrared spectroscopy—FTIR. *The Canadian Journal of Chemical Engineering*, [e-journal] 98(1), pp. 25–33. <http://dx.doi.org/10.1002/cjce.23664>.

Gutiérrez-Zapata, H. M., Alvear-Daza, J. J., Rengifo-Herrera, J. A. and Sanabria, J., 2017. Addition of Hydrogen Peroxide to Groundwater with Natural Iron Induces Water Disinfection by Photo - Fenton at Circumneutral

pH and other Photochemical Events. *Photochem. Photobiol.*, [e-journal] 93(5), pp. 1224–1231. <http://dx.doi.org/10.1111/php.12779>.

Gutiérrez-Zapata, H. M., Sanabria, J. and Rengifo-Herrera, J. A., 2017. Addition of hydrogen peroxide enhances abiotic sunlight-induced processes to simultaneous emerging pollutants and bacteria abatement in simulated groundwater using CPC solar reactors. *Solar Energy*, [e-journal] 148, pp. 110–116. <http://dx.doi.org/10.1016/j.solener.2017.03.068>.

Huang, Y. F., Ang, S. Y., Lee, K. M. and Lee, T. S., 2015. Quality of Water Resources in Malaysia. In: T. S. Lee, ed. 2015. *Research and Practices in Water Quality*: InTech.

Ismail, A. A., van de Voort, F. R. and Sedman, J., 2007. Chapter 4 Fourier Transform Infrared Spectroscopy: Principles and Applications. *Techniques and Instrumentation in Analytical Chemistry*, [e-journal] 1997, pp. 93–139. [http://dx.doi.org/10.1016/s0167-9244\(97\)80013-3](http://dx.doi.org/10.1016/s0167-9244(97)80013-3).

Jang, S.-C., Hong, S.-B., Yang, H.-M., Lee, K.-W., Moon, J.-K., Seo, B.-K., Huh, Y. S. and Roh, C., 2014. Removal of Radioactive Cesium Using Prussian Blue Magnetic Nanoparticles. *Nanomaterials (Basel, Switzerland)*, [e-journal] 4(4), pp. 894–901. <http://dx.doi.org/10.3390/nano4040894>.

Jiménez, I. D. I. O., García, B. E., Ibanez, G. R., López, J. L. C. and Perez, J. A. S., 2019a. Continuous flow disinfection of WWTP secondary effluents by solar photo-Fenton at neutral pH in raceway pond reactors at pilot plant scale. *Applied Catalysis B: Environmental*. <http://dx.doi.org/10.1016/j.apcatb.2019.01.093>.

Jiménez, I. D. I. O., López, J. L. C., Ibáñez, G. R., Gracia, B. E. and Pérez, J. A. S., 2019b. Kinetic assessment of antibiotic resistant bacteria inactivation by solar photo-Fenton in batch and continuous mode for wastewater reuse. *Water Research*. <http://dx.doi.org/10.1016/j.watres.2019.04.059>.

Kim, J. Y., Lee, C., Sedlak, D. L., Yoon, J. and Nelson, K. L., 2010. Inactivation of MS2 coliphage by Fenton's reagent. *Water research*, [e-journal] 44(8), pp. 2647–2653. <http://dx.doi.org/10.1016/j.watres.2010.01.025>.

Kohantorabi, M., Giannakis, S., Gholami, M. R., Feng, L. and Pulgarin, C., 2018. A systematic investigation on the bactericidal transient species generated by photo-sensitization of natural organic matter (NOM) during solar and photo-Fenton disinfection of surface waters. *Applied Catalysis B: Environmental*. <http://dx.doi.org/10.1016/j.apcatb.2018.12.012>.

Krishnan, S., Rawindran, H., Sinnathambi, C. M. and Lim, J. W., 2017. Comparison of various advanced oxidation processes used in remediation of industrial wastewater laden with recalcitrant pollutants. *IOP Conference Series: Materials Science and Engineering*, [e-journal] 206. <http://dx.doi.org/10.1088/1757-899X/206/1/012089>.

La Obra Jiménez, I. de, Giannakis, S., Grandjean, D., Breider, F., Grunauer, G., Casas López, J. L., Sánchez Pérez, J. A. and Pulgarin, C., 2020. Unfolding the action mode of light and homogeneous vs. heterogeneous photo-Fenton in bacteria disinfection and concurrent elimination of micropollutants in urban wastewater, mediated by iron oxides in Raceway Pond Reactors. *Applied Catalysis B: Environmental*, [e-journal] 263, p. 118158–118158. <http://dx.doi.org/10.1016/j.apcatb.2019.118158>.

Lee Goi, C., 2020. The river water quality before and during the Movement Control Order (MCO) in Malaysia. *Case Studies in Chemical and Environmental Engineering*, [e-journal] 2, p. 100027–100027. <http://dx.doi.org/10.1016/j.cscee.2020.100027>.

Leonel, A. G., Mansur, A. A. P. and Mansur, H. S., 2020. Advanced Functional Nanostructures based on Magnetic Iron Oxide Nanomaterials for Water Remediation: A Review. *Water research*. <http://dx.doi.org/10.1016/j.watres.2020.116693>.

Li, B., 2014. Comparison of bacterial inactivation efficiency and disinfection byproduct formation from different disinfection processes. *All Theses*.

Li, F., Yang, Q., Qiu, F. and Liu, Y., 2016. Modification of superparamagnetic iron oxide nanoparticles with poly(diallyldimethylammonium chloride) at air atmosphere. *Polymers for Advanced Technologies*, [e-journal] 27(11), pp. 1530–1534. <http://dx.doi.org/10.1002/pat.3834>.

Li, Y., Yang, D., Wang, S., Li, C., Xue, B., Yang, L., Shen, Z., Jin, M., Wang, J. and Qiu, Z., 2018. The Detailed Bactericidal Process of Ferric Oxide Nanoparticles on *E. coli*. *Molecules (Basel, Switzerland)*, [e-journal] 23(3). <http://dx.doi.org/10.3390/molecules23030606>.

Lim, J. Y., Yoon, J. W. and Hovde, C. J., 2012. A Brief Overview of Escherichia coli O157:H7 and Its Plasmid O157. *J Microbio Biotechnol*, 20(1), pp. 5–14.

Linden, K. and Murphy, J. R., 2017. PHYSICAL AGENTS. <http://dx.doi.org/10.14321/waterpathogens.70>.

Litter, M. I. and Slodowicz, M., 2017. An overview on heterogeneous Fenton and photoFenton reactions using zerovalent iron materials. *Journal of Advanced Oxidation Technologies*, [e-journal] 20(1). <http://dx.doi.org/10.1515/jaots-2016-0164>.

Liu, C., Xie, X., Zhao, W., Liu, N., Maraccini, P. A., Sassoubre, L. M., Boehm, A. B. and Cui, Y., 2013. Conducting nanosponge electroporation for affordable and high-efficiency disinfection of bacteria and viruses in water. *Nano letters*, [e-journal] 13(9), pp. 4288–4293. <http://dx.doi.org/10.1021/nl402053z>.

Liu, J., Dong, C., Deng, Y., Ji, J., Bao, S., Chen, C., Shen, B., Zhang, J. and Xing, M., 2018. Molybdenum sulfide Co-catalytic Fenton reaction for rapid and efficient inactivation of *Escherichia coli*. *Water Research*. <http://dx.doi.org/10.1016/j.watres.2018.08.039>.

López, A. V., López, K. H., Giannakis, S. and Benítez, N., 2017. Effect of reactor material and its reuse on photo-Fenton process efficiency at near-neutral pH: alterations in *E. coli* inactivation and resorcinol degradation kinetics in water. *Journal of Photochemistry and Photobiology A: Chemistry*. <http://dx.doi.org/10.1016/j.jphotochem.2017.04.019>.

Low, S. C., Ng, Q. H. and Tan, L. S., 2019. Study of magnetic-responsive nanoparticle on the membrane surface as a membrane antifouling surface coating. *Journal of Polymer Research*, [e-journal] 26(3). <http://dx.doi.org/10.1007/s10965-019-1734-4>.

Marjanovic, M., Giannakis, S., Grandjean, D., Alencastro, L. F. d. and Pulgarin, C., 2018. Effect of μM Fe addition, mild heat and solar UV on sulfate radical-mediated inactivation of bacteria, viruses, and micropollutant degradation in water. *Water research*, [e-journal] 140, pp. 220–231. <http://dx.doi.org/10.1016/j.watres.2018.04.054>.

Matsumoto, T., Tatsuno, I. and Hasegawa, T., 2019. Instantaneous Water Purification by Deep Ultraviolet Light in Water Waveguide: *Escherichia Coli* Bacteria Disinfection, 11(968).

Meng, X., Wu, J., Kang, J., Gao, J., Liu, R., Gao, Y., Wang, R., Fan, R., Khoso, S. A., Sun, W. and Hu, Y., 2018. Comparison of the reduction of chemical oxygen demand in wastewater from mineral processing using the coagulation–flocculation, adsorption and Fenton processes. *Minerals Engineering*, [e-journal] 128, pp. 275–283. <http://dx.doi.org/10.1016/j.mineng.2018.09.009>.

Moncayo-Lasso, A., Sanabria, J., Pulgarin, C. and Benítez, N., 2009. Simultaneous *E. coli* inactivation and NOM degradation in river water via photo-Fenton process at natural pH in solar CPC reactor. A new way for enhancing solar disinfection of natural water. *Chemosphere*, [e-journal] 77, pp. 296–300. <http://dx.doi.org/10.1016/j.chemosphere.2009.07.007>.

Moradi, M., Kalantary, R. R., Esrafil, A., Jafari, A. J. and Gholami, M., 2017. Visible light photocatalytic inactivation of *Escherichia coli* by natural pyrite assisted by oxalate at neutral pH. *Journal of Molecular Liquids*, [e-journal] 248, pp. 880–889. <http://dx.doi.org/10.1016/j.molliq.2017.10.115>.

Motshekga, S. C., Sinha Ray, S. and Maity, A., 2018. Synthesis and characterization of alginate beads encapsulated zinc oxide nanoparticles for bacteria disinfection in water. *Journal of colloid and interface science*, [e-journal] 512, pp. 686–692. <http://dx.doi.org/10.1016/j.jcis.2017.10.098>.

Mukherjee, M. and De, S., 2015. Reduction of microbial contamination from drinking water using an iron oxide nanoparticle-impregnated ultrafiltration mixed matrix membrane: preparation, characterization and antimicrobial properties. *Environmental Science: Water Research & Technology*, [e-journal] 1(2), pp. 204–217. <http://dx.doi.org/10.1039/C4EW00094C>.

Naderi, M., 2015. Surface Area: Brunauer-Emmett-Teller (BET). In: 2015. *Progress in Filtration and Separation*: Elsevier, pp. 585–608.

Nahim-Granados, S., Pérez, J.A. S. and Polo-Lopez, M.I., 2017. Effective solar processes in fresh-cut wastewater disinfection_ Inactivation of pathogenic *E. coli* O157_H7 and Salmonella enteritidis. *Catalysis Today*. <http://dx.doi.org/10.1016/j.cattod.2017.10.042>.

Nangmenyi, G., Li, X., Mehrabi, S., Mintz, E. and Economy, J., 2011. Silver-modified iron oxide nanoparticle impregnated fiberglass for disinfection of bacteria and viruses in water. *Materials Letters*, [e-journal] 65(8), pp. 1191–1193. <http://dx.doi.org/10.1016/j.matlet.2011.01.042>.

National Geographic Society, 2020. *Rivers and Streams*. [online] Available at: <https://www.nationalgeographic.org/topics/resource-library-rivers-and-streams/?q=&page=1&per_page=25> [Accessed 15 July 2020].

Ndounla, J., Kenfack, S., Wéthé, J. and Pulgarin, C., 2014. Relevant impact of irradiance (vs. dose) and evolution of pH and mineral nitrogen compounds during natural water disinfection by photo-Fenton in a solar CPC reactor. *Applied Catalysis B: Environmental*, [e-journal] 148-149, pp. 144–153. <http://dx.doi.org/10.1016/j.apcatb.2013.10.048>.

Ndounla, J., Spuhler, D., Kenfack, S., Wéthé, J. and Pulgarin, C., 2013. Inactivation by solar photo-Fenton in pet bottles of wild enteric bacteria of natural well water: Absence of re-growth after one week of subsequent storage. *Applied Catalysis B: Environmental*, [e-journal] 129, pp. 309–317. <http://dx.doi.org/10.1016/j.apcatb.2012.09.016>.

New, C. Y., A., U., Premarathne, J.M.K.J.K., Thung, T. Y., Lee, E., Chang, W. S., Loo, Y. Y., Kwan, S. Y., Tan, C. W., Kuan, C. H. and R., S., 2017. Microbiological food safety in Malaysia from the academician's perspective. *Food Research*, [e-journal] 1(6), pp. 183–202. <http://dx.doi.org/10.26656/fr.2017.6.013>.

Nurliyana, M. R., Sahdan, M. Z., Wibowo, K. M., Muslihati, A., Saim, H., Ahmad, S. A., Sari, Y. and Mansor, Z., 2018. The Detection Method of Escherichia coli in Water Resources: A Review. *Journal of Physics: Conference Series*, [e-journal] 995, p. 12065–12065. <http://dx.doi.org/10.1088/1742-6596/995/1/012065>.

O'Dowd, K. and Pillai, S. C., 2020. Photo-Fenton disinfection at near neutral pH: Process, parameter optimization and recent advances. *Journal of*

Environmental Chemical Engineering, [e-journal] 8(5), p. 104063–104063. <http://dx.doi.org/10.1016/j.jece.2020.104063>.

Odonkor, S. T. and Mahami, T., 2020. *Escherichia coli* as a Tool for Disease Risk Assessment of Drinking Water Sources. *International journal of microbiology*, [e-journal] 2020, p. 2534130–2534130. <http://dx.doi.org/10.1155/2020/2534130>.

Onwuegbuzie, A. J. and Frels, R., 2016. *Seven Steps to a Comprehensive Literature Review: A Multimodal and Cultural Approach*. Croydon: CPI Group (UK) Ltd.

Ortega-Gómez, E., Fernández-Ibáñez, P., Ballesteros Martín, M. M., Polo-López, M. I., Esteban García, B. and Sánchez Pérez, J. A., 2012. Water disinfection using photo-Fenton: Effect of temperature on *Enterococcus faecalis* survival. *Water research*, [e-journal] 46(18), pp. 6154–6162. <http://dx.doi.org/10.1016/j.watres.2012.09.007>.

Ortega-Gómez, E., Martín, M. M. B., Carratalà, A., Ibañez, P. F., Pérez, J. A. S. and Pulgarín, C., 2015. Principal parameters affecting virus inactivation by the solar photo-Fenton process at neutral pH and μM concentrations of H_2O_2 and $\text{Fe}^{2+/3+}$. *Applied Catalysis B: Environmental*. <http://dx.doi.org/10.1016/j.apcatb.2015.03.016>.

Othman, F., Sakai, N. and Chowdhury, M. S., 2015. Assessment of microorganism pollution of Selangor River, Malaysia. *International Journal of Advances in Agricultural & Environmental Engineering*, [e-journal] 1(2). <http://dx.doi.org/10.15242/IJAAEE.C0215147>.

Pereira, L. C. d. O., Rosso, T., Campos, J. C. and Giordano, G., 2011. Fenton's reagent application in the domestic sewers disinfection. *An Interdisciplinary Journal of Applied Science*, [e-journal] 6(1), pp. 65–76. <http://dx.doi.org/10.4136/ambi-agua.174>.

Pillai N, V., 2020. Research Methodology: Literature Review. <http://dx.doi.org/10.13140/RG.2.2.19772.18560>.

Polo-López, M. I., Nahim-Granados, S. and Fernández-Ibáñez, P., 2018. Homogeneous Fenton and Photo-Fenton Disinfection of Surface and Groundwater. *Applications of Advanced Oxidation Processes (AOPs) in Drinking Water*. http://dx.doi.org/10.1007/698_2017_129.

Porras, J., Giannakis, S., Torres-Palma, R. A., Fernandez, J. J., Bensimon, M. and Pulgarin, C., 2018. Fe and Cu in humic acid extracts modify bacterial inactivation pathways during solar disinfection and photo-Fenton processes in water. *Applied Catalysis B: Environmental*, [e-journal] 235, pp. 75–83. <http://dx.doi.org/10.1016/j.apcatb.2018.04.062>.

Price, R. G. and Wildeboer, D., 2017. *E. coli* as an Indicator of Contamination and Health Risk in Environmental Waters. In: A. Samie, ed. 2017. *Escherichia*

coli - Recent Advances on Physiology, Pathogenesis and Biotechnological Applications: InTech.

Priyanka and Choudhary, O. P., 2018. Uses of Transmission Electron Microscope in Microscopy and its Advantages and Disadvantages. *International Journal of Current Microbiology and Applied Sciences*, [e-journal] 7(05), pp. 743–747. <http://dx.doi.org/10.20546/ijcmas.2018.705.090>.

Qu, J., Dong, Y., Wang, Y. and Xing, H., 2015. A novel sensor based on Fe₃O₄ nanoparticles-multiwalled carbon nanotubes composite film for determination of nitrite. *Sensing and Bio-Sensing Research* 3, pp. 74–78.

Rincón, A.-G. and Pulgarin, C., 2006. Comparative evaluation of Fe³⁺ and TiO₂ photoassisted processes in solar photocatalytic disinfection of water. *Applied Catalysis B: Environmental*, [e-journal] 63(3-4), pp. 222–231. <http://dx.doi.org/10.1016/j.apcatb.2005.10.009>.

Rodríguez-Chueca, J., Ormad, M. P., Mosteo, R., Sarasa, J. and Ovelleiro, J. L., 2015. Conventional and Advanced Oxidation Processes Used in Disinfection of Treated Urban Wastewater. *Water Environment Research*, [e-journal] 87(3), pp. 281–288. <http://dx.doi.org/10.2175/106143014X13987223590362>.

Rodríguez-Chueca, J., Mosteo, R., Ormad, M. P. and Ovelleiro, J. L., 2012. Factorial experimental design applied to Escherichia coli disinfection by Fenton and photo-Fenton processes. *Solar Energy*, [e-journal] 86(11), pp. 3260–3267. <http://dx.doi.org/10.1016/j.solener.2012.08.015>.

Rodríguez-Chueca, J., Ormad, M. P., Mosteo, R. and Ovelleiro, J. L., 2015. Kinetic modeling of Escherichia coli and Enterococcus sp. inactivation in wastewater treatment by photo-Fenton and H₂O₂/UV-vis processes. *Chemical Engineering Science*. <http://dx.doi.org/10.1016/j.ces.2015.08.051>.

Rodríguez-Chueca, J., Polo-López, M. I., Mosteo, R., Ormad, M. P. and Fernández-Ibáñez, P., 2013. Disinfection of real and simulated urban wastewater effluents using a mild solar photo-Fenton. *Applied Catalysis B: Environmental*, [e-journal] 150-151, pp. 619–629. <http://dx.doi.org/10.1016/j.apcatb.2013.12.027>.

Ruales-Lonfat, C., Benítez, N., Sienkiewicz, A. and Pulgarín, C., 2014. Deleterious effect of homogeneous and heterogeneous near-neutral photo-Fenton system on Escherichia coli. Comparison with photo-catalytic action of TiO₂ during cell envelope disruption. *Applied Catalysis B: Environmental*, [e-journal] 160-161, pp. 286–297. <http://dx.doi.org/10.1016/j.apcatb.2014.05.001>.

Rubio, D., Nebot, E., Casanueva, J. F. and Pulgarin, C., 2013. Comparative effect of simulated solar light, UV, UV/H₂O₂ and photo-Fenton treatment (UV-Vis/H₂O₂/Fe^{2+,3+}) in the Escherichia coli inactivation in artificial seawater. *Water research*, [e-journal] 47(16), pp. 6367–6379. <http://dx.doi.org/10.1016/j.watres.2013.08.006>.

- Saadatkhah, N., Carillo Garcia, A., Ackermann, S., Leclerc, P., Latifi, M., Samih, S., Patience, G. S. and Chaouki, J., 2020. Experimental methods in chemical engineering: Thermogravimetric analysis—TGA. *The Canadian Journal of Chemical Engineering*, [e-journal] 98(1), pp. 34–43. <http://dx.doi.org/10.1002/cjce.23673>.
- Salgado, P., Frontela, J. L. and Vidal, G., 2020. Optimization of Fenton Technology for Recalcitrant Compounds and Bacteria Inactivation. *catalysts*, [e-journal] 10. <http://dx.doi.org/10.3390/catal10121483>.
- Saqib Ishaq, M., Afsheen, Z. and Khan, A., 2019. Disinfection Methods. In: S. Bahadar Khan, and K. Akhtar, eds. 2019. *Photocatalysts - Applications and Attributes*: IntechOpen.
- Schuttlefield, J. D. and Grassian, V. H., 2008. ATR-FTIR Spectroscopy in the Undergraduate Chemistry Laboratory: Part I. Fundamentals and Examples. *Journal of Chemical Education*, 85(2).
- Selvakumar, A., Tuccillo, M. E., Muthukrishnan, S. and Bay, A. B., 2009. Use of Fenton's Reagent as a Disinfectant. *Remediation*, pp. 135–142. <http://dx.doi.org/10.1002/rem.20208>.
- Singh, P., Sharma, K., Hasija, V., Sharma, V., Sharma, S., Raizada, P., Singh, M., Saini, A. K., Hosseini-Bandegharai, A. and Thakur, V. K., 2019. Systematic review on applicability of magnetic iron oxides–integrated photocatalysts for degradation of organic pollutants in water. *Materials Today Chemistry*, [e-journal] 14, p. 100186–100186. <http://dx.doi.org/10.1016/j.mtchem.2019.08.005>.
- Snyder, H., 2019. Literature review as a research methodology: An overview and guidelines. *Journal of Business Research*, [e-journal] 104, pp. 333–339. <http://dx.doi.org/10.1016/j.jbusres.2019.07.039>.
- Tang, C. Y. and Yang, Z., 2017. Transmission Electron Microscopy (TEM). In: 2017. *Membrane Characterization*: Elsevier, pp. 145–159.
- Templier, M. and Paré, G., 2015. A Framework for Guiding and Evaluating Literature Reviews. *Communications of the Association for Information Systems*, 37, pp. 112–137.
- Tong, M., Liu, F., Dong, Q., Ma, Z. and Liu, W., 2019. Magnetic Fe₃O₄-deposited flower-like MoS₂ nanocomposites for the Magnetic Fe₃O₄-deposited flower-like MoS₂ nanocomposites for the Fenton-like Escherichia coli disinfection and diclofenac degradation. *Journal of Hazardous Materials*. <http://dx.doi.org/10.1016/j.jhazmat.2019.121604>.
- Topac, B. S. and Alkan, U., 2016. Comparison of solar/H₂O₂ and solar photo-fenton processes for the disinfection of domestic wastewaters. *KSCE Journal of Civil Engineering*, [e-journal] 20(7), pp. 2632–2639. <http://dx.doi.org/10.1007/s12205-016-0416-6>.

UN-Water, 2020. *UN World Water Development Report 2020 'Water and Climate Change'*. [online] Available at: <<https://www.unwater.org/world-water-development-report-2020-water-and-climate-change/#:~:text=UN%20World%20Water%20Development%20Report%2020%20'Water%20and%20Climate%20Change',-UN%20DWater&text=This%20will%20be%20a%20considerable,are%20witho ut%20safely%20managed%20sanitation.>> [Accessed 29 December 2020].

Valero, P., Giannakis, S., Mosteo, R., Ormad, M. P. and Pulgarin, C., 2017. Comparative effect of growth media on the monitoring of *E. coli* inactivation and regrowth after solar and photo-Fenton treatment. *Chemical Engineering Journal*, [e-journal] 313, pp. 109–120. <http://dx.doi.org/10.1016/j.cej.2016.11.126>.

Wang, X., Zhang, X., Zhang, Y., Wang, Y., Sun, S.-P., Wu, W. D. and Wu, Z., 2020. Nanostructured Semiconductor Supported Iron Catalysts for Heterogeneous Photo-Fenton Oxidation: A Review. *Journal of Materials Chemistry A*. <http://dx.doi.org/10.1039/D0TA04541A>.

Wei Wu, Zhaohui Wu, Taekyung Yu, Changzhong Jiang and Woo-Sik Kim, 2015. Recent progress on magnetic iron oxide nanoparticles: synthesis, surface functional strategies and biomedical applications. *Sci. Technol. Adv. Mater.*, [e-journal] 16. <http://dx.doi.org/10.1088/1468-6996/16/2/023501>.

Xu, C., Akakuru, O. U., Zheng, J. and Wu, A., 2019. Applications of Iron Oxide-Based Magnetic Nanoparticles in the Diagnosis and Treatment of Bacterial Infections. *Frontiers in bioengineering and biotechnology*, [e-journal] 7, p. 141–141. <http://dx.doi.org/10.3389/fbioe.2019.00141>.

Yu, C.-J., Lin, C.-Y., Liu, C.-H., Cheng, T.-L. and Tseng, W.-L., 2010. Synthesis of poly(diallyldimethylammonium chloride)-coated Fe₃O₄ nanoparticles for colorimetric sensing of glucose and selective extraction of thiol. *Biosensors and Bioelectronics*, [e-journal] 26, pp. 913–917. <http://dx.doi.org/10.1016/j.bios.2010.06.069>.

Zare, K., Gupta, V. K., Moradi, O., Makhlof, A. S. H., Sillanpää, M., Nadagouda, M. N., Sadegh, H., Shahryari-ghoshekandi, R., Pal, A., Wang, Z.-j., Tyagi, I. and Kazemi, M., 2015. A comparative study on the basis of adsorption capacity between CNTs and activated carbon as adsorbents for removal of noxious synthetic dyes: a review. *Journal of Nanostructure in Chemistry*, [e-journal] 5(2), pp. 227–236. <http://dx.doi.org/10.1007/s40097-015-0158-x>.

Zhang, M.-H., Dong, H., Zhao, L., Wang, D.-X. and Di Meng, 2019. A review on Fenton process for organic wastewater treatment based on optimization perspective. *The Science of the total environment*, [e-journal] 670, pp. 110–121. <http://dx.doi.org/10.1016/j.scitotenv.2019.03.180>.